

A PROCESS TO EVALUATE COMMERCIAL SOFTWARE PACKAGES THAT  
ESTIMATE MEASUREMENT UNCERTAINTY THROUGH SIMULATION

by

Jonathan Marvin Beaman

A dissertation submitted to the faculty of  
The University of North Carolina at Charlotte  
in partial fulfillment of the requirements  
for the degree of Doctor of Philosophy in  
Mechanical Engineering

Charlotte

2011

Approved by:

---

Dr. Edward P. Morse

---

Dr. James F. Cuttino

---

Dr. Angela D. Davies

---

Dr. Robert J. Hocken

---

Dr. Thomas R. Lucas

©2011  
Jonathan Marvin Beaman  
ALL RIGHTS RESERVED

## ABSTRACT

JONATHAN MARVIN BEAMAN. A process to evaluate commercial software packages that estimate measurement uncertainties through simulation. (Under the direction of DR. EDWARD PHILLIP MORSE).

Coordinate Measuring Machines (CMMs) can be used to measure a great variety of parts. Essentially, any three-dimensional surface can be evaluated. Characterizing the measurement uncertainty in a way that maintains traceability in accordance with international standards can be difficult since there are many variables that influence a measurement, such as geometry type, nominal scale, fixturing, orientation, number of measuring points, and probe configuration. Task-specific uncertainty is measurement uncertainty related to a particular measurement scenario. The idea of using statistically-based simulations, in particular Monte-Carlo type simulations, to help determine these uncertainties, has been previously introduced as a practical method. The work in this dissertation describes the concepts and implementation of two commercially available software simulation packages, VCMM and PUNDIT. A process used for evaluating commercial software packages was implemented by way of comparing software estimates for uncertainty to those calculated from calibrated artifact measurement (substitution method) for a variety of measurands. This process indicates directly how well each software performs for the cases tested, but also provides a framework for future verification processes. The results indicate that realistic uncertainty estimates can be attained by simulation, in the context of the experimental conditions, though a broader scope for the simulations, inclusive of multiple conditions for each measurement task, gives improved results.

## ACKNOWLEDGMENTS

I wish to thank Dr. Edward Morse, Greg Caskey, Tracy Beauregard, and all of the other faculty, staff, and graduate students that I have had the opportunity to work with at The University of North Carolina at Charlotte.



## TABLE OF CONTENTS

CHAPTER 1: INTRODUCTION	1
1.1 Description of Coordinate Measuring Machines	2
1.2 Measurement Uncertainty and Task Specific Uncertainty	4
1.3 Determining Task Specific Uncertainties	8
1.4 Purpose for Simulating Measurement	10
1.5 Structure of this Document	11
CHAPTER 2: VIRTUAL METHODS INVESTIGATED	12
2.1 How Simulation Methods Work	12
2.2 Simulation Methods Tested	15
2.3 Purpose for Testing Particular Simulation Methods	17
CHAPTER 3: VCMM AND PUNDIT SOFTWARE PACKAGES	19
3.1 VCMM	19
3.2 PUNDIT	39
CHAPTER 4: TESTING	50
4.1 Experimental Procedure for Tests of Simulation Methods	51
4.1.1 Software Inputs	53
4.1.2 Ball Plate Measurement	59
4.1.3 Ball Plate Measurement Results	63
4.2 Results	67
4.2.1 All Measurands	68
4.2.2 Ring Tests	69
4.2.3 Line Tests	87

4.2.4	Point to Point Distance Tests	90
4.2.5	Sphere Tests	97
4.2.6	Cylinder Tests	107
4.2.7	Summary by Measurand	114
4.2.8	Notes on Findings	115
CHAPTER 5: CONCLUSIONS AND REMARKS		119
REFERENCES		124

## Chapter 1: INTRODUCTION

Task specific uncertainty in the context of Coordinate Measuring Machine (CMM) measurements refers to uncertainty resulting from the measurement of a particular geometry and scale in a particular configuration within the machine volume. The calculation of a reliable estimate for this uncertainty can be very complicated without the aid of standards, experience, and even computer simulations. The importance of the concepts of uncertainty and traceability have been recognized as the desire to control manufacturing processes and assess the quality of dimensional values for products continually increases. CMMs, are popular and versatile, but their complexity makes it difficult to reliably document the uncertainties associated with the measurements produced with them. The idea of using computers and statistically based simulations to help determine these uncertainties has been previously introduced as a practical method [1][2][3][4] et al.. The work in this dissertation assesses the results of two commercially available software simulation packages by implementing a procedure of comparison to experimental data (via substitution method) for several measurands on a specific machine. The results indicate that realistic uncertainty estimates can be attained by simulation, in the context of the experimental conditions (on the order of 1 to 3 micrometers deviation from experiment), though a broader scope for the simulations, inclusive of multiple conditions for each measurement task, gives improved results. Attention is also drawn to the fact that the process requires expertise, likely above the

skill level of the typical technician or operator and that certain extrinsic influences must be verified and included in the uncertainty estimate determined by simulation.

### 1.1 Description of Coordinate Measuring Machines

A CMM is a coordinate measuring device, meaning the coordinates of points are reported, which can be used to compose a measurement. CMMs commonly have three orthogonal axes, establishing a cartesian reference frame, though there are variations, such as the inclusion of a rotary axis. The combination of three axial movements allows free movement in three-dimensional space within the constraints of the measurement volume. A probe, fixed to one of the axes, measures discrete points on the surface of a part. Physically contacting probes, the type discussed in this dissertation, directly contact the part and record a measurement 'point' by a switching mechanism or an analogous type contact sensor. A collection of these points is used to evaluate a measurand, e.g. a circle or plane. CMMs, by their nature, are flexible measuring devices that can measure a wide variety of geometries of various scales in varied orientations and positions. [5] gives a thorough description of CMMs and their functionality.

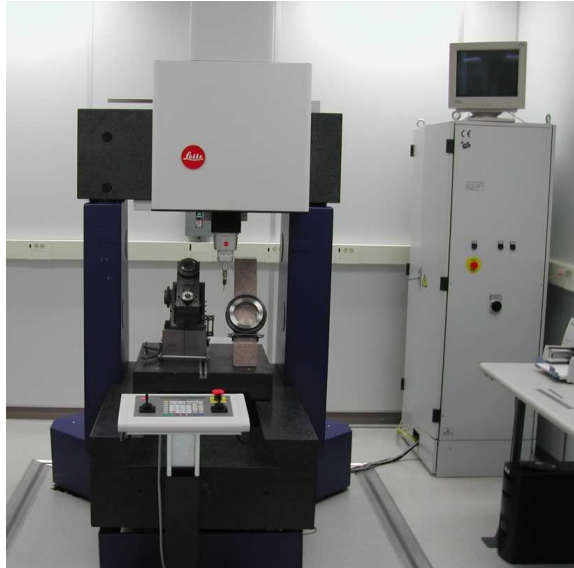


Figure 1: Photograph of Leitz PMM Used in Study

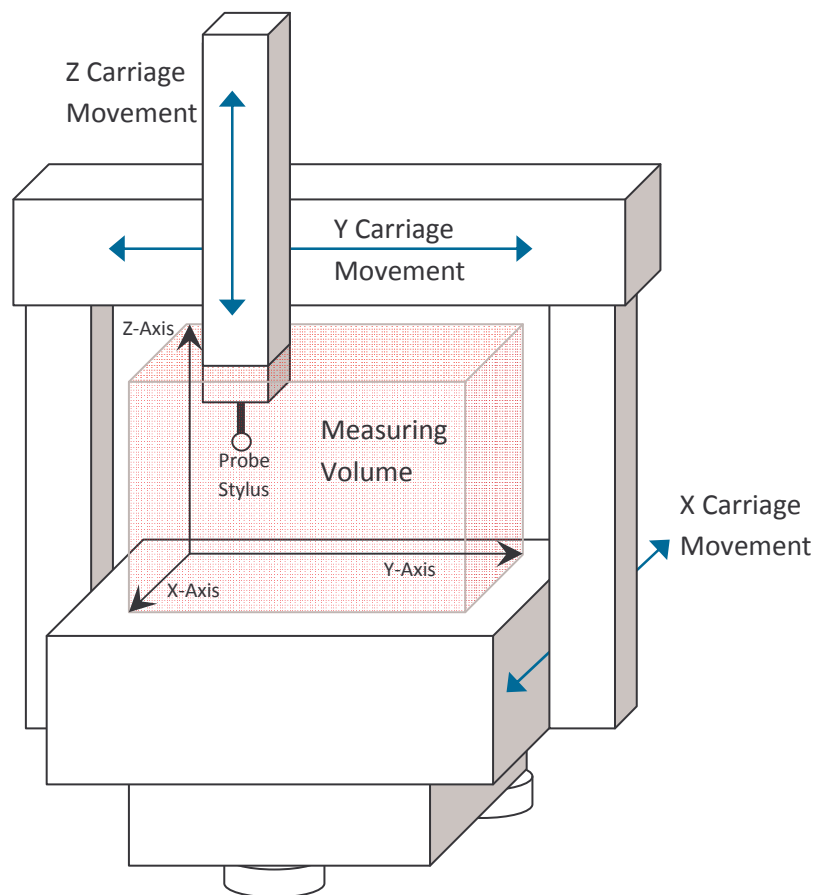


Figure 2: CMM Coordinate Frame, Measuring Volume, and Moving Axes

Additional components typical to most CMM configurations include axis scales, a numeric controller, a computer interface with programming software, and some form of software correction used to compensate estimated systematic errors.

## 1.2 Measurement Uncertainty and Task Specific Uncertainty

A measurement is the comparison of an object of unknown dimension to a reference value. As the VIM [6], International Vocabulary of Metrology, defines it, more generally, it is a, “process of experimentally obtaining one or more quantity values that can reasonably be attributed to a quantity.”

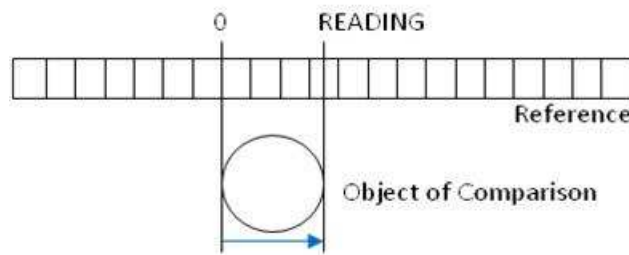
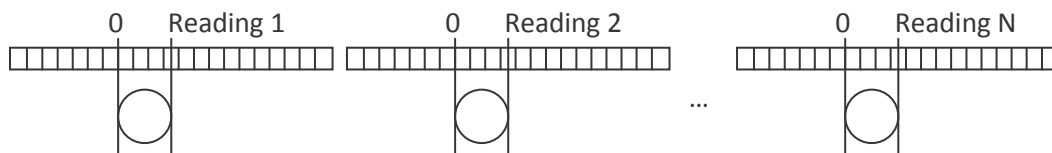


Figure 3: Basis of Measurement

Any comparison is, however, imperfect, as information is lost in the observation. [5][7] That is, with repeated comparisons of identical object and reference, on a scale with high enough resolution, different measurement values will result. Therefore, many values can be attributed to the reference comparison and any measurement is inexact.



Reading 1  $\neq$  Reading 2  $\neq$  Reading N

Figure 4: Repeated Comparisons Will Yield Varied Readings

Measurement Uncertainty describes the confidence in a comparison used to establish a measurement, since any one reading is only one possible value of the measurement. It is a statistical evaluation that quantifies the range of values for measurement.

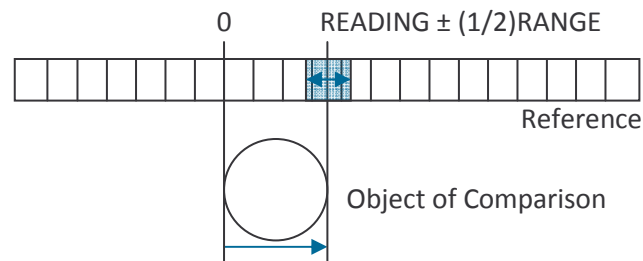


Figure 5: Uncertainty Describes a Range of Possible Measurement Observations

International and national standards organizations have attempted to define uncertainty and unify the way in which it is quantified. Currently, the VIM[6] formally defines measurement uncertainty as a, “non-negative parameter characterizing the dispersion of the quantity values being attributed to a measurand, based on the information used.” The intent is to apply probability mathematics to describe the range (or dispersion) of values that might be expected when making a measurement. This implies that a coverage interval be used to quantify the range. This may be, for example, a standard deviation. In order for any metrological process to be reliable (such as monitoring a process control or ensuring interchangeability of manufactured components for assembly) and to ensure reliability of global comparisons of measured quantities, measurement uncertainty must be ascertained.

In determining this range of values, or measurement uncertainty, attributed to a measurement, the sources of the variation and their magnitudes have to be determined

[8][9][10]. In practice, most CMM applications are indirect comparisons to a universal reference. A universal reference is established, for example, by an international agreement, defining the standard to some physical constant which is known exactly. The universal reference is used to make a ‘chain’ of reference comparisons, ensuring the same reference is ultimately used by and made available to all. In this process, every comparison, establishing a new ‘sub’-reference, contributes to the uncertainty of the previous comparison. In this way, any reference used to establish the uncertainty of any CMM is ‘traceable’ to the universal reference. The VIM[6] definition of Traceability is the “...property of a measurement result whereby the result can be related to a reference through a documented unbroken chain of calibrations, each contributing to the measurement uncertainty.” Through this method, the actual error of the measurement is constrained.

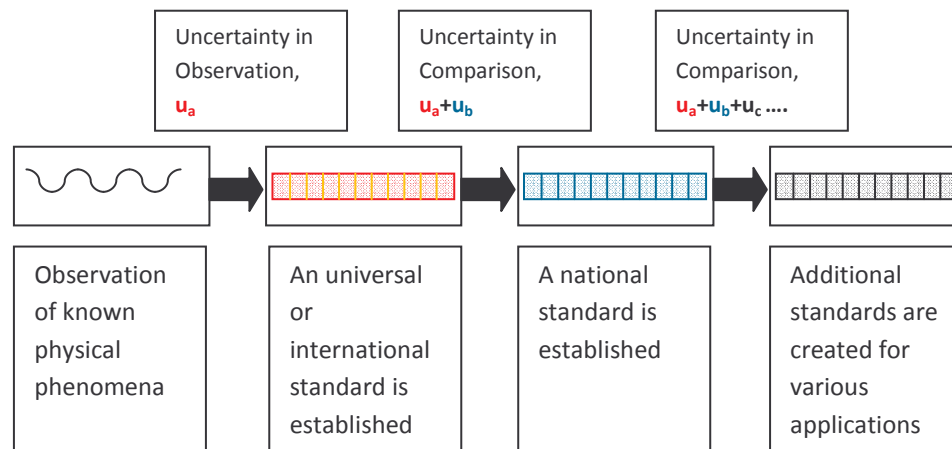


Figure 6: Cumulative Uncertainties in the Chain of Standards, From Creation of an International Standard to the End User



Since CMMs were created to measure essentially any surface within its three dimensional volume, the types of measurement tasks are numerous. Even for similar geometries, the scale, orientation in which it is measured, and probing strategy used may differ. The uncertainty associated with any particular ‘task’ will therefore, vary, though they are measured with the same device. [5] describes measurement uncertainty as, “The collection of (all possible) measurement errors...” and [11] defines task specific uncertainty as, “...the measurement uncertainty that results...when a specific feature is measured with a specific inspection plan.” Each task will have a set of quantities that influence the measurement and it’s range of possible values. These are called input quantities and can be defined as distributions of values, in keeping with the concept of traceability. [11] summarizes the sources of uncertainty, as related to task specific uncertainty, into five main categories: hardware, workpiece, sampling strategy, fitting and evaluation algorithms, and extrinsic factors.

The calculation of a measurement uncertainty for any one task can be thought of as a combination of these effects. The GUM[8], Guide to the Expression of Uncertainty in Measurement, defines the calculation for ‘combined’ uncertainty and defines the model for the measurement, including input quantities, as  $y(x_i) = f(x_1, x_2, \dots, x_n)$ . Each input quantity will have a standard uncertainty (defined as a standard deviation of its range),  $u(x_i)$ . The equation for combined uncertainty is stated as,

with,  $y(x_i) = f(x_1, x_2, \dots, x_n)$

$$u_c^2(y) = \sum_{i=1}^N \left( \frac{\partial f}{\partial x_i} \right)^2 u^2(x_i) + 2 \sum_{i=1}^{N-1} \sum_{j=i+1}^N \left( \frac{\partial f}{\partial x_i} \right) \left( \frac{\partial f}{\partial x_j} \right) u(x_i, x_j)$$

Equation 1: Combined Uncertainty [8]

The partial derivatives are called sensitivity coefficients. They can be thought of as linear approximations of the effects that changes in the input quantity will have on the measurement result [7]. The first summation term can be thought of as a linear combination of the standard uncertainties, where the double summation terms includes the covariances of the inputs and account for correlated input quantities.

Analysis of task specific uncertainty in this way is called sensitivity analysis and can be a difficult or an impossible procedure [4][11][12]. Task specific uncertainty is therefore an important issue in order to maintain traceability and made all the more complex to determine. There are alternate methods of determining task specific uncertainties, two of them, by thorough measurement of a calibrated artifact and by simulation of measurements, are discussed in the following section.

### 1.3 Determining Task Specific Uncertainties

There are alternate methods to sensitivity analysis for determining task-specific measurement uncertainties. The basic concepts of the calibrated artifact method (substitution method) and the Monte-Carlo simulation method are discussed here and results of both are presented in this dissertation.

In order to maintain an ‘unbroken chain of comparisons’ to a reference, an accepted method of determining task specific measurement uncertainty is to measure an artifact which is ‘close’ to the part measurand to be evaluated in nearly identical conditions. This should be repeated a statistically acceptable number of times until a distribution of results can be realized that describes the uncertainty associated with the measurand, machine, and conditions [13]. This method, also known as the substitution method, may be thought of as an analog to the sensitivity analysis method and is

compliant with the GUM. In measuring the artifact, all sources of uncertainty are included in the value range that results and are directly accounted for. The resulting uncertainty value is then valid for future measurements of the measurand as long as the conditions during the artifact evaluation remain consistent. In practice, this means an acceptable uncertainty for the artifact used and a range of conditions affecting the variation in measurement must be determined (typically in accordance with a measurement standard). [13] outlines the procedures for this method.

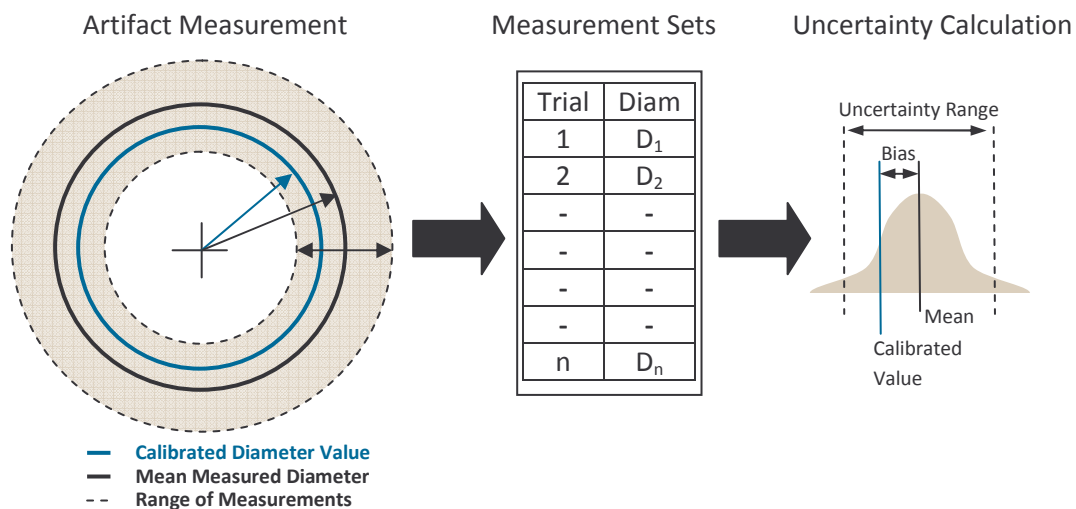


Figure 7: Task Specific Uncertainty Estimation from Calibrated Artifact Measurement

Another method of determining task-specific measurement uncertainty is by Monte-Carlo simulation. Theoretically, if a sufficient mathematical model of the CMM motions applied in measuring a point in space is used and terms that describe the errors in motion can be propagated to accurately describe the effects on the measurement point, then a simulation of real CMM behavior can be applied. In general, the errors that influence a measurement point are not known exactly. The errors are determined in practice, in terms of an uncertainty value, that is a distribution of possible errors. By

applying a Monte-Carlo method to selecting individual errors from the error uncertainties (distributions), the theoretical model of the CMM can then be used computationally to determine virtual measurement points used to determine virtual measurement tasks. The distribution of the virtual measurement results is in turn used to calculate a task specific measurement uncertainty, much in the way that the calibrated artifact method does.

Both methods are used to determine uncertainties in order to evaluate two commercial versions of the virtual simulation method (VCMM and PUNDIT). The ‘artifact’ method is used determine reference uncertainties for a particular set of mesaurands and is compared to the results of the ‘virtual’ methods. Some examples of previous testing in this area and on validation techniques are in [14][15][16][17].

#### 1.4 Purpose for Simulating Measurement

In order to reduce costs and make more practical the determination of task specific uncertainties, simulating the propagation of errors with computational methods could theoretically allow uncertainty terms to be ‘virtually’ determined. In effect, the versatility of the CMM, which is its greatest advantage, would be more manageable in terms of complying with standard traceability.

Compliance of the software itself to standards and the practicality of using the software is an important issue, though. The idea of Monte-Carlo style simulations has been around for some time in the application of determining measurement uncertainties. For CMMs, the idea of replacing statistical observations for every possible scenario is appealing economically and in making traceability for CMM measurements possible for a wider range of users. However, it must be ascertained whether a software package is capable of handling the complexities of such a task and whether the ultimate goal of

traceability is met, both in implementation commercially and in the definition of the standards.

### 1.5 Structure of this Document

This dissertation will first describe the concepts of the virtual methods investigated and show some of the differences and similarities of each. Next, the particular software packages, VCMM and PUNDIT are described in more detail, with a full description of their implementation. The experimental procedure is then described, including a description of the ‘real-life’ measurements for comparison as well as the inputs used for the software simulations. Results of the testing for several different measurands is shown as a comparison between the real-life measurement uncertainties and the simulated ones. Finally, a conclusion of the results is given, commenting on the performance of the software and future work that might be suggested. The objective is to ascertain whether a commercially available method of determining simulated uncertainties is valid, in the sense that it performs under the limited conditions of the experiment.

## Chapter 2: VIRTUAL METHODS INVESTIGATED

The software packages evaluated are virtual methods because they model the behavior of a real CMM, in effect producing sets of measurement data they way a physical CMM would. In this way, uncertainties are produced from the virtual measurement data sets that can be evaluated, statistically, for uncertainty, as real measurement data would be. Monte-Carlo type simulations have been addressed by the GUM[8] and their use is outlined in [18]

### 2.1 How Simulation Methods Work

All machines will have errors, an inexact functioning relative to the intent of the design, which requires an uncertainty assigned to their output. For a measuring system with three orthogonal axes with linear motions, such as a typical CMM, there are 21 errors in positioning, assuming a rigid body model. Each carriage axis may be characterized as having 6 degrees of freedom. There are 3 possible translational errors and 3 possible rotational errors per axis. There are also 3 possible alignment or squareness errors between the axes.[19][5]

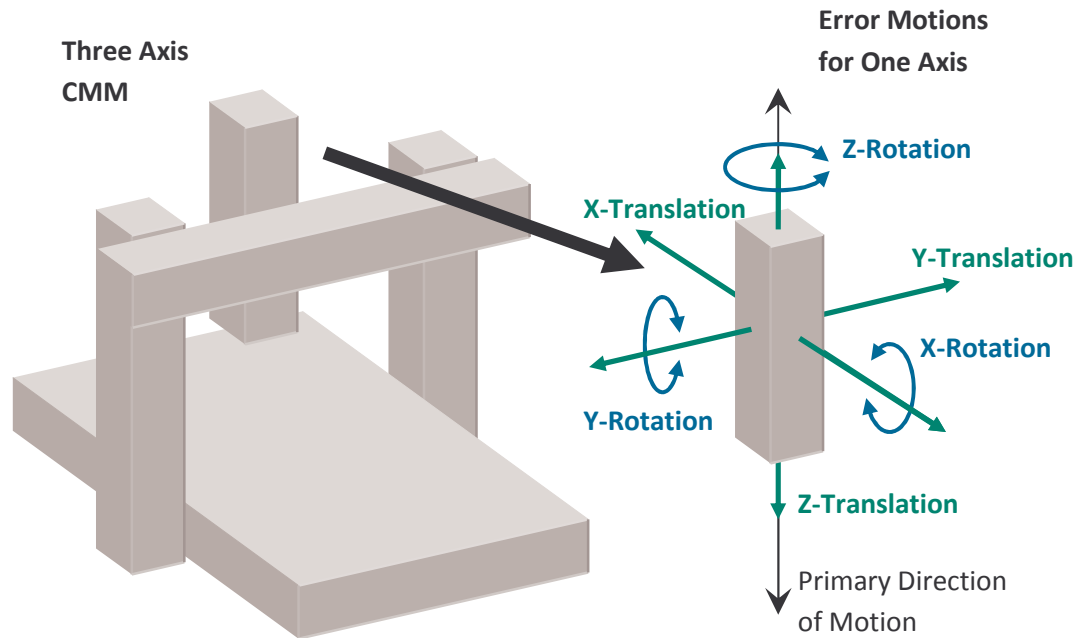


Figure 8: 6-DOF Error Motion per Axis; 3-Translational and 3-Rotational Errors

There are many sources or input quantities that may contribute to these geometric errors. Primary among these are thermal effects, vibrational effects, loading effects, etc. The probing system, which may be modeled kinematically as a length extension of the axis it is attached to, has additional errors related to the dynamics of its contact detection mechanism. There are also extrinsic effects, not directly related to the machine's functionality, such as thermal effects and form error of the part, operator error, and software fitting algorithm errors that affect the measurement reading.

A simulation, may incorporate the kinematic model of a particular machine geometry and superimpose systematic and random errors to simulate positional errors for any given measurement point.

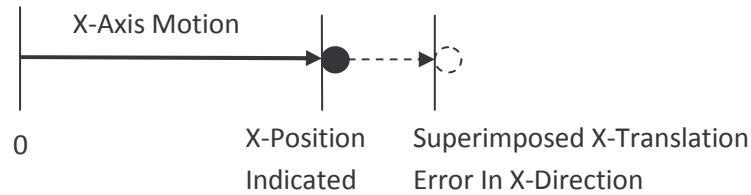


Figure 9: One Dimension Example, Systematic Error Superimposed On Indicated Position

The errors which affect the position indication of the CMM will in general be known within a possible range of values, having systematic and random components. The error state of the machine for any particular instance is therefore not known to an exact value in three dimensions [5][11]. The effect on position of the CMM at a particular location is a bounded region that is a culmination of all error ranges. The Monte-Carlo simulation in principal accounts for all estimated error ranges and determines a range of possible outcomes, based on their contribution. In a simplified example, say the model of a process outcome,  $Y$ , is  $Y = A + B + C$ , where  $A$ ,  $B$ , and  $C$  are input quantities, each a distribution of values with a range defined by a standard deviation. Each cycle of the Monte-Carlo simulation would use a randomly selected input value,  $A_i$ ,  $B_i$ ,  $C_i$  within the defined standard deviation range of each (standard deviation is a  $\pm$  value) and propagate these through the model for  $Y$  and yield a value  $Y_i$ . Repeating this cycle many times will yield a distribution of values,  $Y_{sim}$ . The distribution shape for  $Y_{sim}$  will depend on the shape of the input quantities' distributions. If  $A$ ,  $B$ , and  $C$  were distributed normally, then the outcome of the simulation,  $Y_{sim}$ , would also have a normal distribution.



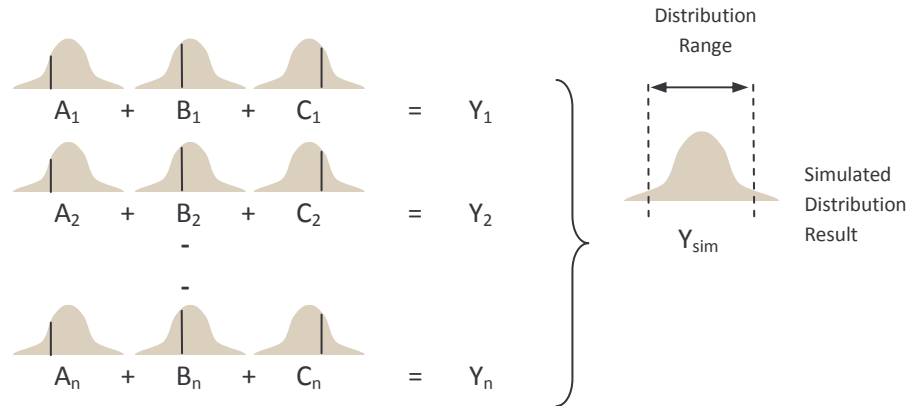


Figure 10: Simplified Example of Monte-Carlo Simulation Concept

The example above is an illustration of the concept of applying Monte-Carlo methods to CMM measurement simulations. When determining measurement uncertainties for CMM tasks, a similar model is applied, though the determination of input quantities is more complex. However, the combination of these effects, all having probability distributions, is simplified by the random selection mechanism of this type of simulation. In theory, the results of the simulation would give realistic outcomes (measurement points) without having to determine analytical values for the input quantities effects as with the sensitivity analysis method.

## 2.2 Simulation Methods Tested

Two simulation software packages were tested, VCMM and PUNDIT, one using the virtual CMM method, and one using a method called simulation by constraints, respectively. Both use a kinematic model of the CMM's behavior to determine how errors are propagated and produce distributions of measurement points, but differ primarily in the handling of input error distributions.

The Virtual CMM (VCMM) method, developed by PTB, is an application of parametric and other source error distributions to a kinematic model of the machine

positioning. Errors are determined in individual scenarios by the Monte-Carlo method from defined distributions, and propagated to simulate positioning and probing inaccuracies of nominal measurement points. Sets of these measurement points, used to calculate measurement features are produced as a result. In this way, an error distribution for the measurand is developed, and interpreted as an uncertainty. This method requires each parametric error to be determined with systematic and random components. The systematic 'state' of the machine is determined by an artifact measurement procedure and input to the kinematic model. The random errors define ranges for the Monte-Carlo error selection. The simulated model for the machine accounts for the particulars of the design, as well as the conditions that have an effect on machine positioning, such as thermal influences. Essentially, the VCMM concept is to create a model representing the parametric state (complete description of all 21 errors) of the CMM. This state is varied within the ranges determined by the influence quantities input to the simulation. The measurement states are considered 'virtual' measurements of a single machine. The result should produce hypothetical measurement sets of sufficient range and distribution that would be produced by the machine being modeled.

The simulation by constraints method, developed by NIST, and used by PUNDIT, is similar to the VCMM method in that it approximates error sources and propagates them through a kinematic model as parametric errors. As the name implies, certain functional errors can be considered to be constrained within bounds that for practical reasons are easier to approximate and verify than a full parametric set of errors.[12][2] By this method, the Monte-Carlo scheme is used to randomly select error states, in effect creating a set of virtual machines. This is the primary difference in the simulation by

constraints method and VCMM. The parametric states are not necessarily a representation of the particular CMM being evaluated. The performance evaluation values, for example the Maximum Permissible Error (MPE) [20], do not represent a complete parametric state, but are used to constrain the possible values a parametric state may have.[2]

Each state that can perform within the given performance criteria is considered valid and is added to a set of virtual machines and are used to create virtual measurement points. Uncertainties are then calculated from the measurement results distribution created by a number of the virtual machines.

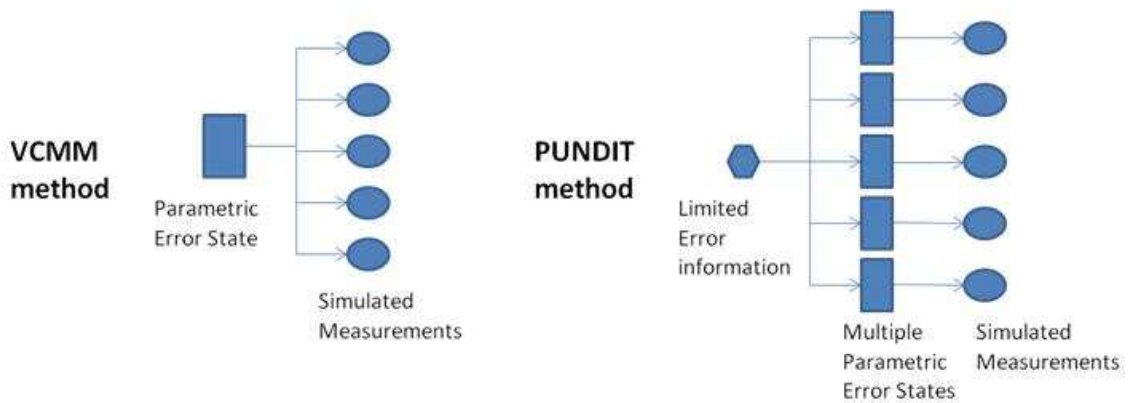


Figure 11: Comparison of VCMM and Simulation by Constraints Concepts

### 2.3 Purpose for Testing Particular Simulation Methods

There are two questions for evaluating the software simulation methods, does the software execute the functionality as designed and does the theory behind the design hold true. The software, from a standpoint of coding, is assumed to work as it should for this study, i.e. functionality is as stated by the manufacturer. This evaluation is of application, the results are used to examine the implications of software use, to make suggestions for practical use, and to suggest possible improvements if observed. The

particular software packages, VCMM and PUNDIT, are evaluated to offer a comparison of two particular methods of simulation, each potentially having different applications and uses. VCMM requires testing procedures to determine all parametric errors of the machine and requires interaction with the programming software for the CMM. The SBC method, which is implemented by PUNDIT requires much less information about the state of the machine and is an offline application. The methods may produce different results that may be more or less reliable in comparison, but the evaluation of these methods also relies on the implementation efficacy. The following chapter more closely describes the details of using the software and how simulation parameters are treated.

## Chapter 3: VCMM AND PUNDIT SOFTWARE PACKAGES

Two software simulation packages are evaluated in this dissertation, VCMM and PUNDIT. Each is a Monte-Carlo type simulation that use random selections of variables representing estimated error sources and propagates them through a kinematic model representing a coordinate measuring machine(s). Both could be considered so called virtual CMM simulations [11][2], but they differ primarily in the error estimates that would bound the parametric state of the CMM. VCMM relies on a full parametric error state while PUNDIT utilizes abbreviated performance indicators, a technique called simulation by constraints. Additionally, VCMM would be considered an online application, it is integrated with the CMM software and simulates nominal data from an actual measurement, while PUNDIT, is a separate interface. This chapter describes in more detail the functioning and utilization of the programs.

### 3.1 VCMM

The VCMM package, includes the VCMM component imbedded in the CMM programming software and two interface modules, KALKOM and VCMMTOOL. KALKOM is used to analyze and prepare parametric error estimates describing the machine. The VCMMTOOL module allows additional inputs, such as thermal conditions, additional machine parameters, and workpiece surface parameters and prepares a database describing all error sources to be used by VCMM. VCMM can be called in the CMM programming software to evaluate the uncertainty of a measured

feature. It accesses the database prepared with VCMMTOOL and models a virtual machine that varies, as determined by the range of the various error sources, with each cycle of the simulation. It is a Monte-Carlo style simulation that establishes, through parametric modeling of machine errors and other input quantities, task specific measurement uncertainty.

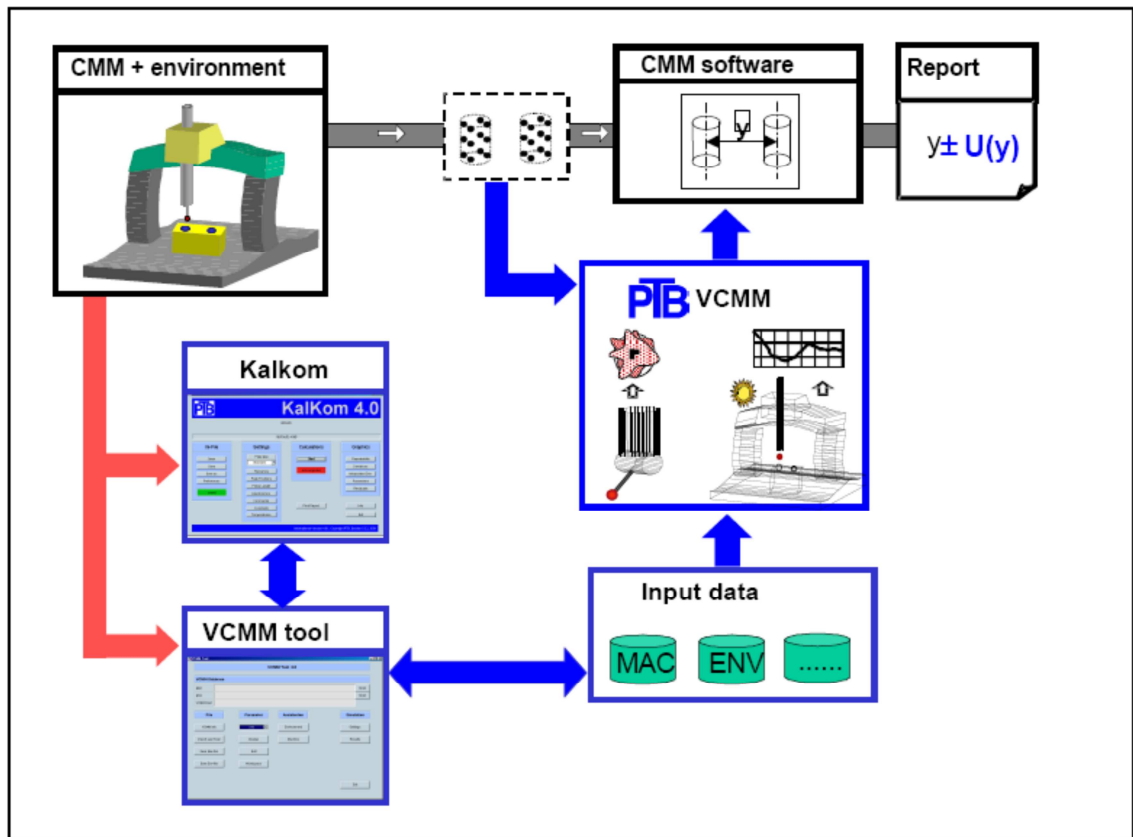


Figure 12: Schematic of VCMM and Component Interaction with the CMM and CMM Software, from VCMM Manual [21]

The VCMM simulation requires that the parametric errors for the CMM be determined by a specific procedure. A calibrated hole or ball plate, with a prescribed measurement strategy and routine, is measured and the resulting ball/hole coordinates are input to the KALKOM module. Based on deviations from the artifact measurement, the

plate orientations, and a fitting algorithm, the parametric errors for the CMM are calculated.

, Figure 15, and Figure 16 show screenshots of the KALKOM interface. The KALKOM output, a partial example is shown in , is a list of each parametric error, discretized to a user specified interval for the numerically error calculation algorithm. For example, the translation error for the X-axis in the X-direction would be represented as a list of coordinate values along the x-axis, say every 20 mm, and the corresponding deviation in micrometers caused by the translation error. Determining errors between the specified interval points is done through linear interpolation of the nearest values. This method of representing the errors is similar to a software correction file used by the CMM operating system when the CMM is calibrated. This allows the VCMM and the operating system software to utilize the error file to superimpose systematic errors determined by KALKOM.

As mentioned, the procedure for determining parametric errors utilizes a ball or hole plate artifact. The artifact is a flat plate with holes or spheres located in a grid pattern at calibrated locations relative to a plate coordinate system. Measurement of the plate is carried out, nominally in the center of the CMM table, in orientations parallel to the major axes of the machine. The sphere or hole locations are measured in a progressive pattern at positions around the perimeter of the plate in two runs, one in reverse of the first pattern. The plate, being in the center of the table, is measured on the front and back sides. The probe stylus for this procedure is oriented normally to the plate, and the lengths are specified to cover, as much as possible, the extents of the axes.

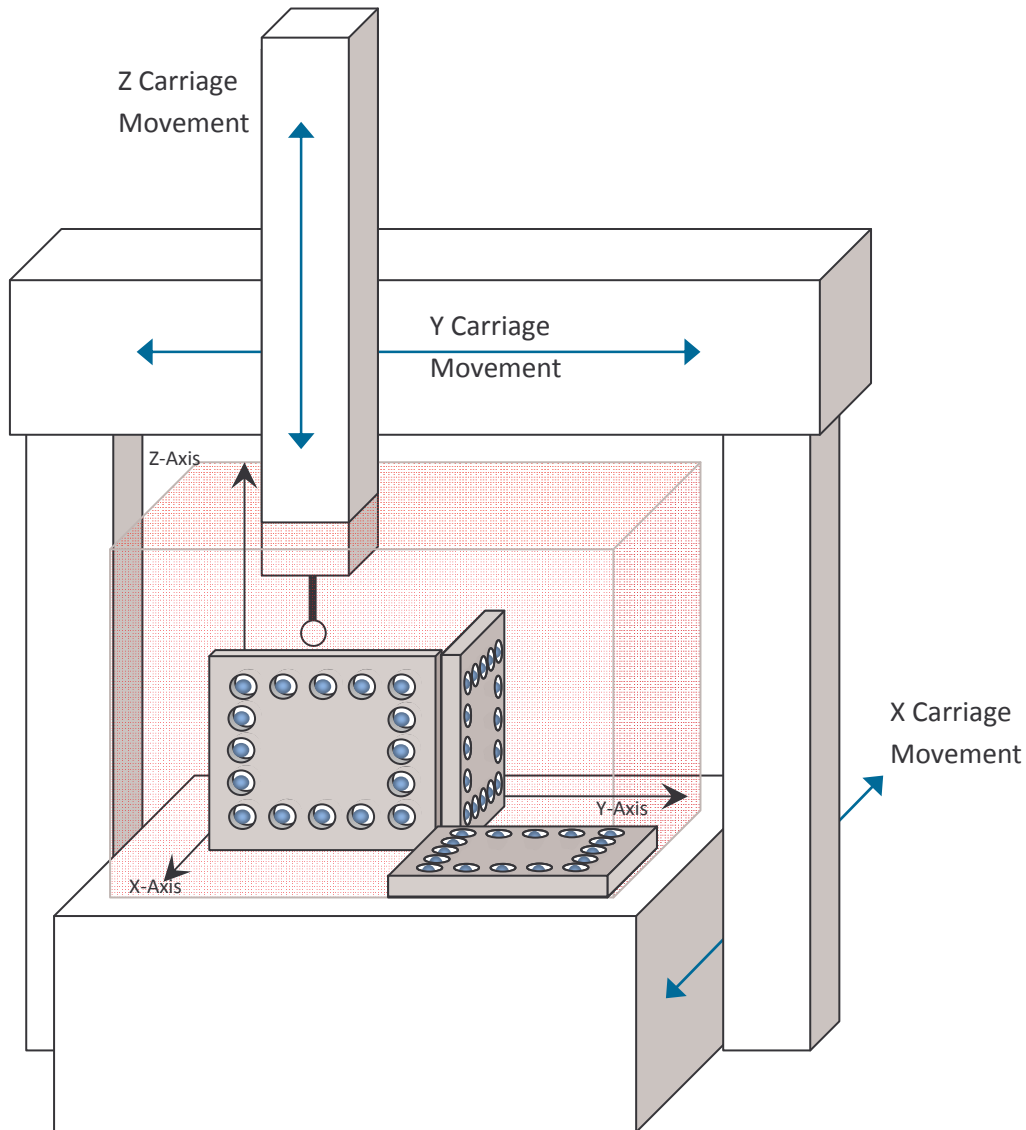


Figure 13: Examples of Calibrated Ball Plate Positions Used for Measuring Parametric Errors

The values for the hole or sphere positions is recorded for each plate orientation and position, and along with the calibrated values, is input to KALKOM by specifying the file location of the plate measurement results. The input of parameters about the plate measurement is done through the KALKOM interface, and examples are shown in Figure



15, Figure 16, and Figure 17. The calibrated plate artifact will in some cases not cover the entire dimension of the machine axis it is being used to evaluate. In those cases, the plate is measured multiple times in overlapping positions, within the same plane. The nominal coordinate values for the plate positions must be specified. Additional parameters that are input are the grid spacing of the spheres or holes for the calibrated plate used, probe lengths and orientations, the axis dimensions, and fitting parameters for the algorithm KALKOM uses to determine the parametric errors, such as the interval spacing the errors will be calculated to and the errorbars to control the smoothness of the fitted error curves.[22]

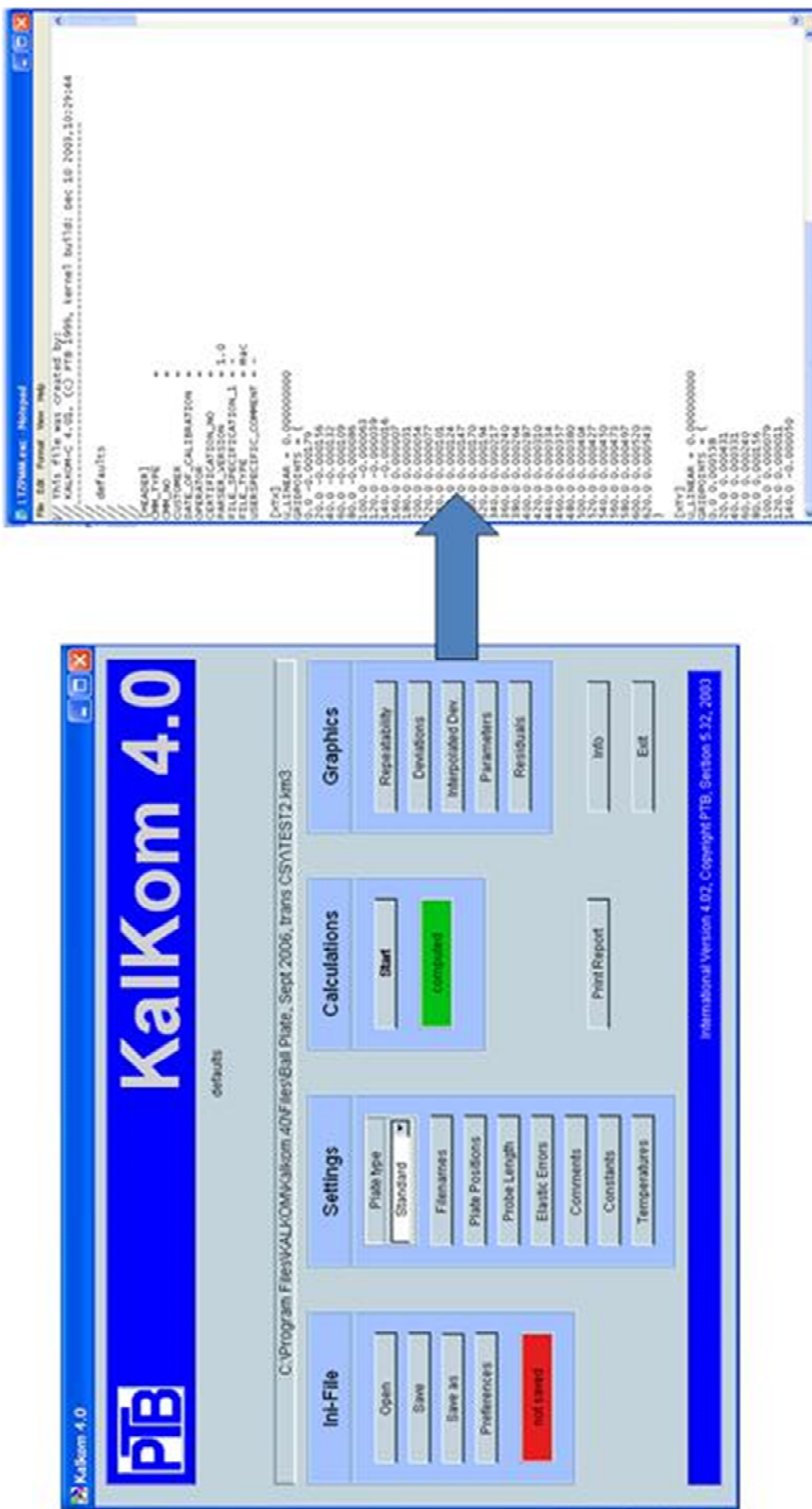
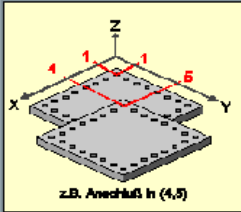


Figure 14: Kalkom Interface with Example of Parametric Data Output

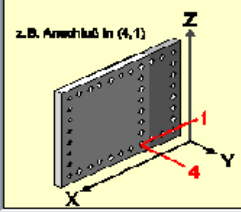
Plate Positions

	X	Y	Z
<b>Position 111 (mm):</b>	60	50.00	100.00
<b>Position 112 (mm):</b>	60.00	50.00	0.00
<input checked="" type="checkbox"/> 21\$	5	1	
<input checked="" type="checkbox"/> 31\$	1	4	
<input checked="" type="checkbox"/> 41\$	5	4	
<input type="checkbox"/> 51\$	0	0	



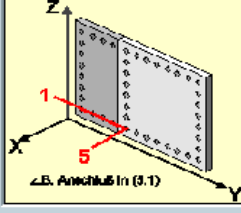
z.B. Anschluss in (4,5)

<b>Position 121 (mm):</b>	60.00	290.00	17.00
<b>Position 122 (mm):</b>	60.00	210.00	17.00
<input checked="" type="checkbox"/> 22\$	5		1
<input type="checkbox"/> 32\$	1		3
<input type="checkbox"/> 42\$	5		3
<input type="checkbox"/> 52\$	0		0



z.B. Anschluss in (4,1)

<b>Position 131 (mm):</b>	200.00	50.00	17.00
<b>Position 132 (mm):</b>	400.00	50.00	17.00
<input checked="" type="checkbox"/> 23\$		4	1
<input type="checkbox"/> 33\$		0	0
<input type="checkbox"/> 43\$		0	0
<input type="checkbox"/> 53\$		0	0



z.B. Anschluss in (3,1)

OK

Cancel

Figure 15: Calibrated Ball/Hole Plate Parameters Example Input, KalKom

Constants			
Spacing of Grid (mm)	<input type="text" value="60"/>		
Bar offset for L-Plates	X	Y	Z
	<input type="text" value="0.00"/>	<input type="text" value="0.00"/>	<input type="text" value="0.00"/>
Errorbars Position +/- ( $\mu\text{m}$ )	<input type="text" value="0"/>		
Errorbars Straightness +/- ( $\mu\text{m}$ )	<input type="text" value="0"/>		
Errorbars Rotation +/- ( $\mu\text{rad}$ )	<input type="text" value="0"/>		
Measuring volume:	X	Y	Z
Start	<input type="text" value="0.00"/>	<input type="text" value="0.00"/>	<input type="text" value="0.00"/>
End	<input type="text" value="600.00"/>	<input type="text" value="500.00"/>	<input type="text" value="400.00"/>
Set first error value to zero for each function	<input type="checkbox"/> On		
Spacing Position [mm]	<input type="text" value="20"/>		
Spacing Straightness [mm]	<input type="text" value="20"/>		
Spacing Rotation [mm]	<input type="text" value="20"/>		
Temperature-Correction by Kalkom	<input type="checkbox"/> On		
2D-Analysis (no vertical positions)	<input type="checkbox"/> On		

Figure 16: Additional Example Plate Parameters, KalKom

The screenshot shows the 'Probe Lengths' dialog box with the following inputs:

Position \$11 (mm):	-140
Position \$12 (mm):	-140
Position \$21 (mm):	-140
Position \$22 (mm):	140
Position \$31 (mm):	-140
Position \$32 (mm):	140
Shift of reference point in Z (mm):	-10

The dialog also features three 3D diagrams illustrating probe configurations and 'OK' and 'Cancel' buttons.

Figure 17: Probe Stylus Inputs for KALKOM

The KALKOM interface also has a graphical output representing various evaluations of the individual plate measurements. In Figure 18 an example of the deviations from calibrated values for one plate measurement and in Figure 19 a repeatability for a single plate measurement is shown (each plate measurements consists of a forward and return sequence, the deviation between each run is shown). The deviations from calibrated values for each plate measurement are used to determine the parametric errors. The errors that are determined depend on the probe and plate orientation during measurement and the deviations of the sphere or hole positions relative to the calibrated values. The interval spacing for each error is user specified and are used to interpolate the error curve fit. Figure 20 and Figure 21 show examples of the calculated error curve for a particular parametric error, with and without errorbars. The effect is to smooth the curve with increased errorbar value. With errorbars set to zero, the

error curve is fit through the center of calculated error value, from the interpolated error values. The calculated parametric errors are used to determine simulated deviations for the respective plate measurements and are compared, shown in Figure 22, to the actual deviations measured.[22]

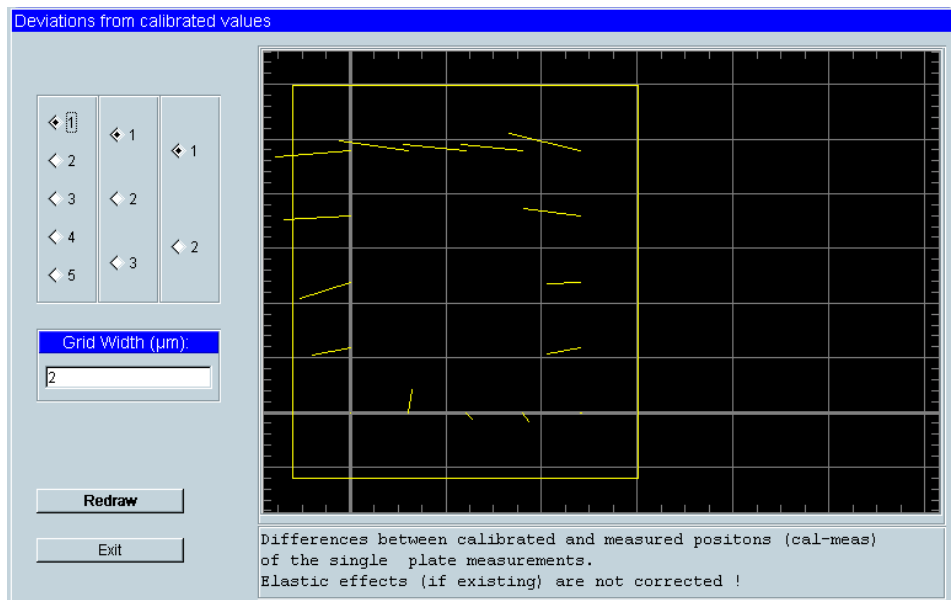


Figure 18: Example of Plate Deviations Determined by KalKom

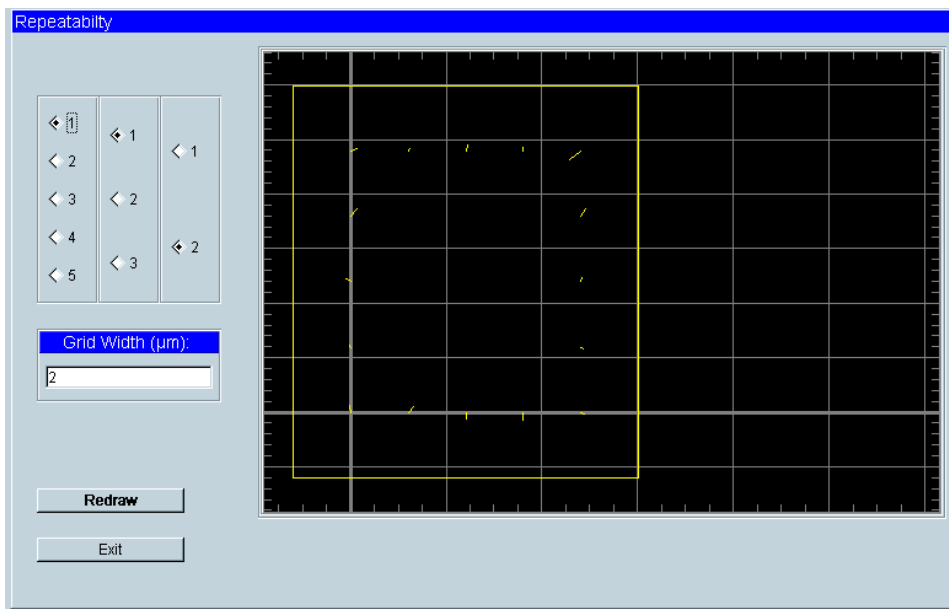


Figure 19: Example of Repeatability of a Plate Measurement, KalKom

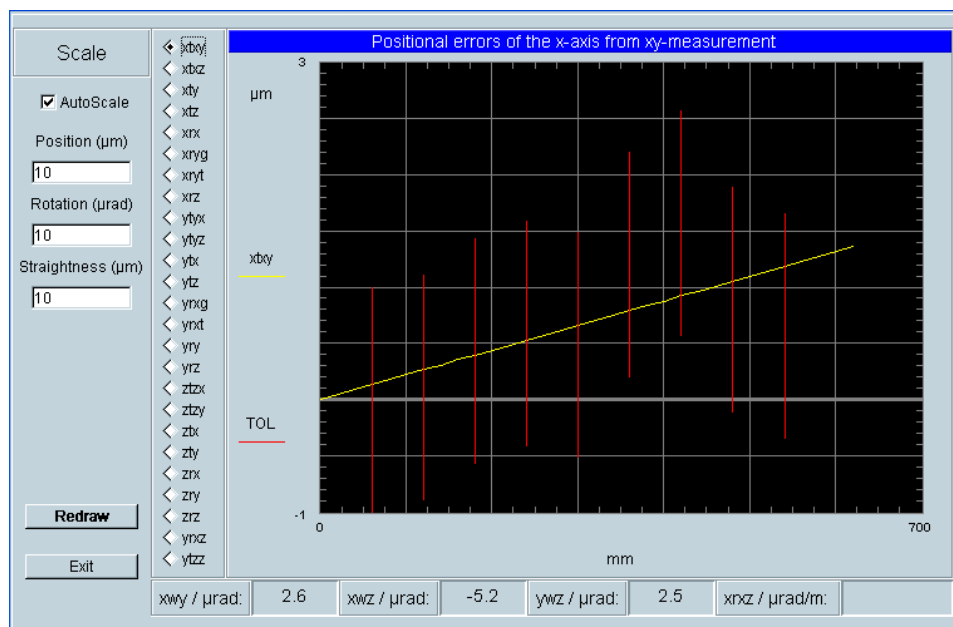


Figure 20: Example of a Parametric Error Fit, With Error Bars, Determined From Plate Measurement, KalKom

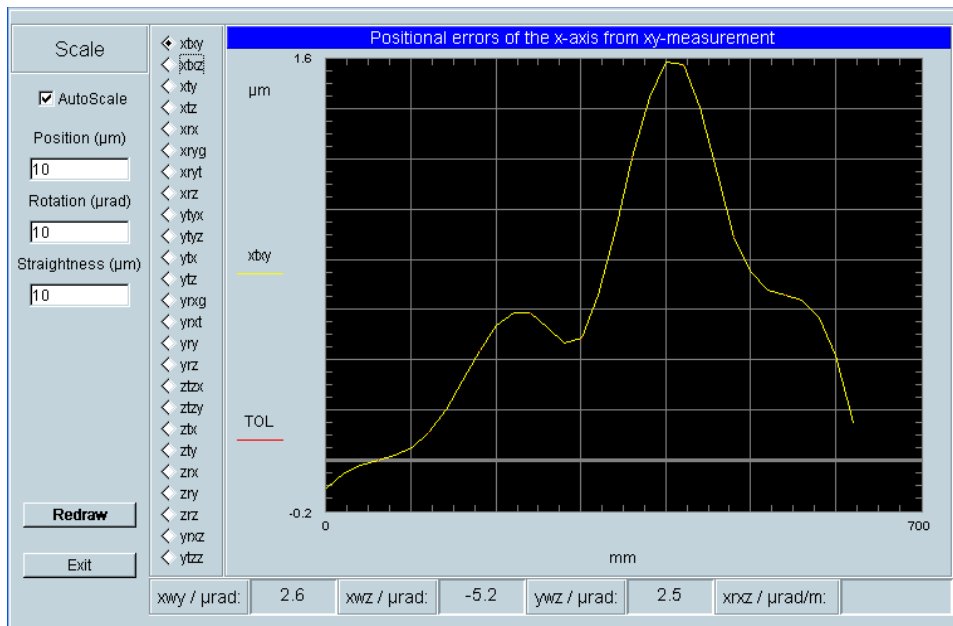


Figure 21: Example of a Parametric Error Fit, Without Error Bars, Determined From Plate Measurement, KalkKom

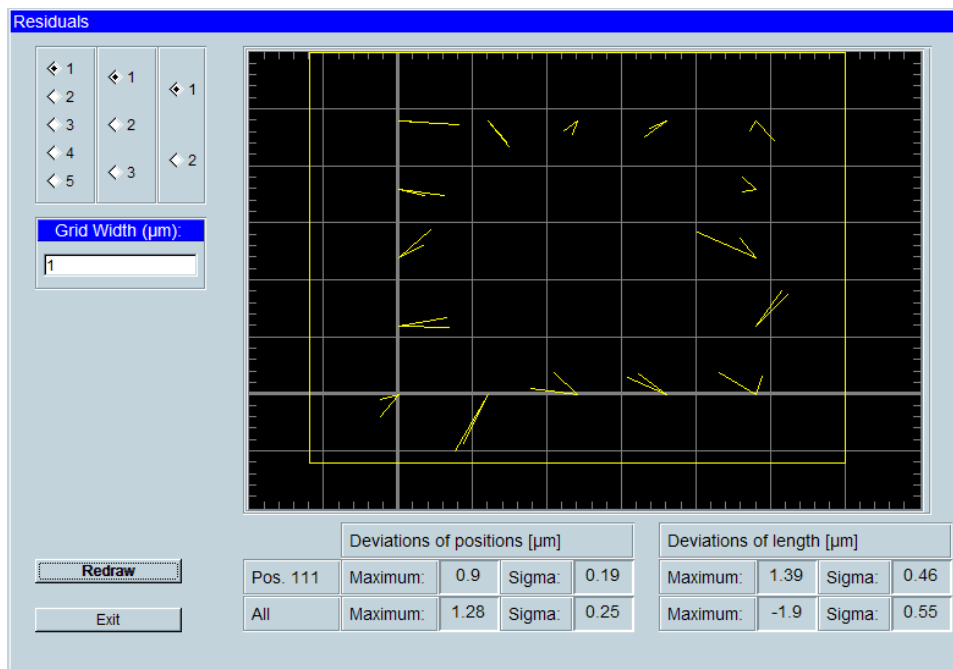


Figure 22: Example of Simulated Deviations for the Calculated Parametric Errors vs. the Actual Deviations Measured



Through VCMMTool a database file containing information about environmental conditions, the kinematic arrangement of the machine axes, certain machine component dimensions, part form errors, and repeatability information are combined with the systematic parametric data. The file can then be accessed by VCMM through the CMM operating software. The primary interface is shown in with an example of the database structure used to pass the simulation parameters to the VCMM software. Figure 24 through Figure 26 show the environmental conditions interface and various parameters that can be used. Values pertaining to the calibrated artifact used in determining the systematic errors (determined in KALKOM) are entered in the machine interface, Figure 27. VCMMTool also has the capability of providing simulations and graphical outputs to show the effects the superposition of the added values and uncertainties of the added error sources will have. Each of the parametric error curves with these added effects can be displayed individually, examples are shown in Figure 28 and Figure 29. Figure 30 shows an example simulation of the ISO 10360 MPE reverification test using the determined systematic and random error effects modeled. These simulations can be used to evaluate the inputs the user has provided.

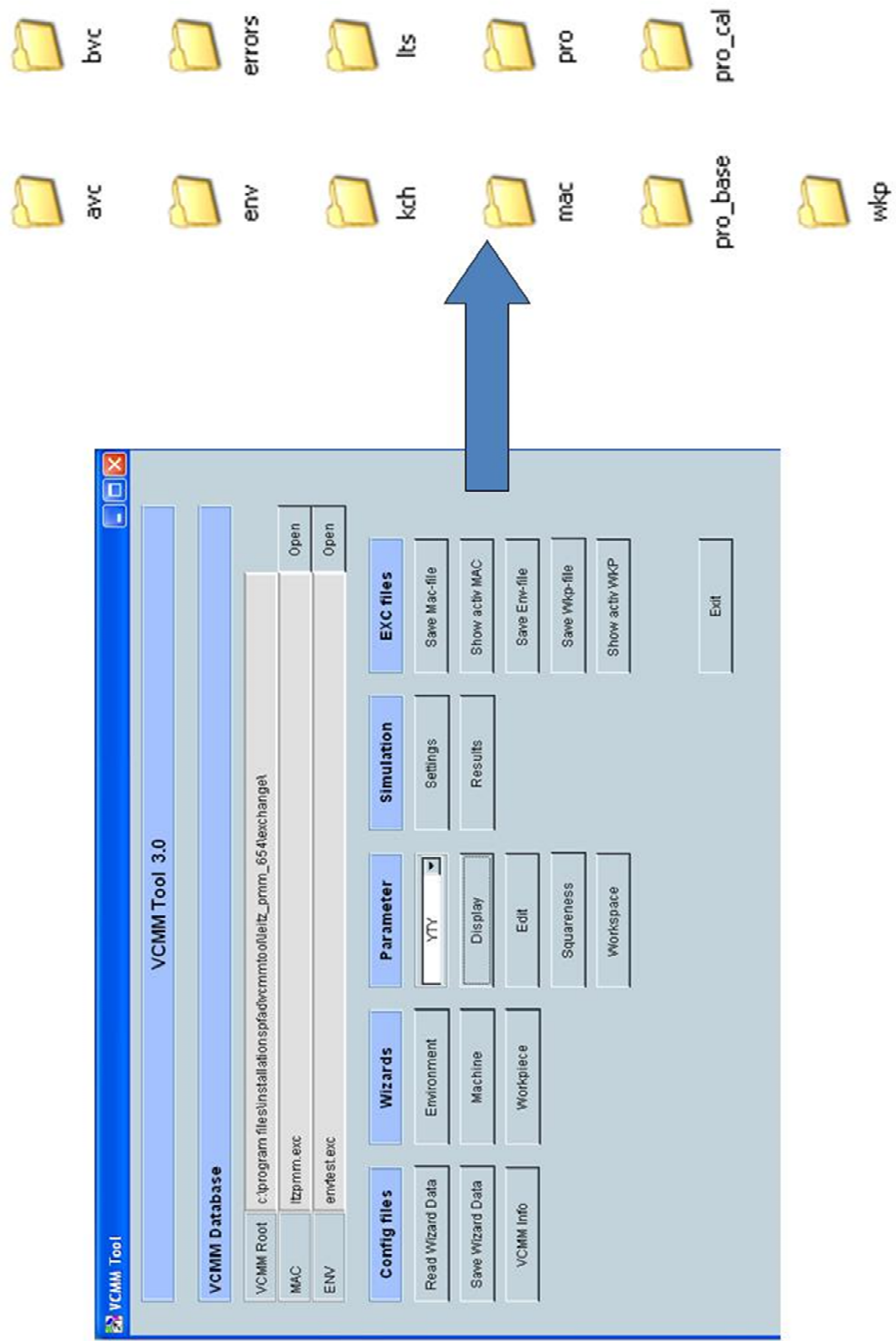


Figure 23: VCMMTool Interface and Database Output

VCMM Wizard: Environment

### Environment parameters (CMM related)

Length of axis:			Expansion coefficient of axis:			
X	600	mm	X	8.5	$\mu\text{m}/(\text{m}^*\text{K})$	
Y	500.0	mm	Y	8.5	$\mu\text{m}/(\text{m}^*\text{K})$	
Z	400.0	mm	Z	8.5	$\mu\text{m}/(\text{m}^*\text{K})$	
Expansion coefficient of scales:			Uncertainties:			Temperature correction:
X	8.3	$\mu\text{m}/(\text{m}^*\text{K})$	X	0.8	$\mu\text{m}/(\text{m}^*\text{K})$	<input type="checkbox"/>
Y	8.3	$\mu\text{m}/(\text{m}^*\text{K})$	Y	0.8	$\mu\text{m}/(\text{m}^*\text{K})$	
Z	8.3	$\mu\text{m}/(\text{m}^*\text{K})$	Z	0.8	$\mu\text{m}/(\text{m}^*\text{K})$	
Height of column:			Distance between columns:			Expansion coefficient of columns:
	1176.6	mm		939.8	mm	
Length of X-slideway:			Thickness of X-slideway:			Width of X-slideway:
	647.7	mm		228.6	mm	
						590.5 mm

Figure 24: Example of VCMMTool inputs for Environmental Parameters, screen 1

VCMM Wizard: Environment

**Environment parameters (CMM related)**

Changes of temperature gradients:			Variation of scale temperatures:			Uncertainty of scale temperatures:		
X	<input type="text" value="0.168799"/>	K/m	X	<input type="text" value="0.1"/>	K	X	<input type="text" value="0.1"/>	K
Y	<input type="text" value="0.1"/>	K/m	Y	<input type="text" value="0.2"/>	K	Y	<input type="text" value="0.1"/>	K
Z	<input type="text" value="0.1"/>	K/m	Z	<input type="text" value="0.2"/>	K	Z	<input type="text" value="0.1"/>	K
Difference of gradients at columns:			Drift of reference point:			Average speed:		
	<input type="text" value="0.2"/>	K/m		<input type="text" value="0.3"/>	μm/h		<input type="text" value="80.0"/>	mm/s

< Back      **Next >**      Cancel

Figure 25: Example of VCMMTool inputs for Environmental Parameters, screen 2

VCMM Wizard: Workpiece

### Environment parameters (Workpiece related)

Uncertainty of workpc. temperature:	Variation of workpc. temperature:	Temperature correction:
<input type="text" value="0.112717"/> K	<input type="text" value="0.1"/> K	<input type="checkbox"/>
Expansion coefficient of workpc.:	Uncertainty of expansion coefficient:	
<input type="text" value="11.8"/> $\mu\text{m}/(\text{m}^*\text{K})$	<input type="text" value="1.2"/> $\mu\text{m}/(\text{m}^*\text{K})$	

< Back   **Finish**   Cancel

Figure 26: Example of VCMMTool inputs for Environmental Parameters, screen 3

VCMM Wizard: Calibration procedure

### Calibration procedure

Calibration uncertainty of standard:

A   $\mu\text{m}$

K   $\mu\text{m/m}$

Gridspacing of standard:

mm

Uncertainty of error components:

Straightness (range)	<input type="text" value="1.0"/>	$\mu\text{m}$	XWY	<input type="text" value="2.0"/>	$\mu\text{rad}$	XRX (linear)	<input type="text" value="2.0"/>	$\mu\text{rad/m}$
Rotation (range)	<input type="text" value="1.0"/>	$\mu\text{rad}$	XWZ	<input type="text" value="2.0"/>	$\mu\text{rad}$	YRY (linear)	<input type="text" value="2.0"/>	$\mu\text{rad/m}$
Position (range)	<input type="text" value="1.0"/>	$\mu\text{m}$	YWZ	<input type="text" value="2.0"/>	$\mu\text{rad}$	ZRZ (linear)	<input type="text" value="2.0"/>	$\mu\text{rad/m}$

Figure 27: Example of VCMMTool inputs for Machine Calibration Parameters

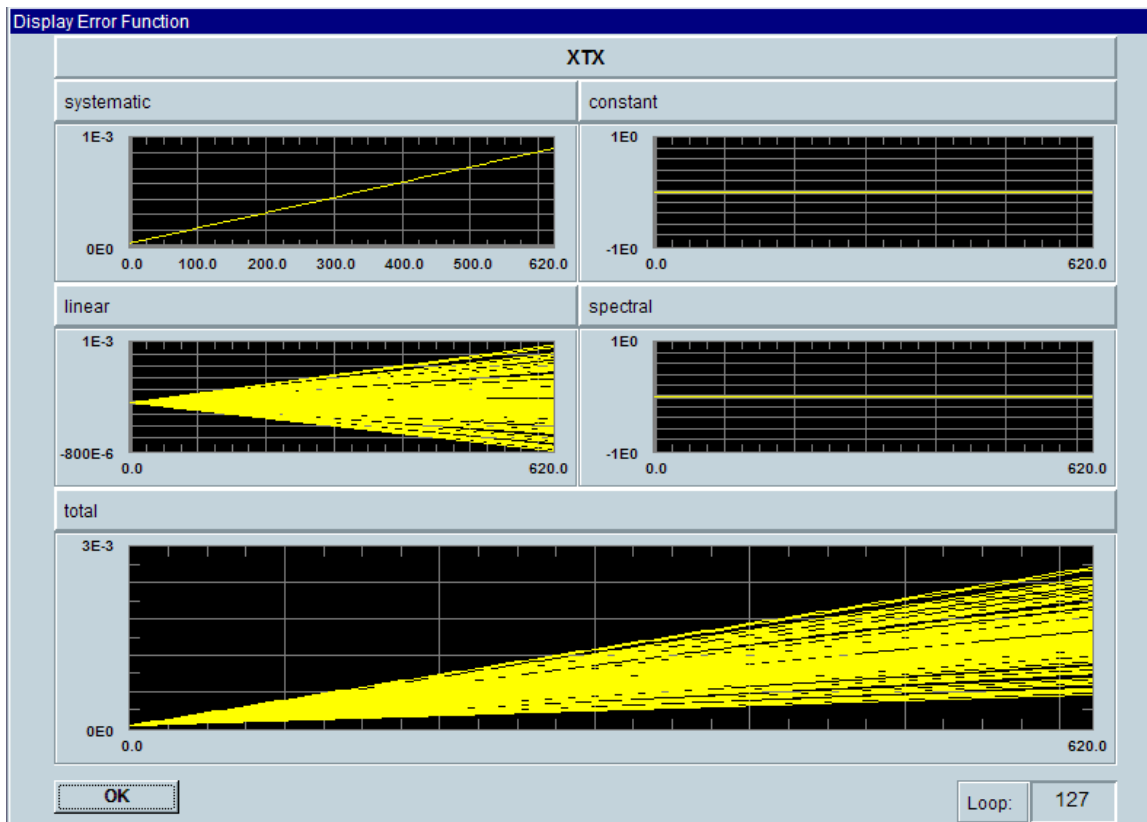


Figure 28: Example of VCMTool simulation for a Scale Error, XTX

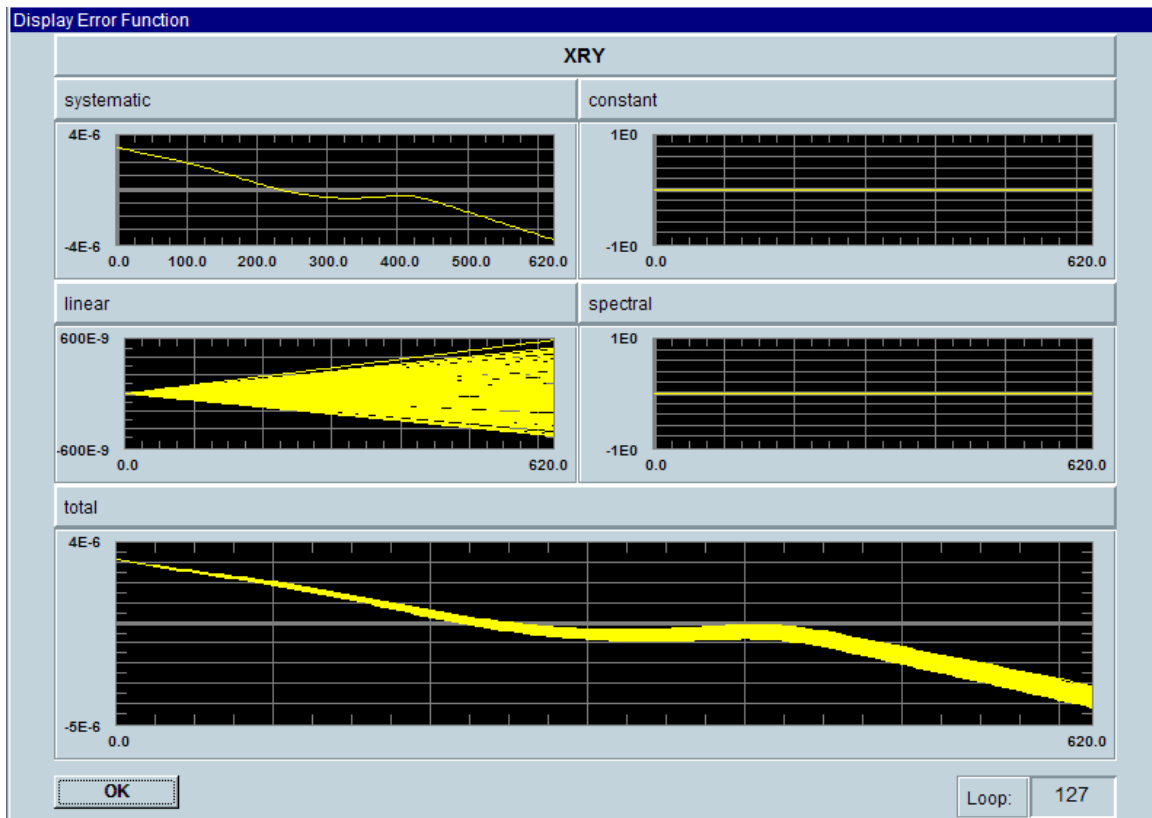


Figure 29: Example of VCMTool Simulation for a Rotational Error, XRY



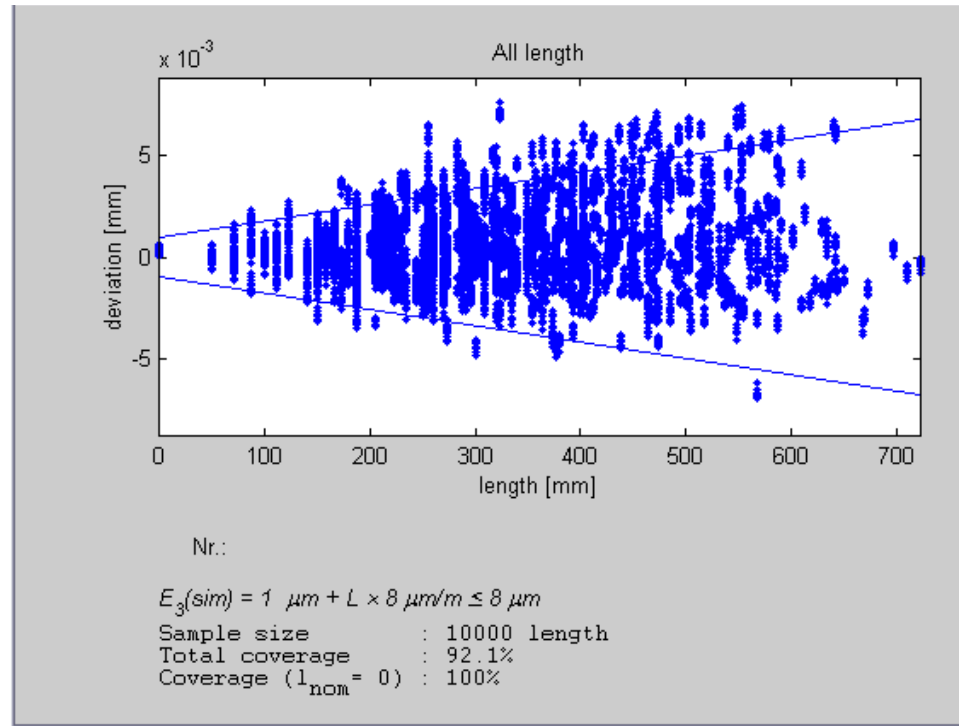


Figure 30: Example of VCMMTool Simulated 10360 CMM Performance Verification Test

VCMM is embedded in the operating software and uses nominal data from the measurement program file and the algorithms used to calculate the physically measured data to return sets of measurement points deviated, theoretically, as the actual measurement points might be. Every set of data essentially represents an individual measurement of a measurand. An uncertainty can then be calculated from the distribution of these values.

### 3.2 PUNDIT

PUNDIT differs from VCMM because it is an offline software and it uses the method of simulation by constraints, instead of a full evaluation of the parametric state. A full parametric option was available for PUNDIT but was not intended for commercial use at the time of testing. Results for this option are included as a comparison. The SBC

method allows an abbreviated representation of machine errors [2]. PUNDIT allows the use of CMM performance evaluations, in the form of MPE's (Maximum Permissible Errors) [20]. These evaluations are typical to CMM specifications and are indicators of the overall performance of the CMM, but are not indicative of the parametric state of the CMM. The errors are considered constrained, and define a state space from which parametric states may be selected. A simplified example, shown in Figure 31, would be to consider a one-dimensional measuring device with two primary geometric errors. If an MPE value were specified for the device, then the resulting state space would be bounded by the region highlighted in green. Parametric error states could be selected from only within this region to prevent the combined error from exceeding the MPE.

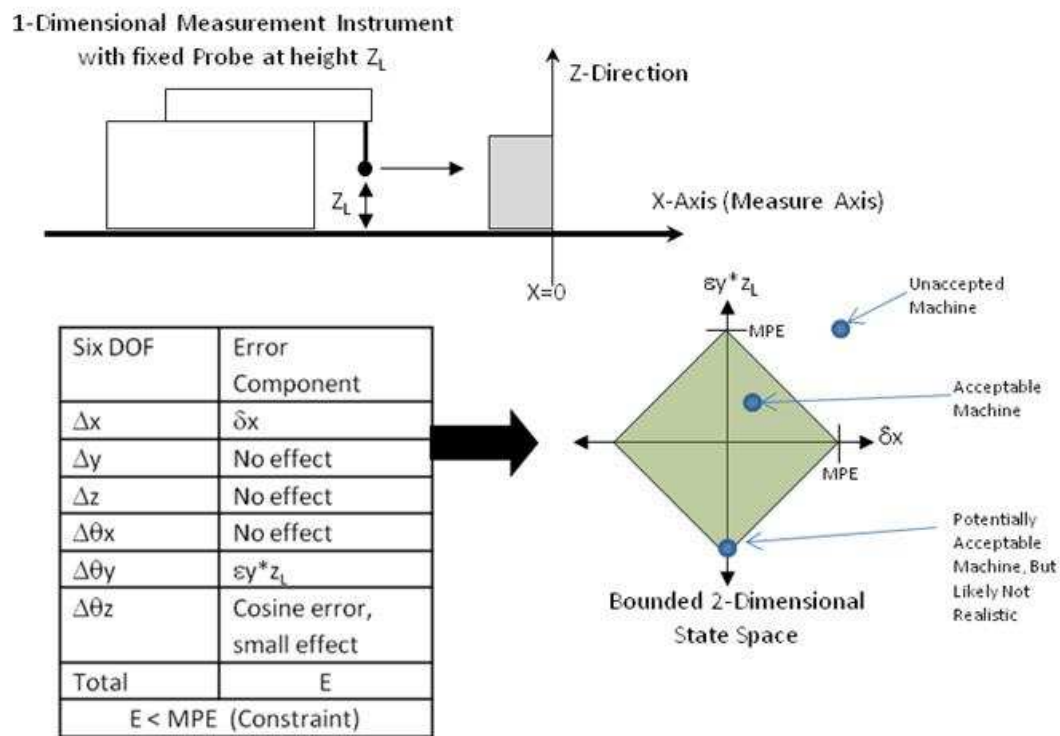


Figure 31: Simplified example of a 1-Dimensional Measuring Machine Illustrating the Simulation by Constraints Concept

It is important to indicate how this method is distinguished from the VCMM method. PUNDIT, like VCMM, produces sets of virtually measured data, but uses a Monte-Carlo method to select machine states (a randomly selected parametric state) that ‘perform’ within the input MPE values instead of varying the estimated parametric state of the machine being evaluated. In this way, a set of ‘machine’ states is created. Measurement points are then created from each machine state, yielding a distribution of measurement results. Other input quantities are also modeled and simulated, including, environmental, part form, and probing performance.

As mentioned, PUNDIT is an offline application. Examples of the user interface are shown in through Figure 38. The functionality of each is described in the PUNDIT manual [23]. There is a single window with tabs to select the various input modes and simulation results. shows the CAD interface and the tolerance definition tab. CAD models can be imported or created to represent the nominal, three-dimensional workpiece geometry of the part evaluated. The geometries being considered for measurement evaluation are defined for the simulation on the graphical model interface. Tolerance definitions can also be applied. shows an example of the CMM tab. Here the kinematic model is selected by type. For instance, a CMM with overhead bridge, vertical ram axis, and moving table. The axial directions and the extents of the measuring axes are also specified. The type of performance evaluation can also be defined on this tab. For instance, the simulation by constraints method with an ISO 10360-2 MPE value may be used. In , an example of a full parametric input is shown. Information concerning the probing system may be defined with the Probe tab shown in Figure 35. Probe configurations including fixed, articulated, and multiple tips may be defined as well as

orientations and lengths of the stylus used. Probing performance evaluation values of several types can also be defined here. The environmental conditions are selected through the Environmental tab, Figure 36, primarily, the workpiece and CMM temperature, temperature variation, the CTE values, and their uncertainties. The Manufacturing tab, Figure 37, allows surface form and roughness information to be added to the workpiece.

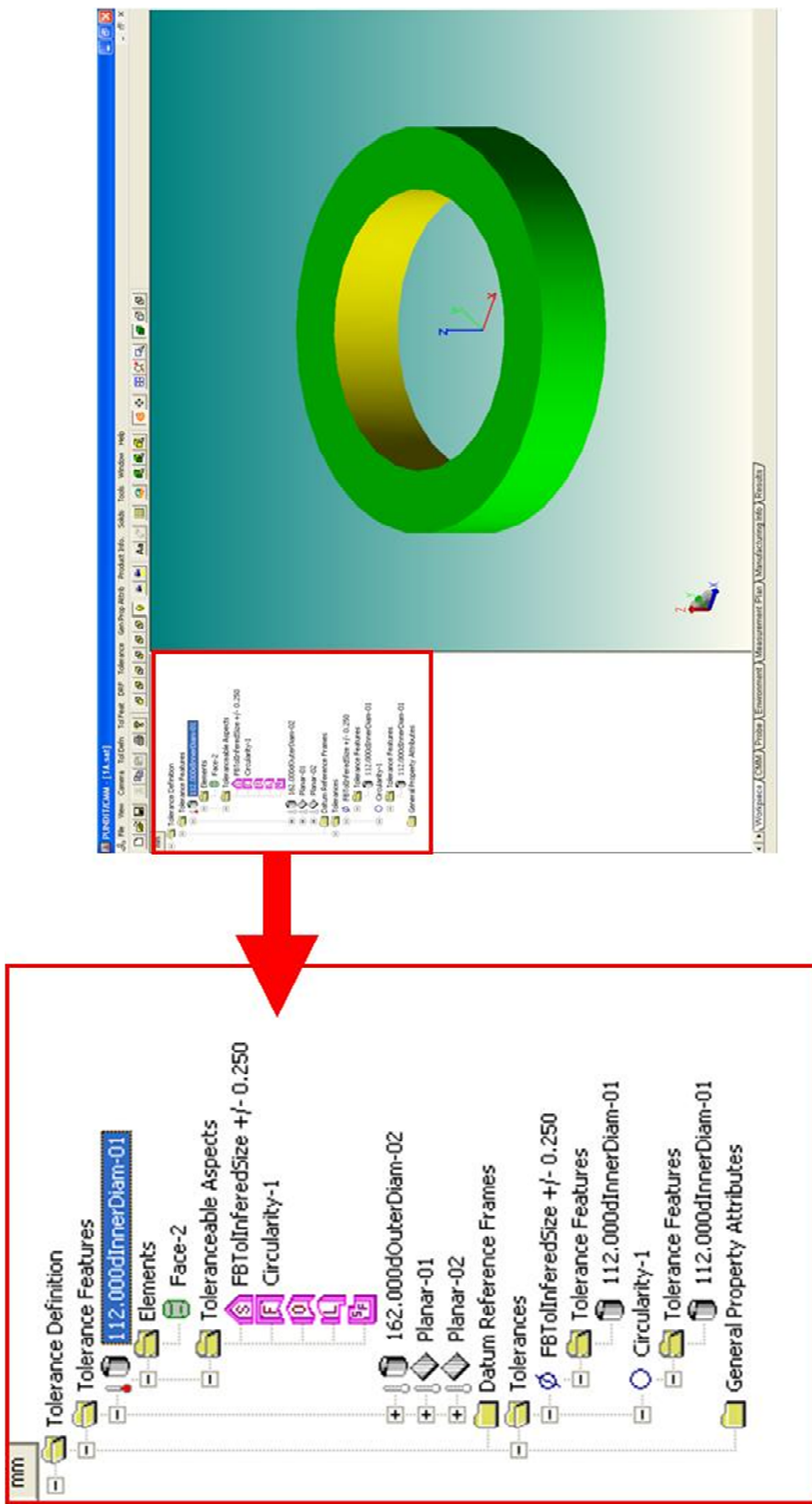


Figure 32: PUNDIT CAD Interface and Tolerance Definition, Workpiece Tab

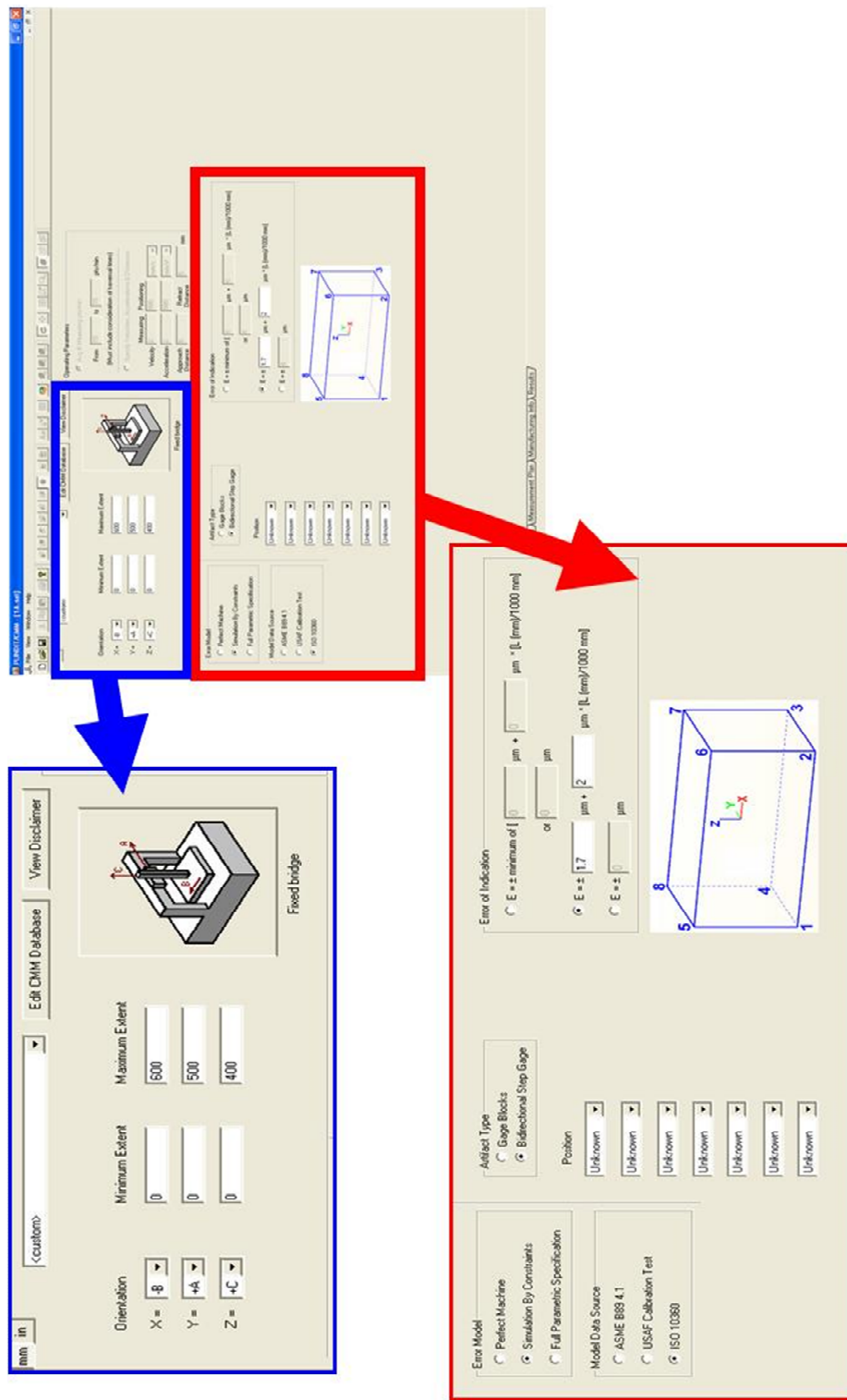


Figure 33: PUNDIT CMM Tab With Examples of CMM Model Selection and MPE Error Input

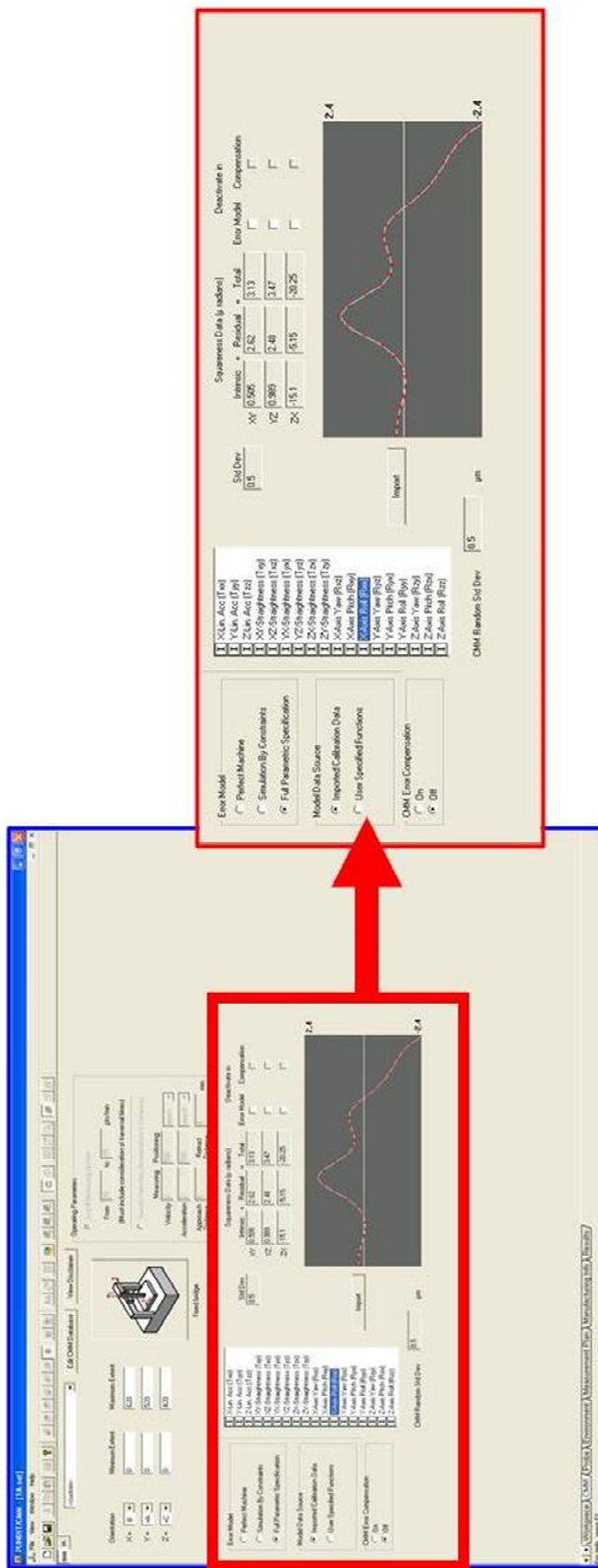


Figure 34: PUNDIT CMM Tab With Example of Parametric Error Input

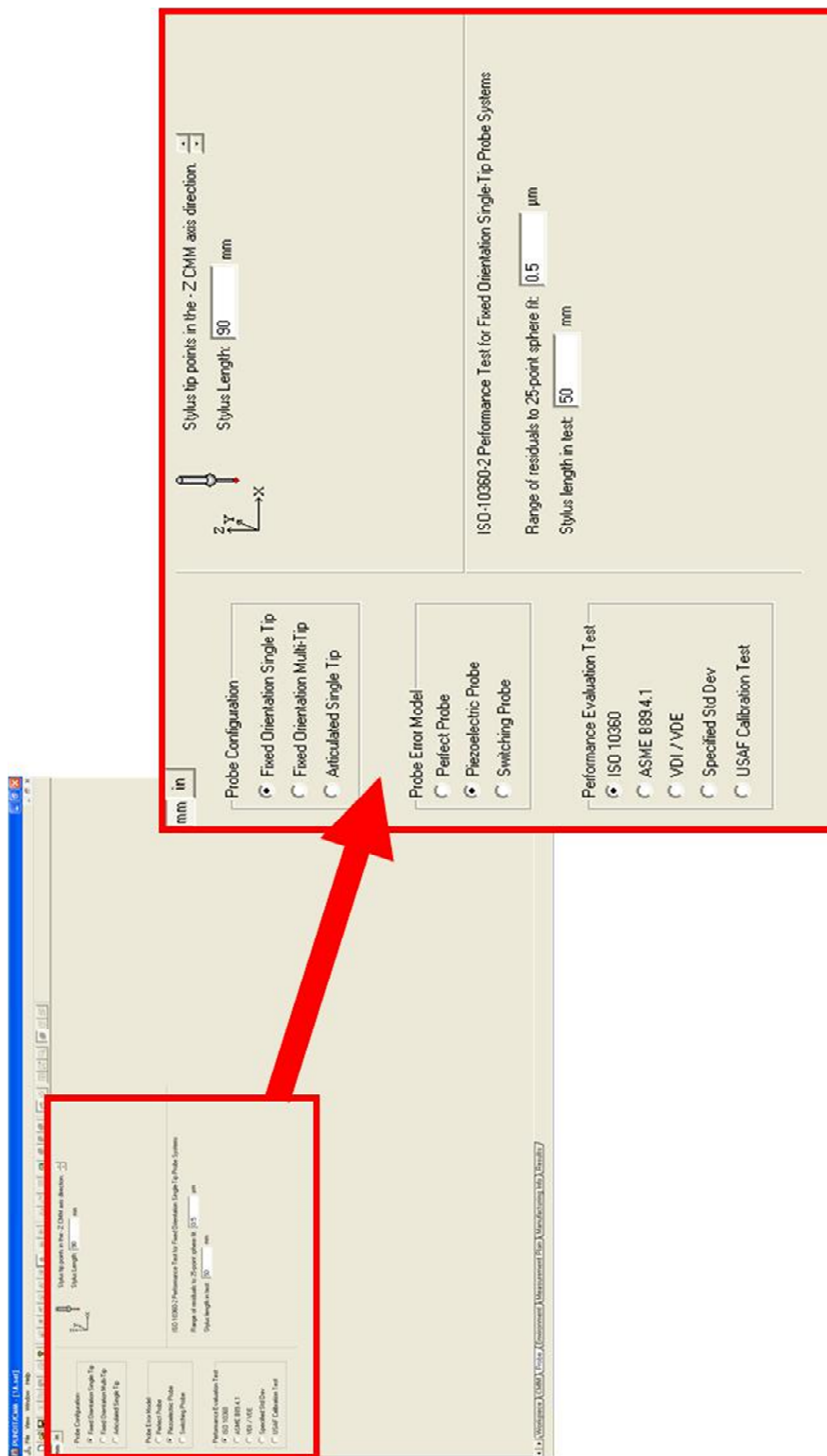


Figure 35: CMM Probe Tab With Example of Probe Type and Performance Input



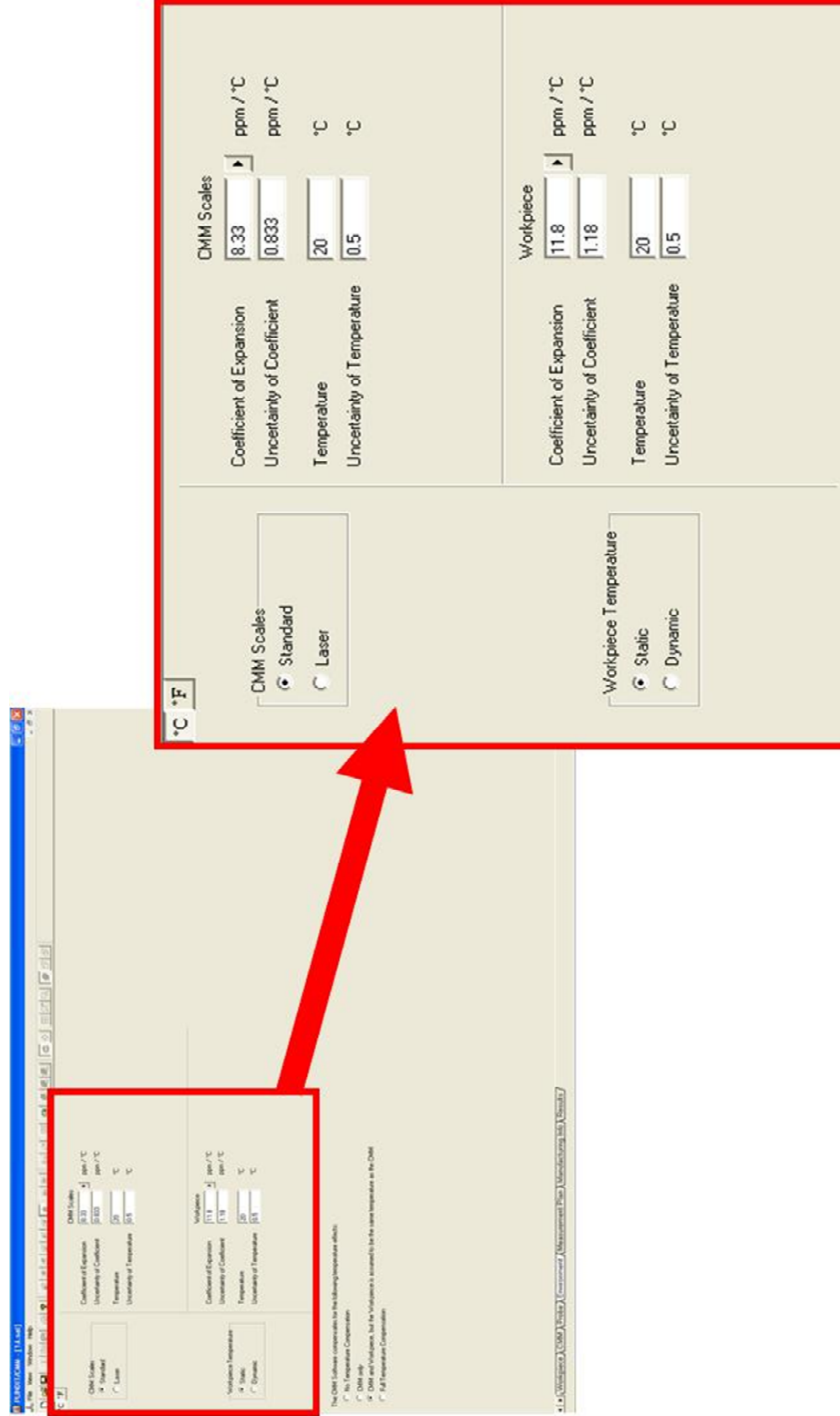


Figure 36: PUNDIT Environment Tab With Example Input for Workpiece and CMM

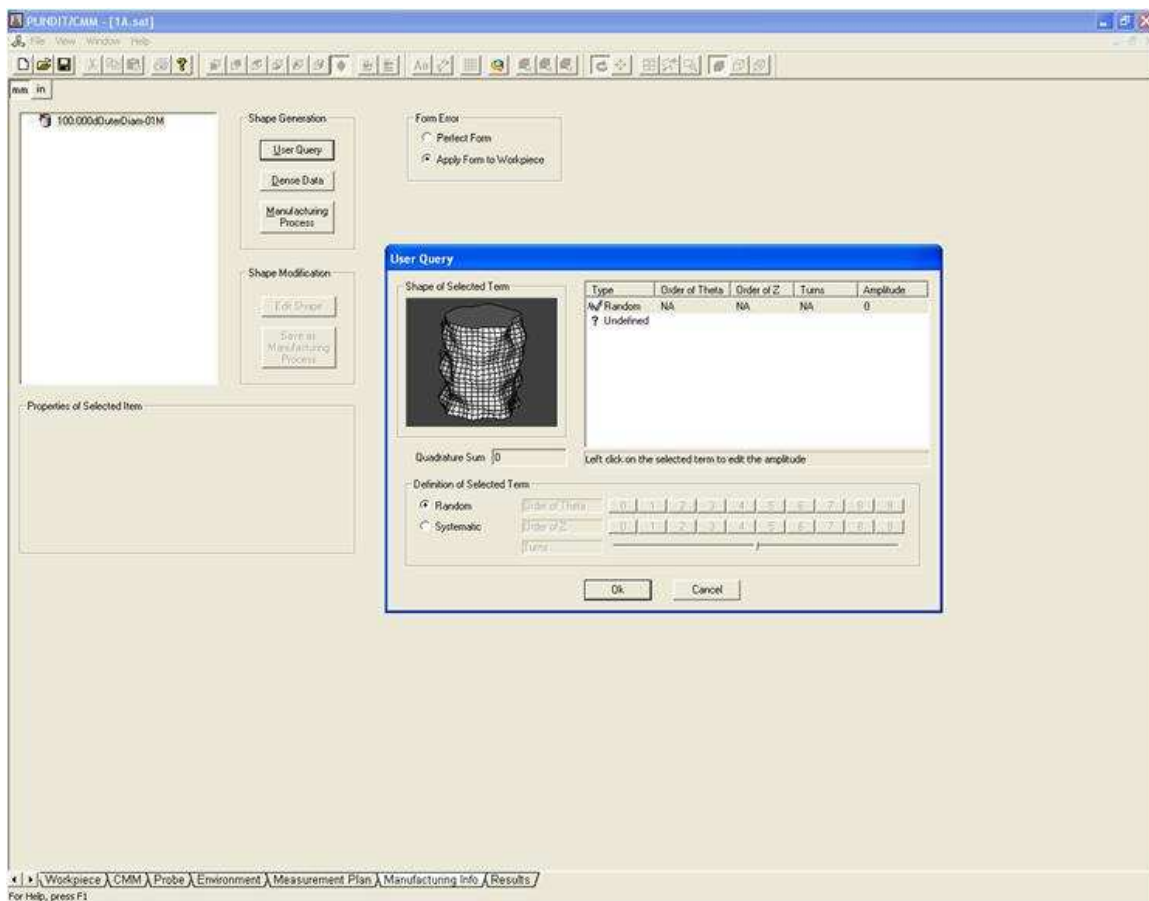


Figure 37: PUNDIT Manufacturing Info Tab

After all inputs are defined, the simulation is run in the Results tab. Figure 38 shows an example of the results of a typical simulation. The distribution of the results is shown graphically as a bar chart. The standard deviation and mean error are shown, and combined to form the uncertainty estimate.

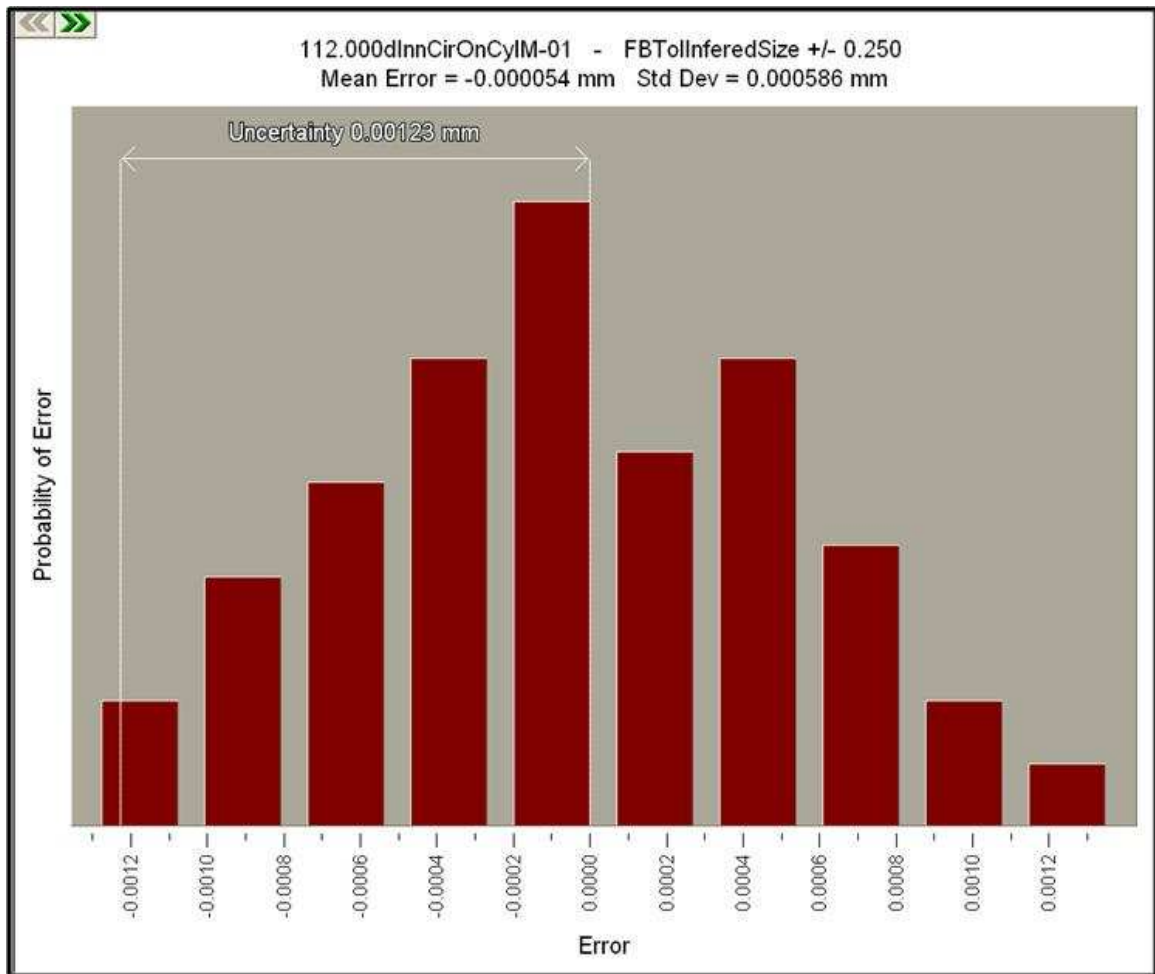


Figure 38: Example of PUNDIT Simulated Uncertainty Result

## Chapter 4: TESTING

In order to evaluate software models of task specific uncertainties, measurements of calibrated artifacts were performed using a Leitz 654 PMM (600mm X 500mm X 400mm, measuring volume). Repeated measurements were taken at different locations within the machine volume. Different artifact orientations were used in order to observe differing values that may arise as a result of varied machine behavior throughout the measuring volume. Uncertainties were calculated for each position and orientation combination. The results of the measurements were compared to software evaluations of the same measurement scenarios to the extent the software inputs allowed. Each software model uses particular inputs to develop an estimation of the measurement uncertainty. In general, the inputs include part geometry, part location, environmental conditions, measurement strategy, part form errors, probing performance, and elements of the machine geometry errors.

The quality of these input values will have a strong influence on the reliability of the software results, and the user must also decide whether the values should attempt to capture the CMM and its environment at a particular point in time or if the inputs should be representative values for a longer time scale. For the experimental comparisons discussed in this paper, the input values should be related to the conditions that exist during the measurements.

#### 4.1 Experimental Procedure for Tests of Simulation Methods

The flowchart shown in Figure 39 describes graphically the contribution of the artifact, the environment, and the measuring machine to the measurement uncertainty. If the influence factors that contribute to the uncertainty are well understood by the user, and the software has the ability to manipulate these data properly, close correlation is to be expected between the measured data and the predicted uncertainty.

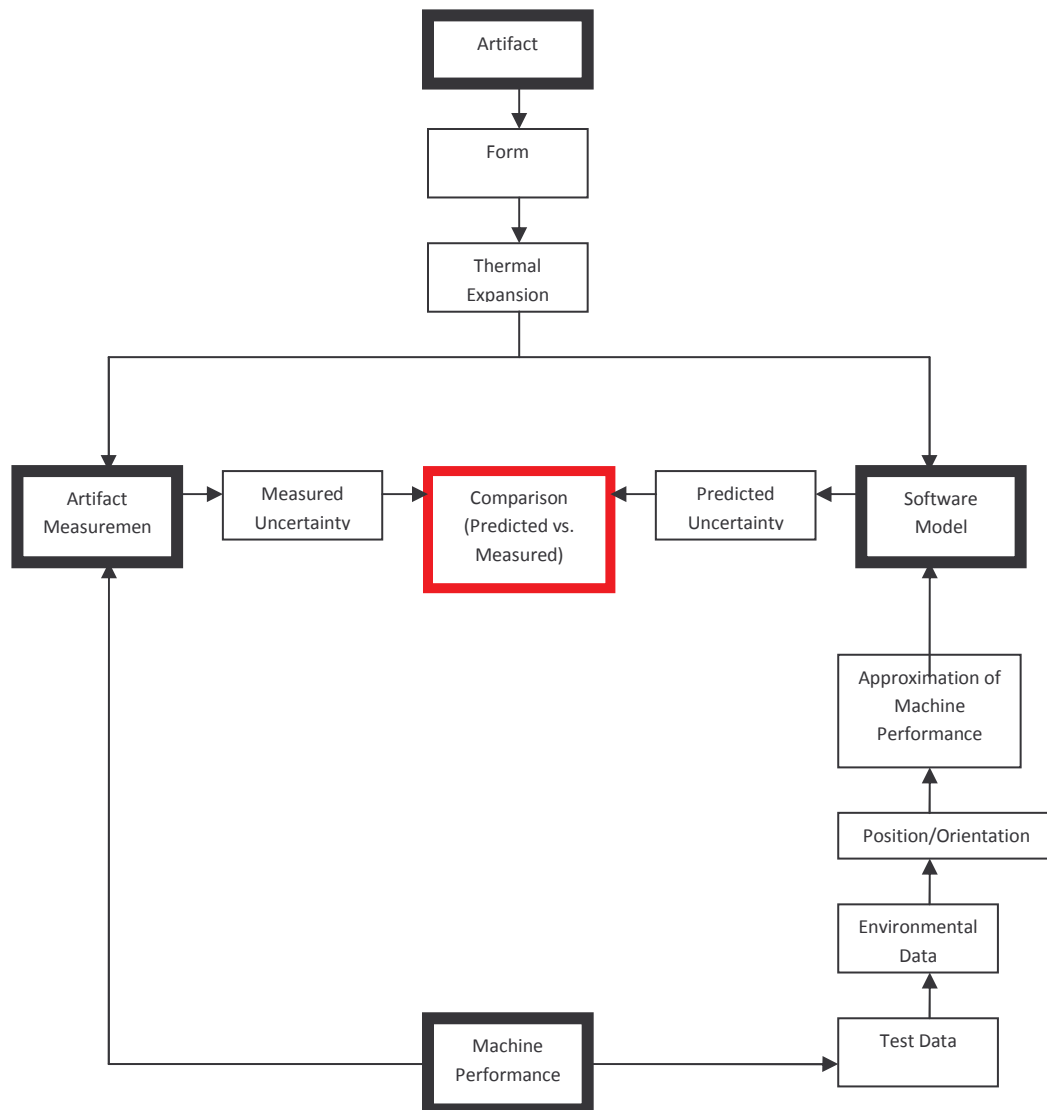


Figure 39: Flow chart for the comparison of experimental and simulated measurements.

The calculation of uncertainty based on the measured data is performed using the method described in ISO TS 15530-3 [13] and outlined in Table 1. This method accounts for both observed variability in the artifact measurements, the uncertainty of the artifact calibration, and the effect of bias that may exist in the measured data.

Table 1: Uncertainty calculation for artifact measurement from ISO TS 15530-3 [13]

$U = k \times \sqrt{u_{cal}^2 + u_p^2 + u_w^2} +  b $	<p>Expanded uncertainty calculation with k - coverage factor (k=2 used for 95% probability).</p>
<p><i>Components:</i></p>	
$u_{cal} = \frac{U_{cal}}{k}$	<p>Standard uncertainty from the artifact calibration certificate (here k is the coverage factor indicated by the certificate).</p>
$u_p = \sqrt{\frac{1}{n-1} \sum_{i=1}^n (y_i - \bar{y})^2}$	<p>Standard uncertainty of measurement procedure, i.e. standard deviation of measurement results.</p>
$u_w = (T - 20^\circ C) \times u_\alpha \times l$	<p>Standard uncertainty due to the manufacturing process and workpiece. In this case only thermal uncertainty is included. <math>u_\alpha</math> is the standard uncertainty for the coefficient of thermal expansion and <math>l</math> is the <i>measured dimension</i>.</p>
$b = \bar{y} - x_{cal}$	<p>Systematic uncertainty, or <i>bias</i> component.</p>

A Leitz 654 PMM was used to conduct all measurement tests. It is was an overhead bridge with moving table configuration. An analog type probe was used in point to point mode. Typical probe calibration form was 0.0005 mm for a 25.0001 mm calibration sphere. The CMM programming software was Quindos V.6, a least squares fitting algorithm was selected for all features measured.

#### 4.1.1 Software Inputs

Table 4, Table 2, and Table 3 lists the inputs or uncertainty contributors to each of the simulation software interfaces. The KALKOM and VCMMTool interfaces are both utilized for preparing the uncertainty inputs for VCMM, with the exception of the actual measurement program containing nominal feature data. KALKOM is used to derive the parametric errors for the machine. This data is then used by VCMMTool to develop further the uncertainty contributors such as environmental data and additional machine data. Table 2 shows the constants used by KALKOM to calculate the parametric errors for measured ball plate data. The inputs used were machine dimensions, plate grid spacing (of the ball plate artifact), and errorbars and spacings used for developing the interpolated parametric errors. The errorbar values are used by KALKOM to control the smoothness of the resulting fitted error. It is defined as "...half of the total range of a symmetric tolerance interval about the calculated 'exact' value of a parametric error function in a grid position." (Kalkom manual)[22]. The value for the errorbars used was the tolerance of the calibration for the ball plate artifact, +/-1.0 micron. Though this parameter is specifically not intended to be used "...in the sense of an uncertainty statement" (VCMM manual)[21], VCMMTool also requires the same value for straightness, rotation, and position 'uncertainty'. The conclusion was to use the specified

artifact uncertainty (for which only position was given) as the value here. The spacing input is intended to be used to control noise in the fitted parametric curves, though no noise was observed from the data calculated, so the value used was not specifically chosen for control of uncertainty of the parametric errors.

Table 2: KALKOM Input Constants

<b>KALKOM INPUTS</b>	
<b>Constants (Mach./Ball Plate):</b>	
X	0-600 mm
Y	0-500 mm
Z	0-400 mm
Errorbars:	
Position, Straightness, Rotation	+/- 1.0 $\mu\text{m}$ , $\mu\text{rad}$
Spacing:	
Position, Straightness, Rotation	20 mm
Plate Grid Spacing	60 mm

Table 3 shows the VCMMTool inputs, which include machine dimensions and environmental conditions. The machine dimensions are straightforward and the thermal data was taken from direct measurement of air temperature as recommended by the VCMM manual. It includes thermal gradients in three dimensions, thermal uncertainties, and thermal variations. Under ‘uncertainty of the error components’: XWY, XWZ, YWZ are defined as “uncertainty of the determination of the rectangularity deviations.” and XRX, YRY, ZRZ are defined as “uncertainty of the determination of the linear components of the roll error of the X-, Y- and Z-axes.” (VCMM manual)[21]. The values used are suggested empirical values in the VCMM manual. The machine scale values were taken from the ambient temperature measurement of the machine portal since no direct measurement of the scales was available. An average of the sensors closest to the table level were used for the X-scale values, and one sensor at the height of the bridge



was used for Z and Y-scale values. With regards to temperature testing - the difference in column thermal gradients was taken from prior testing (December 2006) with sensors arranged in a different configuration from all other thermal values (taken September 2007). The raw data for air temperature measurement (September values) is shown in Figure 40.

Table 3: VCMMTool Input Data

<b>VCMM INPUTS</b>	
<b>Machine:</b>	
X	600 mm
Y	500 mm
Z	400 mm
Height of Column	1176.6mm
Distance Between Columns	939.8mm
Length, X-Slideway	647.7mm
Thickness, X-Slideway	228.6mm
Width, X-Slideway	590.5mm
Parametric Data:	KALKOM Parametric Error Dataset
Probe	VIM_PRBCOR procedure results
Calibration uncert. Of standard	N/A
Uncertainty of error components:	
Straightness, Rotation, Position	1.0 $\mu$ m
XWY, XWZ, YWZ (squareness)	2.0 $\mu$ rad
XRX, YRY, ZRZ (linear components of roll errors)	2.0 $\mu$ rad
<b>Environmental:</b>	
Temperature Gradients:	
X	0.169K/m
Y	0.082 K/m
Z	0.197 K/m
Difference Between Columns	0.196K/m
Scale Temperatures:	
X (variation, uncertainty)	0.147K, 0.112K
Y (variation, uncertainty)	0.222K, 0.100K
Z (variation, uncertainty)	0.223K, 0.100K
Workpiece Temperatures:	
Variation, Uncertainty	0.147K, 0.113K
Expansion Coefficients:	
Workpiece (steel), (alpha, uncertainty)	11.8 $\mu$ m/(m*K), 1.18 $\mu$ m/(m*K)
Axes (granite)	8.5 $\mu$ m/(m*K)
Scales (glass), (alpha, uncertainty)	8.33 $\mu$ m/(m*K), .833 $\mu$ m/(m*K)
Columns (Steel), (alpha, uncertainty)	11.8 $\mu$ m/(m*K)
Other:	
Drift	0. 302 $\mu$ m/h
Average speed	80.0 mm/s

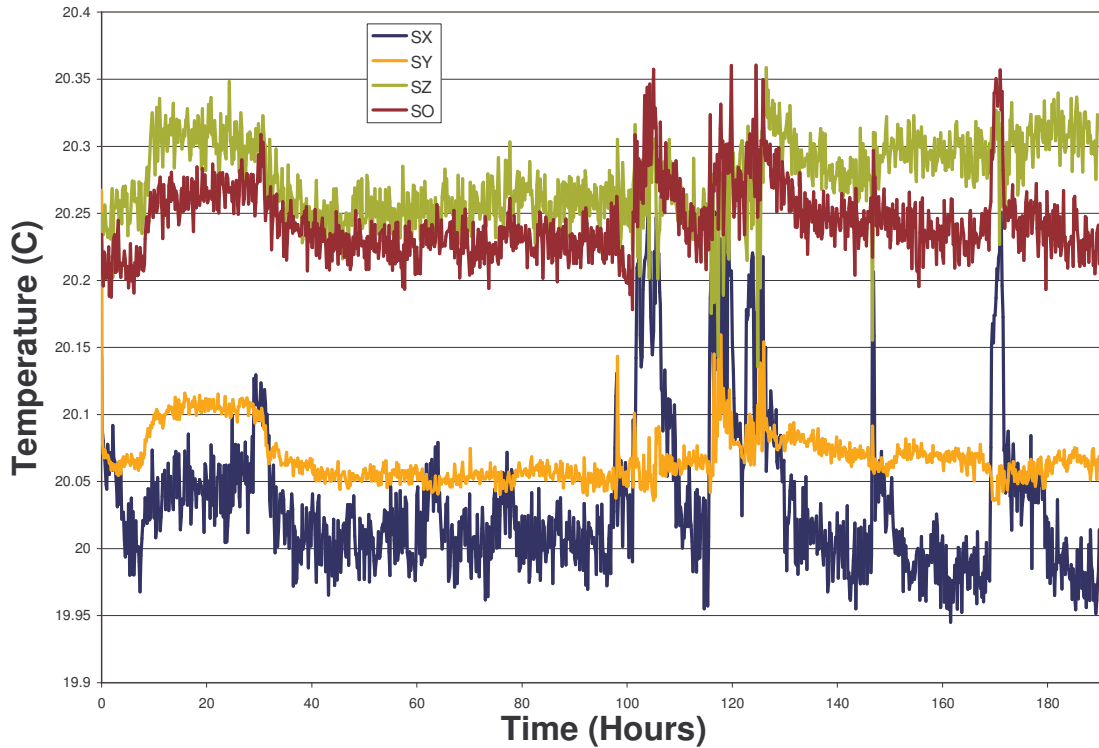


Figure 40: Air Temperatures measurements (190 Hours) at CMM

The values for Pundit, in Table 4, were used for all simulations and include in general a machine definition, probe definition, and environmental conditions. PUNDIT is unique from VCMM in that it has the option for utilizing simulation by constraints and for these experiments the ISO 10360 option was used with the values shown in the table. For full parametric error simulation the corresponding parametric data (derived from KALKOM, a component of the VCMM package) was the same for PUNDIT and VCMM tests. However, the parametric input for PUNDIT requires a standard deviation value for each error and a random error. The ball plate artifact used to attain the parametric errors was calibrated for ball position with an uncertainty of  $\pm 1.0$  micron. Therefore the standard deviation values used were one half of this value (for  $1\sigma$ ; it is assumed that the

uncertainty of the calibration was at  $2\sigma$ ). This constitutes an interval of error about each gridpoint that is used to develop additional random error on top of the mean errors in simulation. (In the case of rotational errors this value was used in conjunction with the probe length used in measuring the ball plate to develop an angular error). The random error was approximated from the repeatability of the forward and backward run of the measurement of the ball plate and was assumed to give a fair estimate of additional random machine error experienced during ball plate measurement. Environmental input includes temperature values for CMM scales and the workpiece, along with expansion coefficients, and uncertainties of all values. The temperature was assumed to be the same for both scales and workpiece. A mean air temperature with an uncertainty of  $2\sigma$  was derived from direct measurement.

Table 4: PUNDIT Software Input Data

<b>PUNDIT INPUTS</b>	
<b>Machine Extents:</b>	
TYPE	Fixed Bridge
X	600 mm
Y	500 mm
Z	400 mm
Machine (simulation by constraints)	$E = \pm 1.2\mu\text{m} + 3.3\mu\text{m}(L/1000\text{mm})$
Parametric Data:	KALKOM Parametric Error Dataset
Individual error standard deviation	0.5 $\mu\text{m}$ Translational/ 1.7 $\mu\text{rad}$ Rotational
Random error standard deviation	0.15 $\mu\text{m}$
Probe	P3=0.8 $\mu\text{m}$ (50 mm length, piezoelectric option used – actual probe head is an LVDT sensor)
<b>Environmental:</b>	
Temperature (scales), uncertainty	20.2°C , 0.22°C
Temperature (part), uncertainty	20.2°C , 0.22°C
Coefficient of thermal expansion (scales, glass) , uncertainty	8.33ppm/°C , 0.833ppm/°C
Coefficient of thermal expansion (workpiece, steel), uncertainty	11.8ppm/°C , 1.18ppm/°C

#### 4.1.2 Ball Plate Measurement

The ball plate was measured on the Leitz 654 PMM at UNCC using the procedures put down by the KALKOM manual. Measurements were made only of spheres around the periphery of the plate, both forward around the perimeter and reverse along the same path. The universal coordinate system defined in the KALKOM manual was used, with the X axis parallel to table movement, the Y axis parallel to the bridge, and the Z axis parallel to the ram. The plates were measured in all three planes in a total of 16 positions, with positive and negative probe orientations. The three number naming convention for the plates was #1# for the XY plane, #2# for the XZ plane, and #3# for the YZ plane, with the first digit being the number of the plate in-plane and the third digit indicating which side of the plate (positive or negative) it was probed, per the KALKOM instructions. The figures below show all plate orientations and positions and the probes used for each.

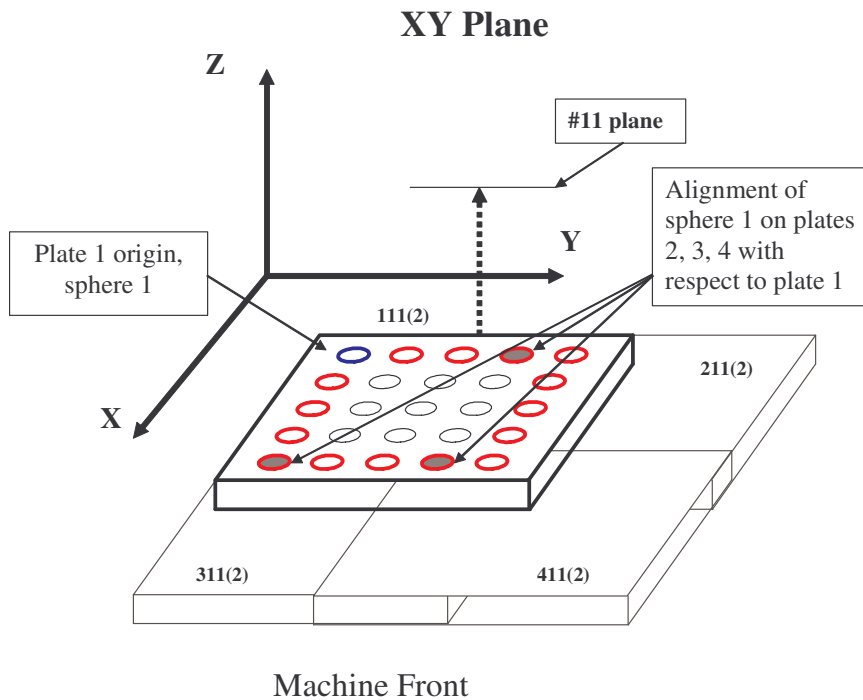


Figure 41: XY Plane Plate Positions

**XY Probe:**Length: 150 mm  
w/ Cube

Figure 42: XY Plane Probe

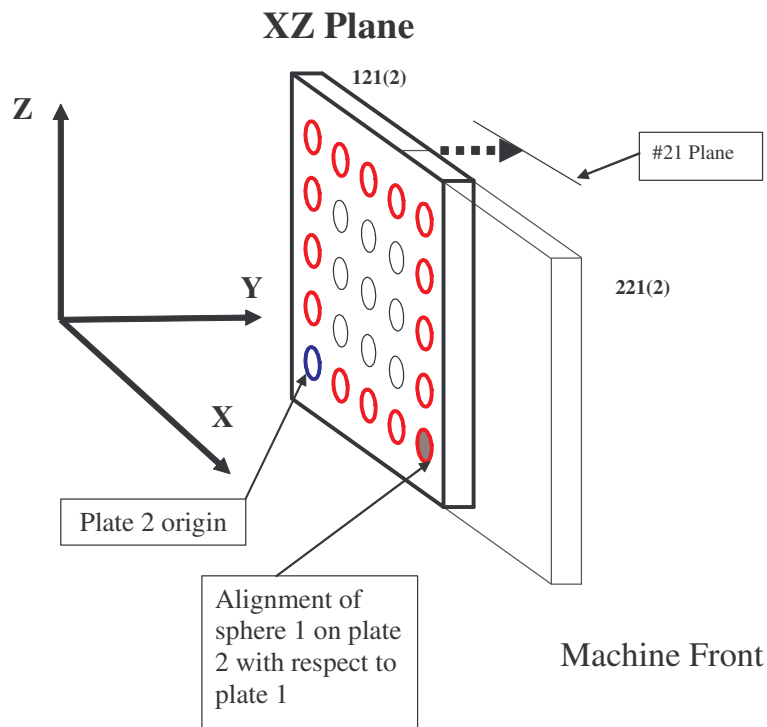


Figure 43: XZ Plane Plate Positions

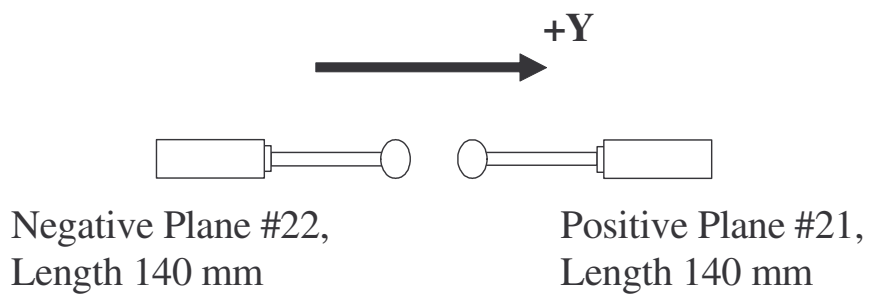
**XZ Probes:**

Figure 44: XZ Plane Probes

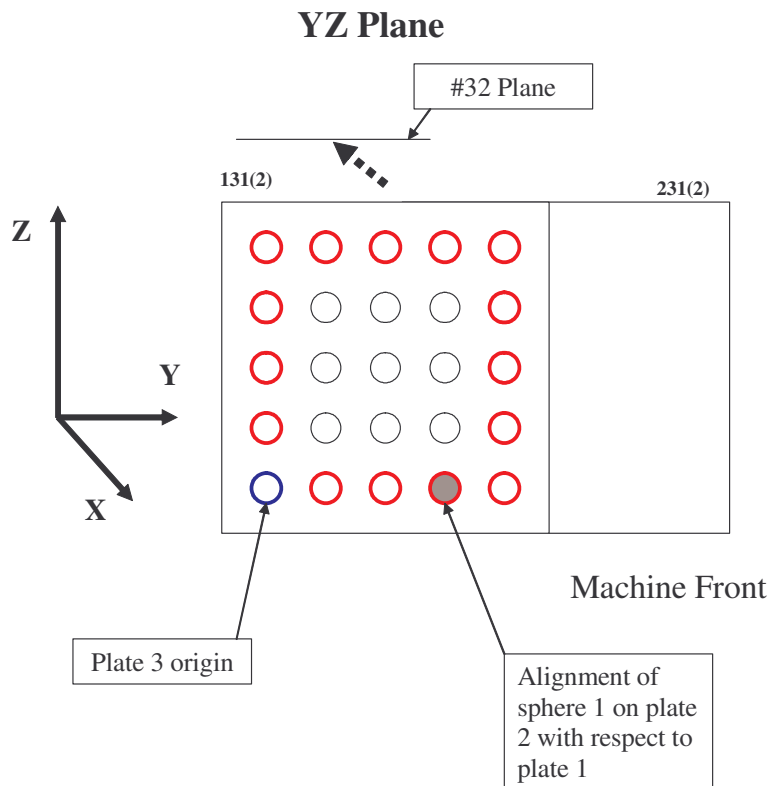


Figure 45: YZ Plane Plate Positions

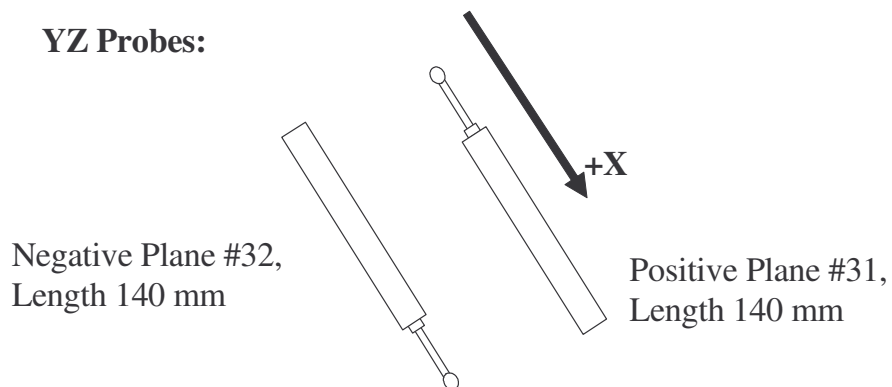


Figure 46: YZ Plane Probes



### 4.1.3 Ball Plate Measurement Results

Table 5 and Table 6 represent the parametric errors determined by the ball plate measurements. Table 5 lists the range of each error for the whole axis and Table 6 shows the error curves for each axis.

Table 5: Parametric Error Ranges  
Error Range (microns/microrads)

XTX	1.226
YTY	1.056
ZTZ	1.556
XTY	0.101
XTZ	0.421
YTX	1.763
YTZ	0.000
ZTX	7.764
ZTY	0.021
XRZ	3.993
XRY	6.885
XRX	4.261
YRZ	22.43
YRX	8.073
YRY	3.708
ZRY	0.913
ZRX	2.064
ZRZ	29.09
XWY	2.620
XWZ	5.147
YWZ	2.477

Table 6: Parametric Errors

<p><b>XTX, Range=1.226 micron</b></p>	<p><b>YTY, Range=1.056 micron</b></p>
<p><b>ZTZ, Range=1.556 micron</b></p>	<p><b>XTY, Range=0.101 micron</b></p>
<p><b>XTZ, Range=0.421 micron</b></p>	<p><b>YTX, Range=1.763 micron</b></p>

Table 6, Continued

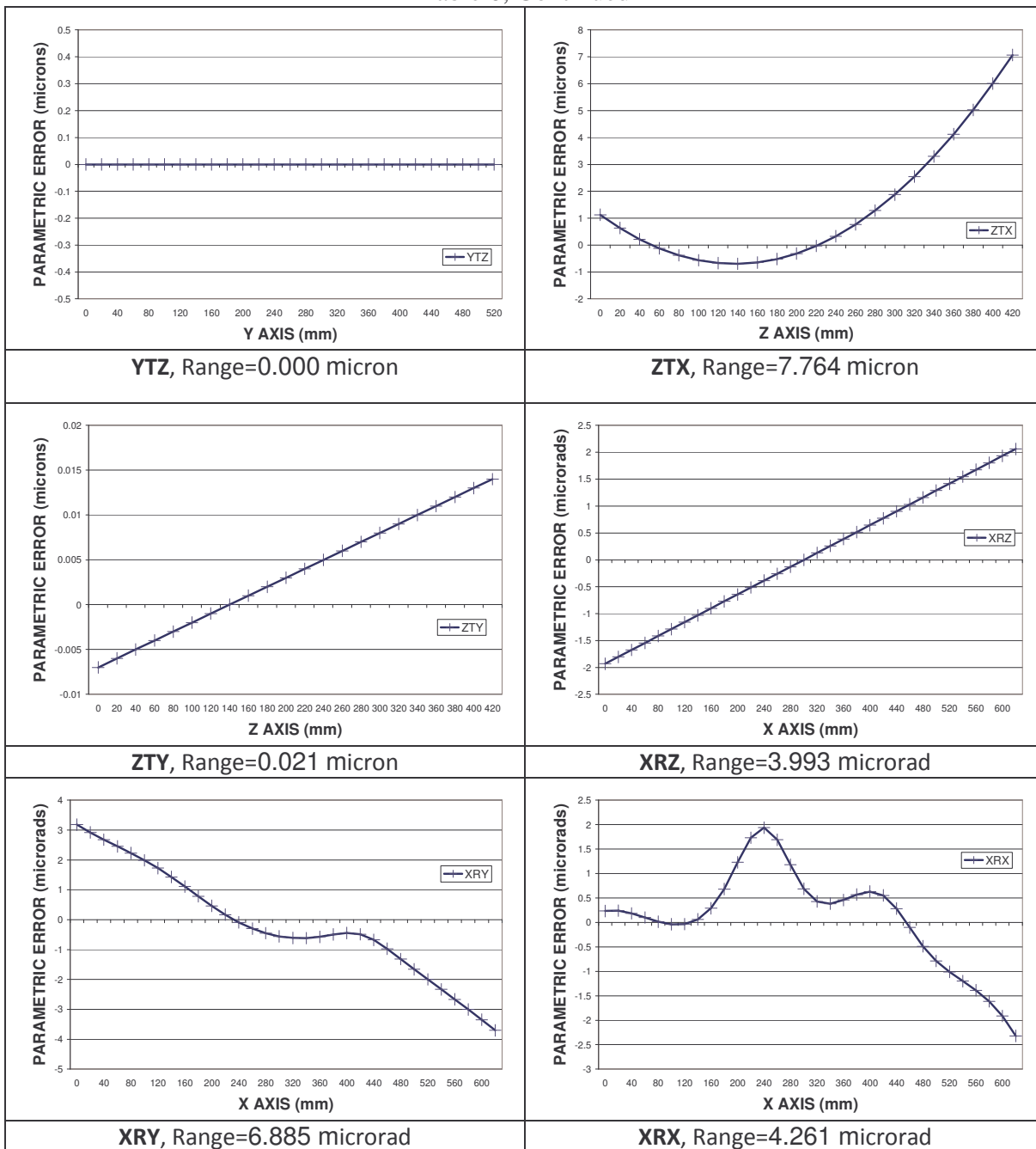
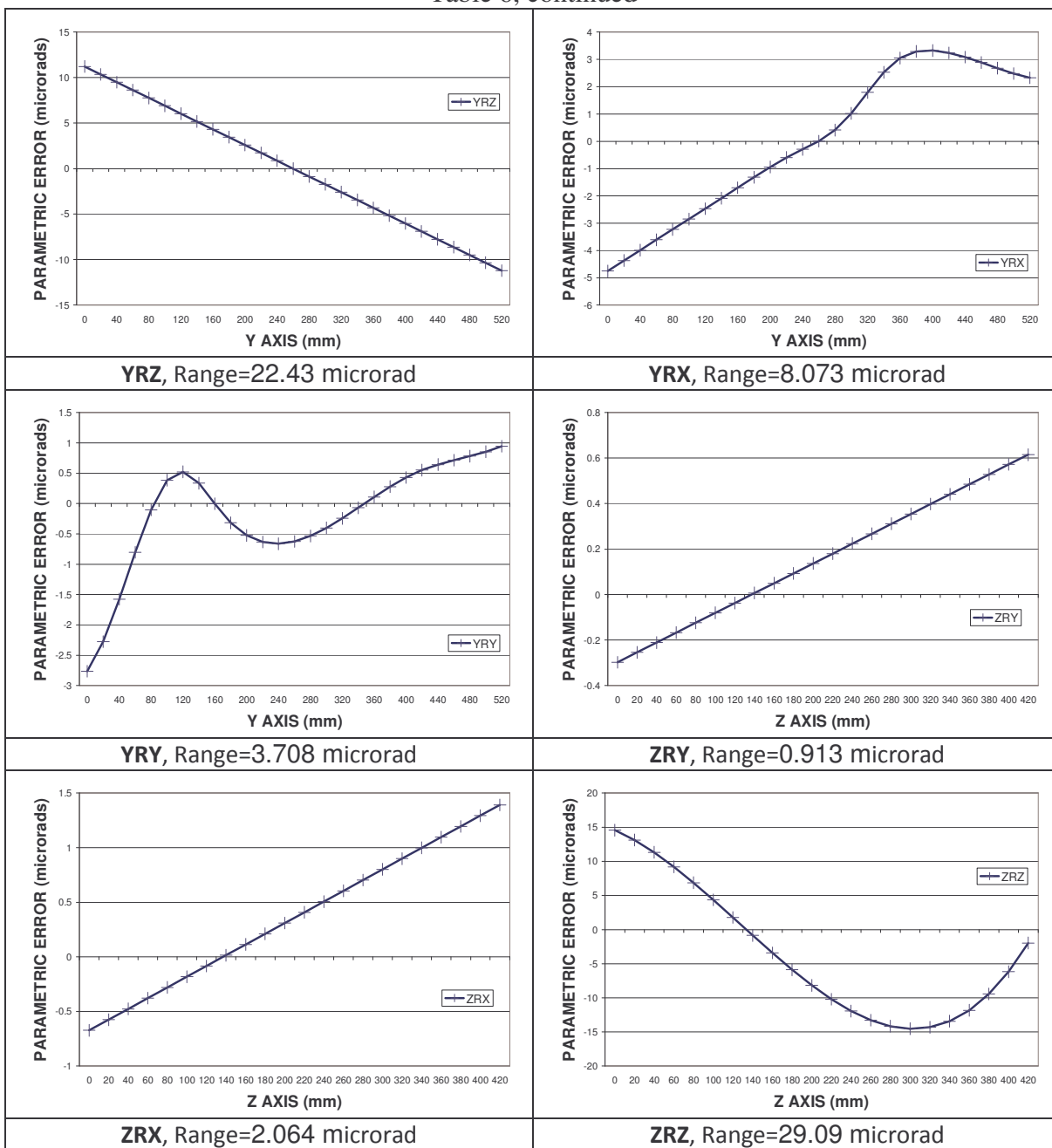


Table 6, continued



## 4.2 Results

The test results are summarized in plots indicating comparisons between the uncertainties determined by each method: by physical experiment and VCMM and PUNDIT simulations. Individual tests were completed for a variety of positions and orientations. Examination of the simulation results for this data reveals the ability of the software to perform for any given measurement task associated with the particular measurand. The results were also averaged across the categories of position and orientation, e.g. all orientations for position '1' are averaged together to form a new category; or all positions for orientation 'A' are averaged. This allows the data to be examined more clearly given the number of data points in some cases, while using a larger basis of data points per category. This also gives an indication of the usefulness of the simulation software in particular scenarios and about the implementation of the software, i.e. it may serve the purpose of informing about overall performance of the machine instead of in just one particular situation. In general, the data is organized in each section by measurand, first by showing the average of results and then by individual position/orientation results.

When comparing the simulated data to the experimental data, a desirable result, besides being close in value to the physical experiment, would be to overestimate it as well. Additionally, when comparing results involving position and orientation, an increase or decrease in the experimentally determined values with position and orientation, mimicked by the simulated data, even if offset, would likewise be a desirable result .

#### 4.2.1 All Measurands

In Figure 47, a summary of all of the measurand uncertainty results determined by experiment, VCMM, PUNDIT (with parametric error inputs), and PUNDIT (using ISO 10360 MPE inputs) are shown. The data is averaged across large and small dimensions (if multiple size artifacts were used) and all positions and orientations tested. Each geometry tested, including circles, point-to-point distances, lines, spheres, and cylinders is shown, with size and form values for circles, spheres, and cylinders. The data is averaged across large and small dimensions (if multiple size artifacts were used) and all positions and orientations tested.

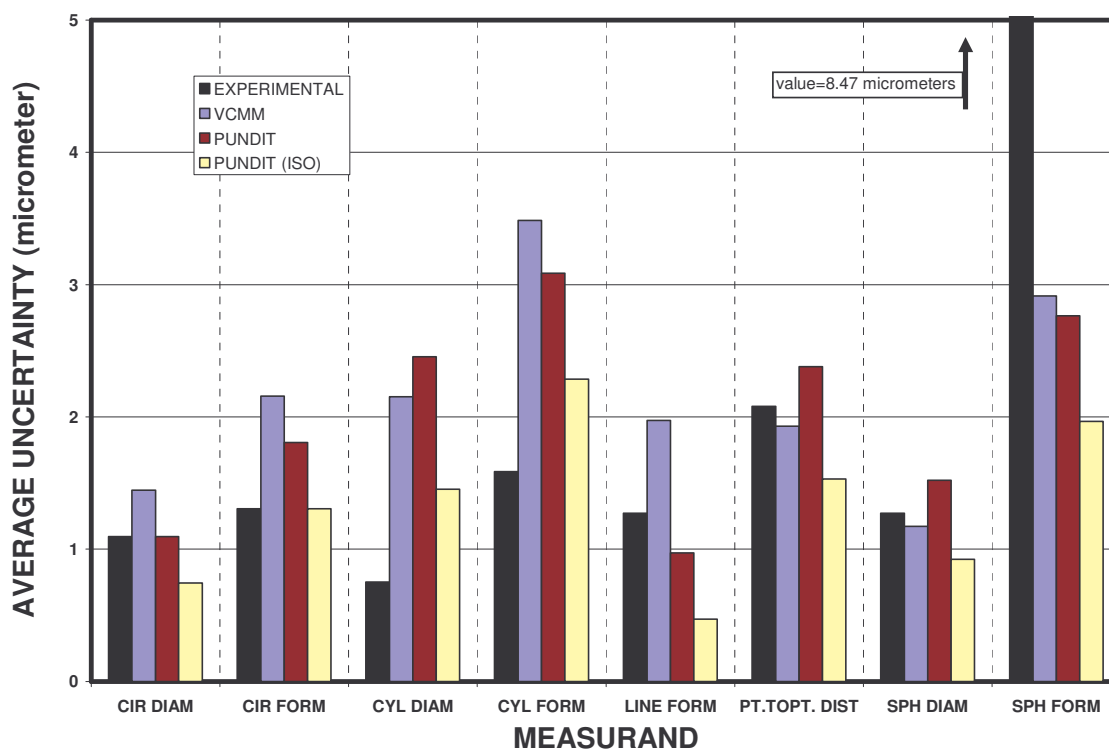


Figure 47: Averages of All Measurand Results

It should be noted that experimental values of uncertainty for sphere form were particularly high due to the design of the larger sphere artifact. The artifact was

manufactured with an intentional form error, for which the exact magnitude and frequency were unknown for these tests. Therefore, only comparisons of the simulated sphere form results amongst themselves are informative.

VCMM and PUNDIT (parametric) results show the largest disparity with the experimental results for cylindrical size and form, both  $> 1.5$  micrometer deviation. All other VCMM and PUNDIT (parametric) results deviate  $< 1.5$  micrometers, excepting the spherical form data. The PUNDIT (ISO) estimations had the smallest absolute deviation from experimental values, at an average of 0.7 micrometers, compared to 0.9 micrometers for PUNDIT (parametric) and 0.8 micrometers for VCMM, though it was the most likely to underestimate the experimental uncertainties.

#### 4.2.2 Ring Tests

Circle measurements were conducted on two Ring Gage artifacts. The smaller ring was 25.000mm (XXX) diameter and the larger was 112.000mm (XX) diameter. All circles were evaluated from 11 measurement points through 360 degrees. Figure 48 shows the positions (1-5) and orientations (A,B,C,F,G,H). The arrows indicate the direction for the normal of each ring. Orientations A,B,C are parallel to the machine axes, while F,G,H are at 45 degrees to normal. Positions 1 and 2 are at the front of the machine table, positions 3 and 4 are at the back of the table, and position 5 is at the center of the table.

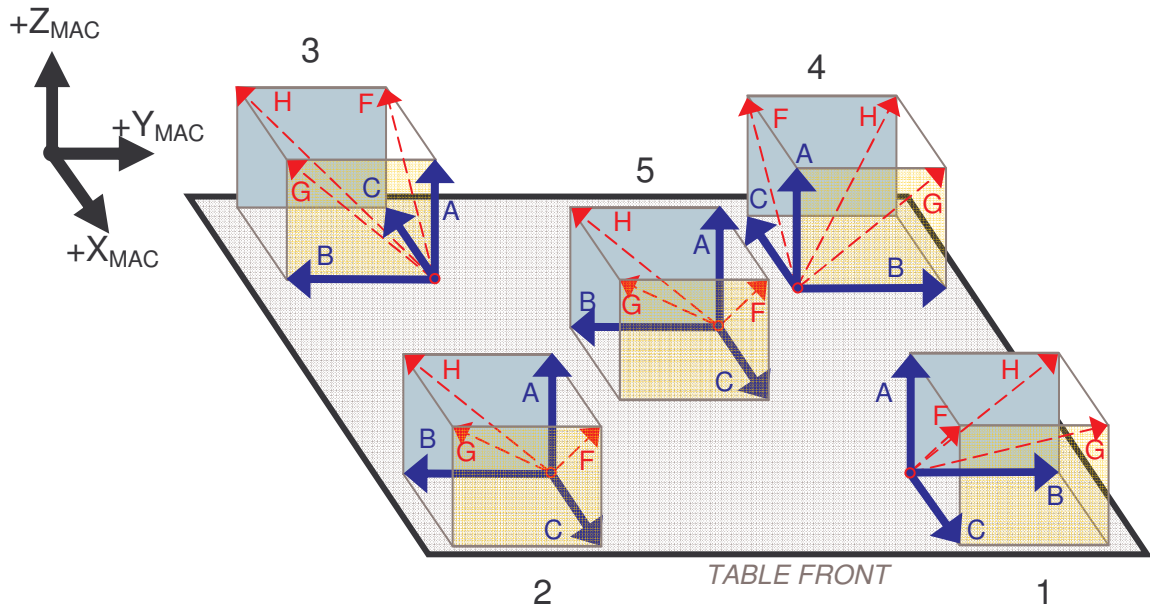


Figure 48: Orientations and Positions for Ring Gage Measurement

The results of the 2D circle measurements are shown in Figure 49 through and in Table 7 through Table 10. Figure 49 shows a summation of all of the circle results. Subsequently, each figure represents either the 25mm gage or the 112mm gage and either diameter evaluations or form (circularity) evaluations, with two plots for each measurand. The first shows an averaged value for all like positions (1, 2, 3, etc.) and orientations (A, B, C, etc.). This was done for the circle results, since owing to the large number of measurement position and orientation combinations, smaller samples (10 measurements) were taken for each. The averaged values for each position and orientation should be more statistically sound though the information is somewhat smoothed. The second shows results for each individual position and orientation combination with the data arranged first by position (i.e. 1A, 2A, 3A, etc.) then by orientation.



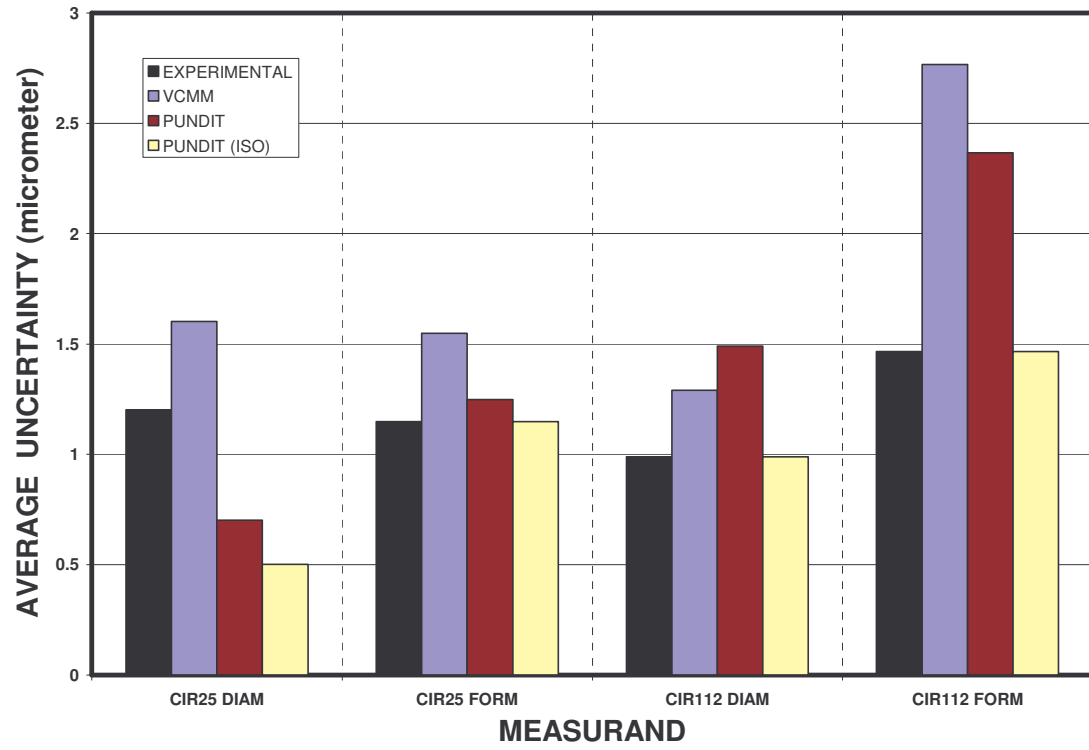


Figure 49: Averages of All 2D Circle Measurements

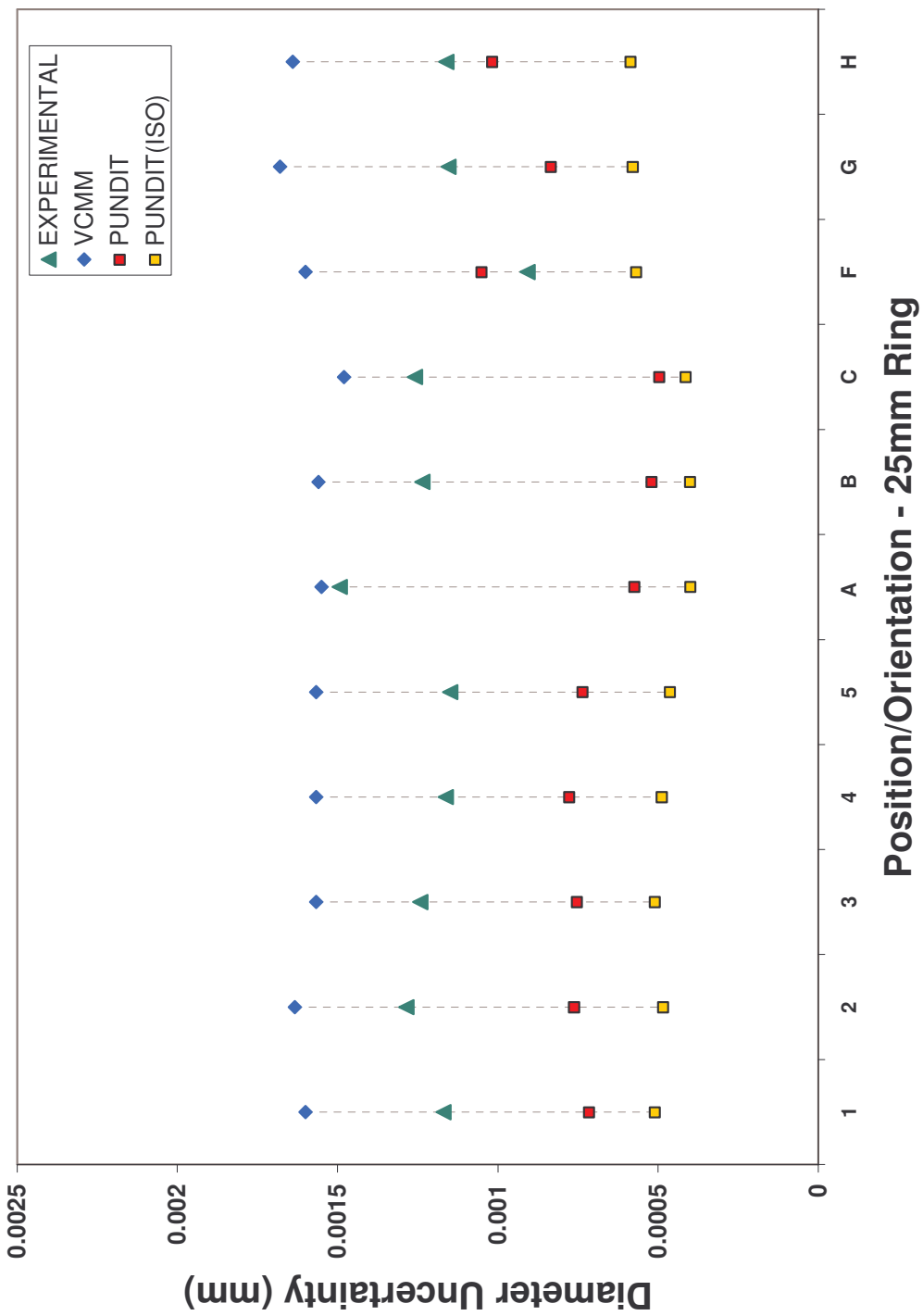


Figure 50: Diameter Results, 25mm Ring Gage, Averaged by Pos./Ori.

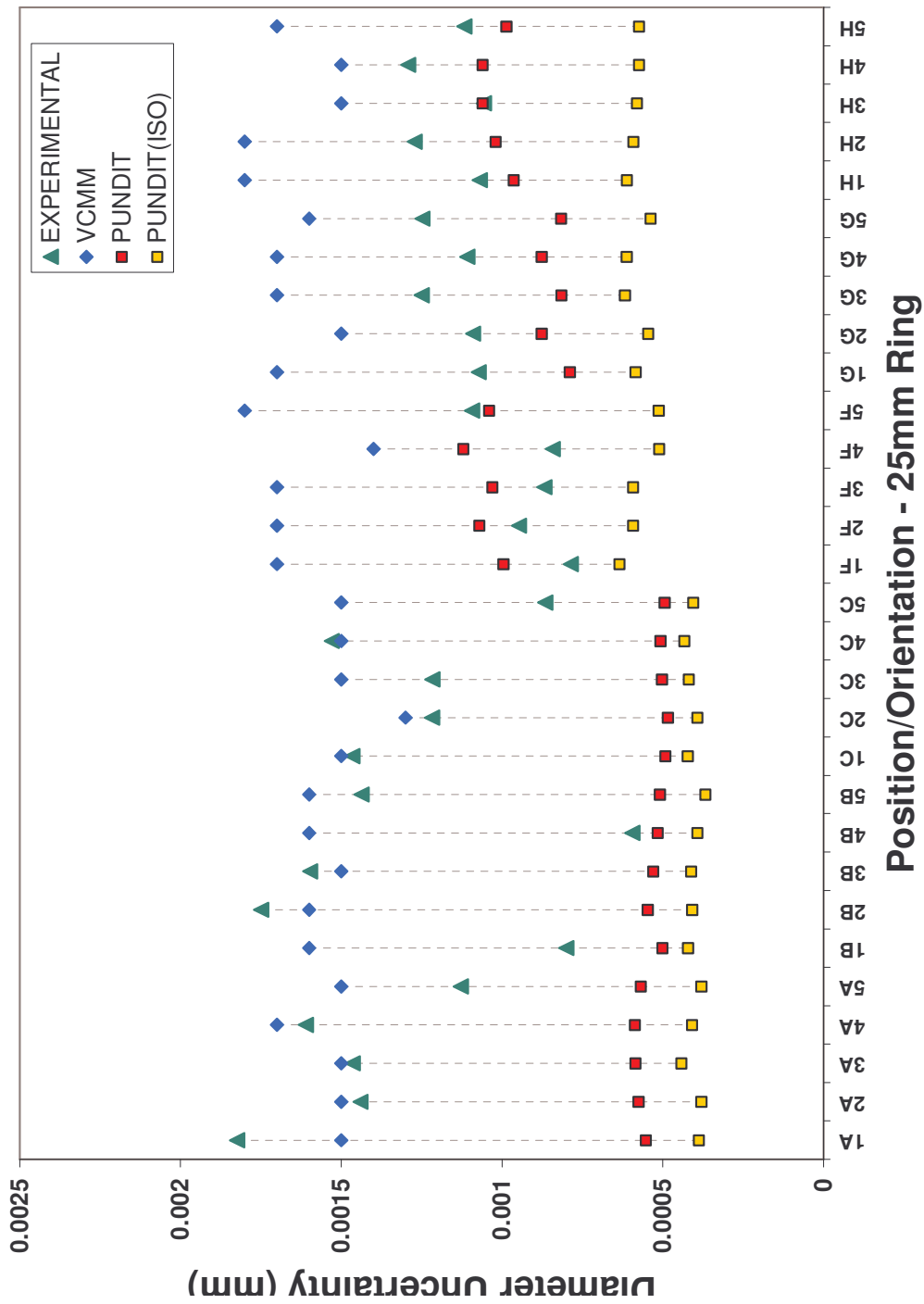


Figure 51: Diameter Results, 25mm Ring Gage

Table 7: Difference in Simulation and Experiment, Diameter, 25mm Ring Gage  
 25mm Ring Gage - Difference in Diameter Uncertainties (Simulation - Experimental) in  
 micrometers

POS.	ORI.	VCMM	PUNDIT(ISO)	PUNDIT(PAR.)
1	A	-0.3	-1.4	-1.3
2	A	0.1	-1.1	-0.9
3	A	0.0	-1.0	-0.9
4	A	0.1	-1.2	-1.0
5	A	0.4	-0.7	-0.6
1	B	0.8	-0.4	-0.3
2	B	-0.1	-1.3	-1.2
3	B	-0.1	-1.2	-1.1
4	B	1.0	-0.2	-0.1
5	B	0.2	-1.1	-0.9
1	C	0.0	-1.0	-1.0
2	C	0.1	-0.8	-0.7
3	C	0.3	-0.8	-0.7
4	C	0.0	-1.1	-1.0
5	C	0.6	-0.5	-0.4
1	F	0.9	-0.2	0.2
2	F	0.8	-0.4	0.1
3	F	0.8	-0.3	0.2
4	F	0.6	-0.3	0.3
5	F	0.7	-0.6	-0.1
1	G	0.6	-0.5	-0.3
2	G	0.4	-0.5	-0.2
3	G	0.5	-0.6	-0.4
4	G	0.6	-0.5	-0.2
5	G	0.4	-0.7	-0.4
1	H	0.7	-0.5	-0.1
2	H	0.5	-0.7	-0.3
3	H	0.4	-0.5	0.0
4	H	0.2	-0.7	-0.2
5	H	0.6	-0.5	-0.1
<b>Average (Absolute Difference)</b>		<b>0.4</b>	<b>0.7</b>	<b>0.5</b>
<b>Maximum (Absolute Difference)</b>		<b>1.0</b>	<b>1.4</b>	<b>1.3</b>

The diameter results indicate that both PUNDIT estimations were below the experimental uncertainty data while the VCMM results were in most cases above the experimental data. In Table 7, the difference values between simulation and experiment have been calculated for each position/orientation as well as the average of the absolute values for the differences and the maximum absolute difference for each simulation

method. Positive difference values within the table are desired since this would indicate that the software predictions did not underestimate uncertainty. The A,B,C orientations indicate larger variations (~1.0 microns) in uncertainty values than the F,G,H orientations (~0.5 microns). However, none of the simulations predicts this range in uncertainties for orientations A,B,C, but both parametric simulations predict the range for F,G,H orientations more closely. Since each of these groups were measured separately at different periods of time the variations could be due to environmental conditions. Additionally, each group required a different probe configuration; the F,G,H group used an adjustable knuckle and the A,B,C group used a cube.

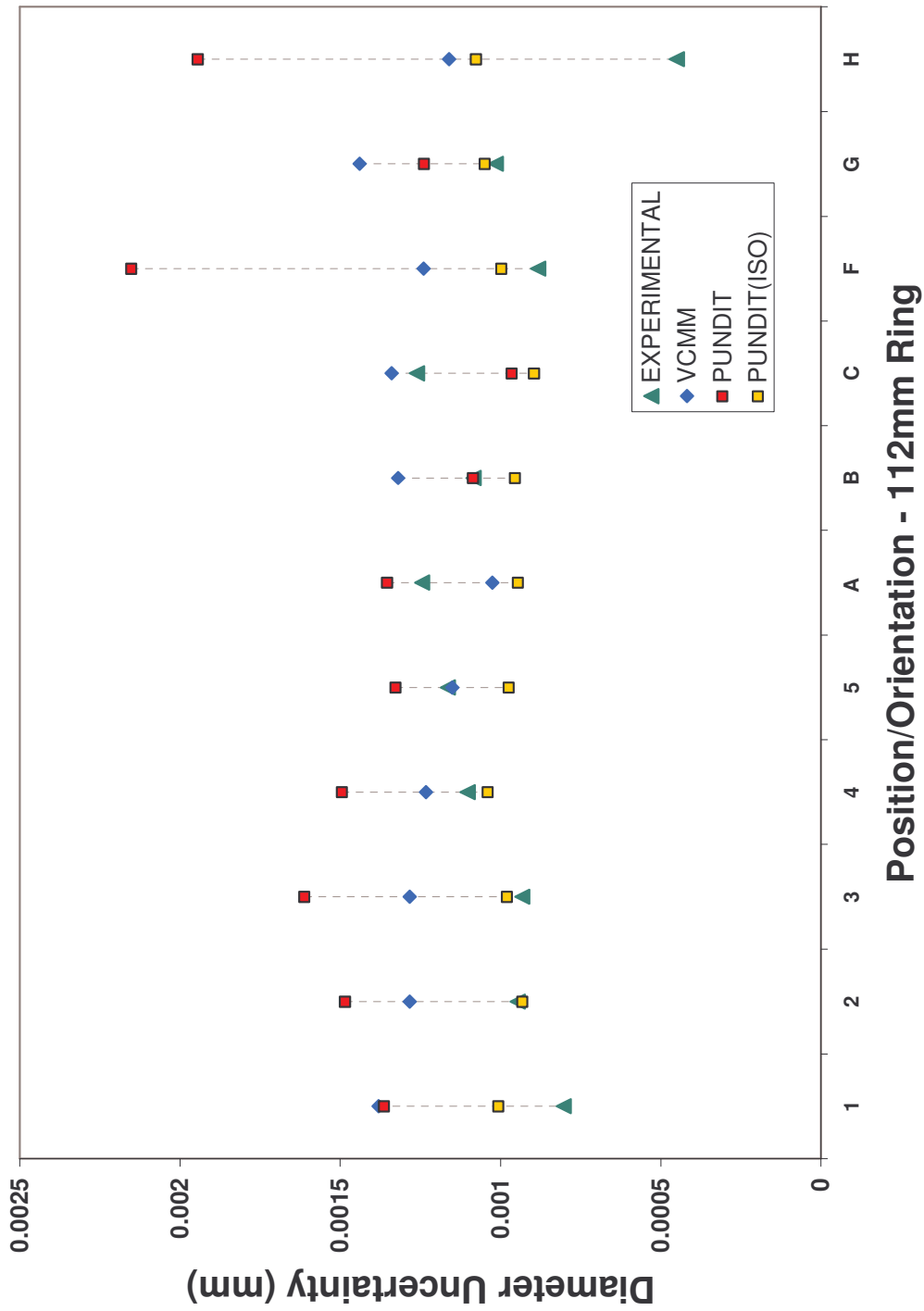


Figure 52: Diameter Results, 112mm Ring Gage, Averaged by Pos./Ori.

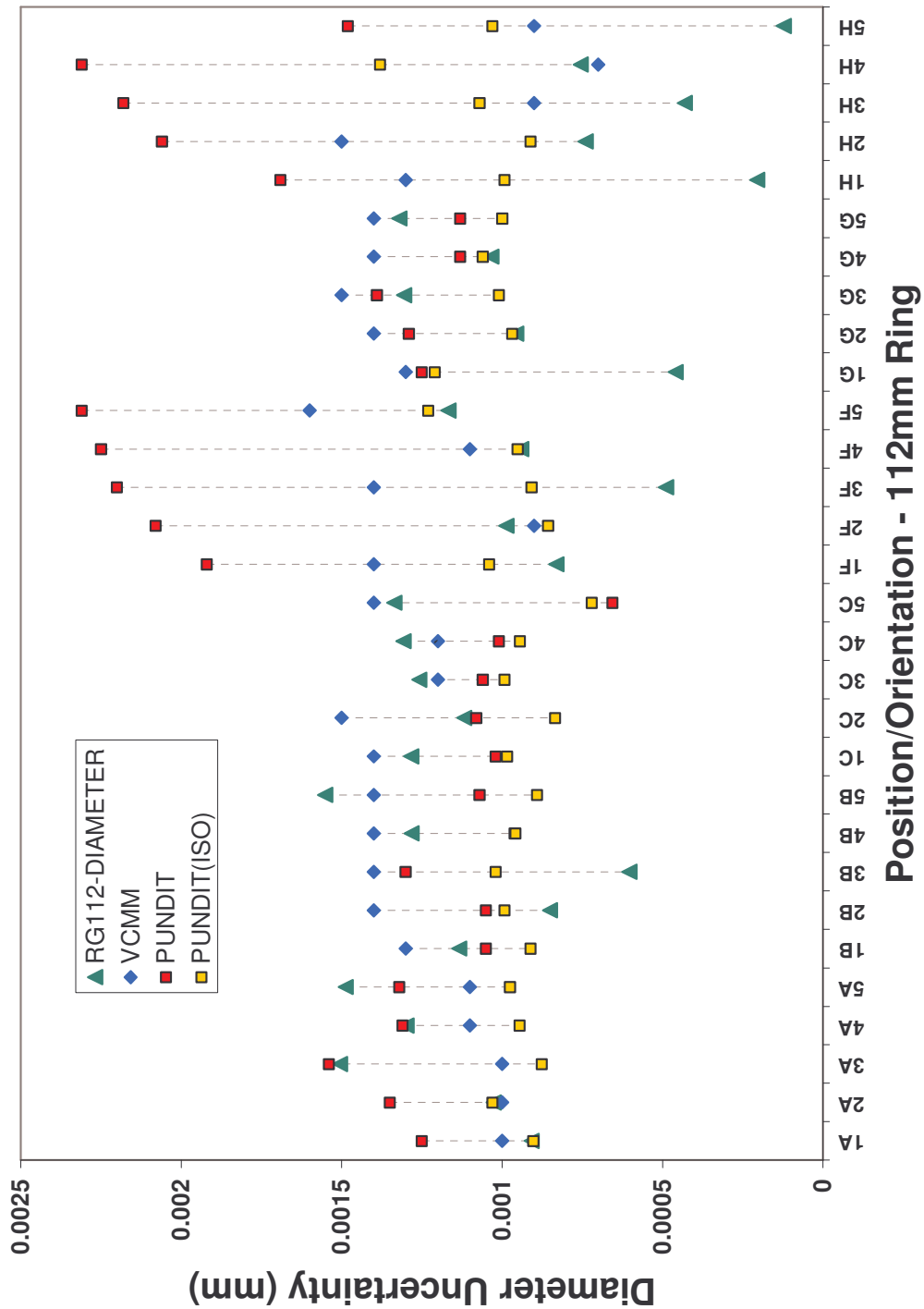


Figure 53: Diameter Results, 112mm Ring Gage

Table 8: Difference in Simulation and Experiment, Diameter, 112mm Ring Gage  
 112mm Ring Gage - Difference in Diameter Uncertainties (Simulation - Experimental) in  
 micrometers

POS.	ORI.	VCMM	PUNDIT(ISO)	PUNDIT(PAR.)
1	A	0.1	0.0	0.3
2	A	0.0	0.0	0.3
3	A	-0.5	-0.6	0.0
4	A	-0.2	-0.4	0.0
5	A	-0.4	-0.5	-0.2
1	B	0.2	-0.2	-0.1
2	B	0.5	0.1	0.2
3	B	0.8	0.4	0.7
4	B	0.1	-0.3	-0.3
5	B	-0.2	-0.7	-0.5
1	C	0.1	-0.3	-0.3
2	C	0.4	-0.3	0.0
3	C	-0.1	-0.3	-0.2
4	C	-0.1	-0.4	-0.3
5	C	0.1	-0.6	-0.7
1	F	0.6	0.2	1.1
2	F	-0.1	-0.1	1.1
3	F	0.9	0.4	1.7
4	F	0.2	0.0	1.3
5	F	0.4	0.1	1.1
1	G	0.8	0.8	0.8
2	G	0.4	0.0	0.3
3	G	0.2	-0.3	0.1
4	G	0.4	0.0	0.1
5	G	0.1	-0.3	-0.2
1	H	1.1	0.8	1.5
2	H	0.8	0.2	1.3
3	H	0.5	0.6	1.7
4	H	-0.1	0.6	1.6
5	H	0.8	0.9	1.4
<b>Average (Absolute Difference)</b>		<b>0.4</b>	<b>0.3</b>	<b>0.6</b>
<b>Maximum (Absolute Difference)</b>		<b>1.1</b>	<b>0.9</b>	<b>1.7</b>

For the 112mm diameter results, all of the simulation packages predict the uncertainties within an average absolute difference of no greater than 0.6 micrometers. However, the PUNDIT results indicate that for the A,B,C orientations the average absolute difference is slightly less than the experimental values and for the F,G,H orientations the average absolute difference is greater than the experimental values. The



PUNDIT results for the F,G,H orientations show much higher variability than for the A,B,C orientations indicating that the modeling is affected by the evaluations involving all three axes as compared to only two. VCMM indicates some increase in variability as well but tracks the experimental values more closely.

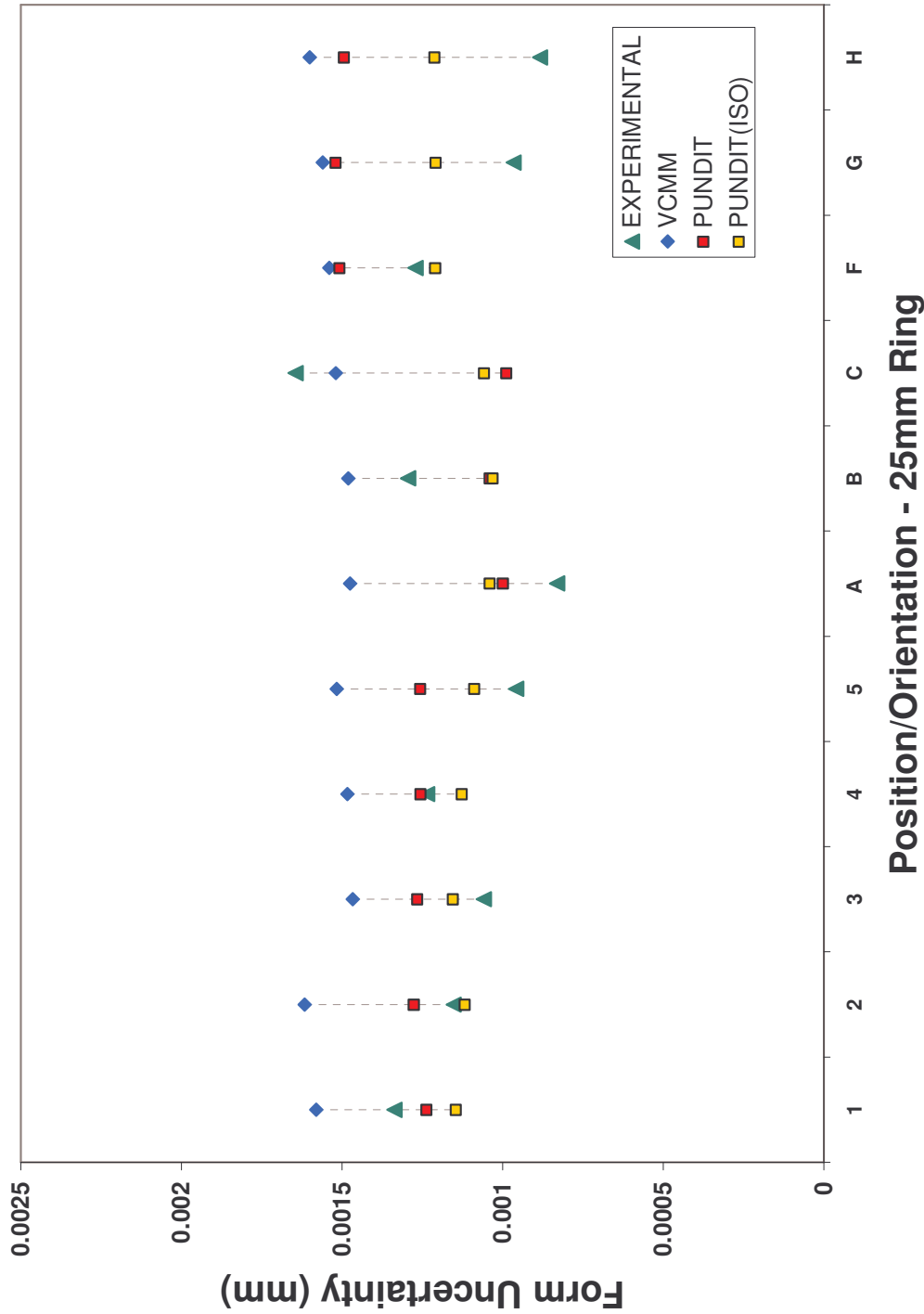


Figure 54: Form Results, 25mm Ring Gage, Averaged by Pos./Ori.

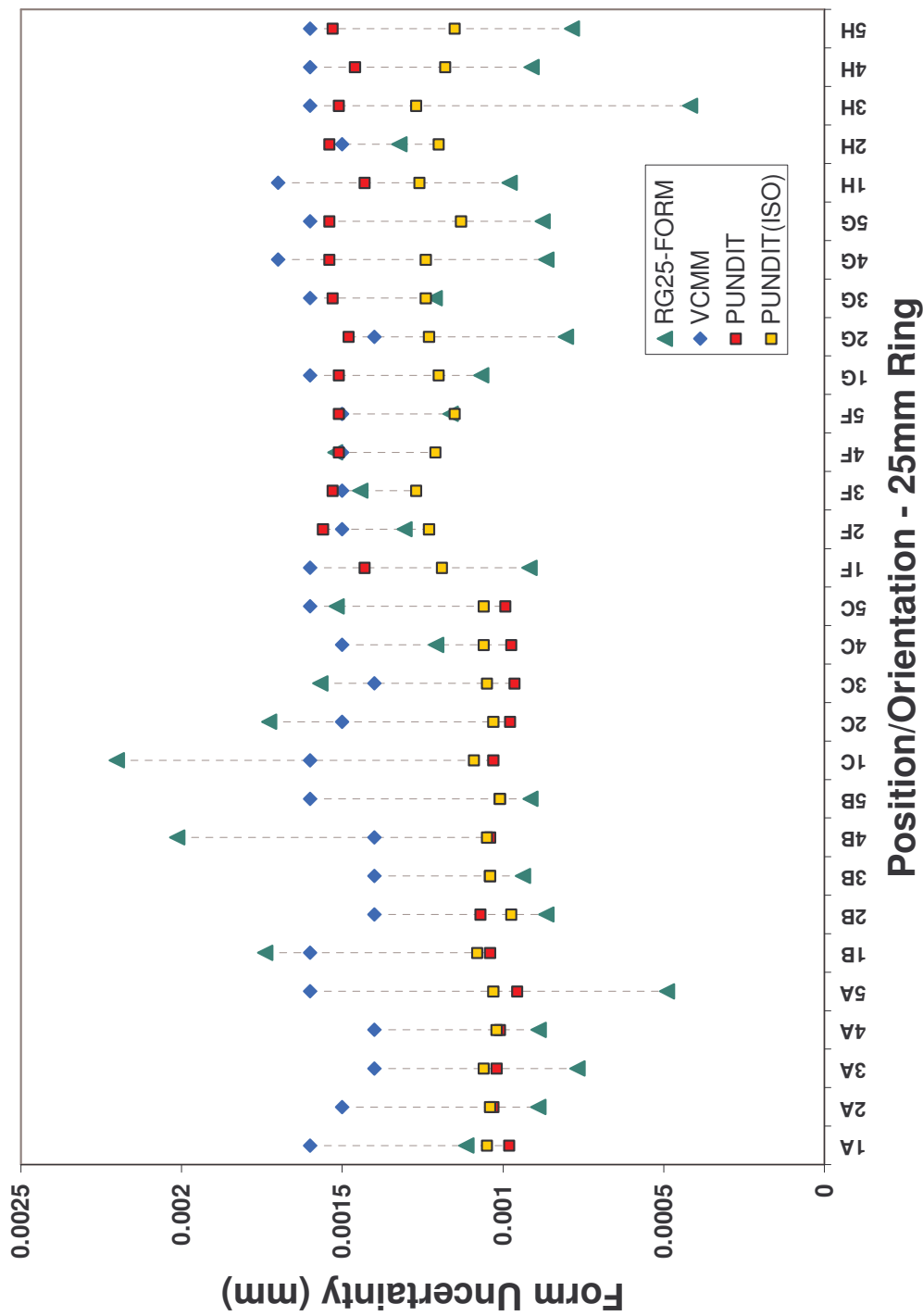


Figure 55: Form Results, 25mm Ring Gage

Table 9: Difference in Simulation and Experiment, Form, 25mm Ring Gage  
 25mm Ring Gage - Difference in Form Uncertainties (Simulation - Experimental) in  
 micrometers

POS.	ORI.	VCMM	PUNDIT(ISO)	PUNDIT(PAR.)
1	A	0.5	-0.1	-0.1
2	A	0.6	0.2	0.1
3	A	0.6	0.3	0.3
4	A	0.5	0.1	0.1
5	A	1.1	0.5	0.5
1	B	-0.1	-0.7	-0.7
2	B	0.5	0.1	0.2
3	B	0.5	0.1	0.1
4	B	-0.6	-1.0	-1.0
5	B	0.7	0.1	0.1
1	C	-0.6	-1.1	-1.2
2	C	-0.2	-0.7	-0.7
3	C	-0.2	-0.5	-0.6
4	C	0.3	-0.1	-0.2
5	C	0.1	-0.5	-0.5
1	F	0.7	0.3	0.5
2	F	0.2	-0.1	0.3
3	F	0.1	-0.2	0.1
4	F	0.0	-0.3	0.0
5	F	0.3	0.0	0.3
1	G	0.5	0.1	0.4
2	G	0.6	0.4	0.7
3	G	0.4	0.0	0.3
4	G	0.8	0.4	0.7
5	G	0.7	0.3	0.7
1	H	0.7	0.3	0.5
2	H	0.2	-0.1	0.2
3	H	1.2	0.9	1.1
4	H	0.7	0.3	0.5
5	H	0.8	0.4	0.7
<b>Average (Absolute Difference)</b>		<b>0.5</b>	<b>0.3</b>	<b>0.4</b>
<b>Maximum (Absolute Difference)</b>		<b>1.2</b>	<b>1.1</b>	<b>1.2</b>

The results for form evaluations for the 25mm ring show variability in the experimental results that is not reflected in the simulated results, though when considering the averaged plots for positions and orientations, , the effect is greatly reduced. All of the simulation results were more likely to overestimate the experimental

values than to underestimate them, though VCMM results tended to exceed the experimental values more consistently for all cases.

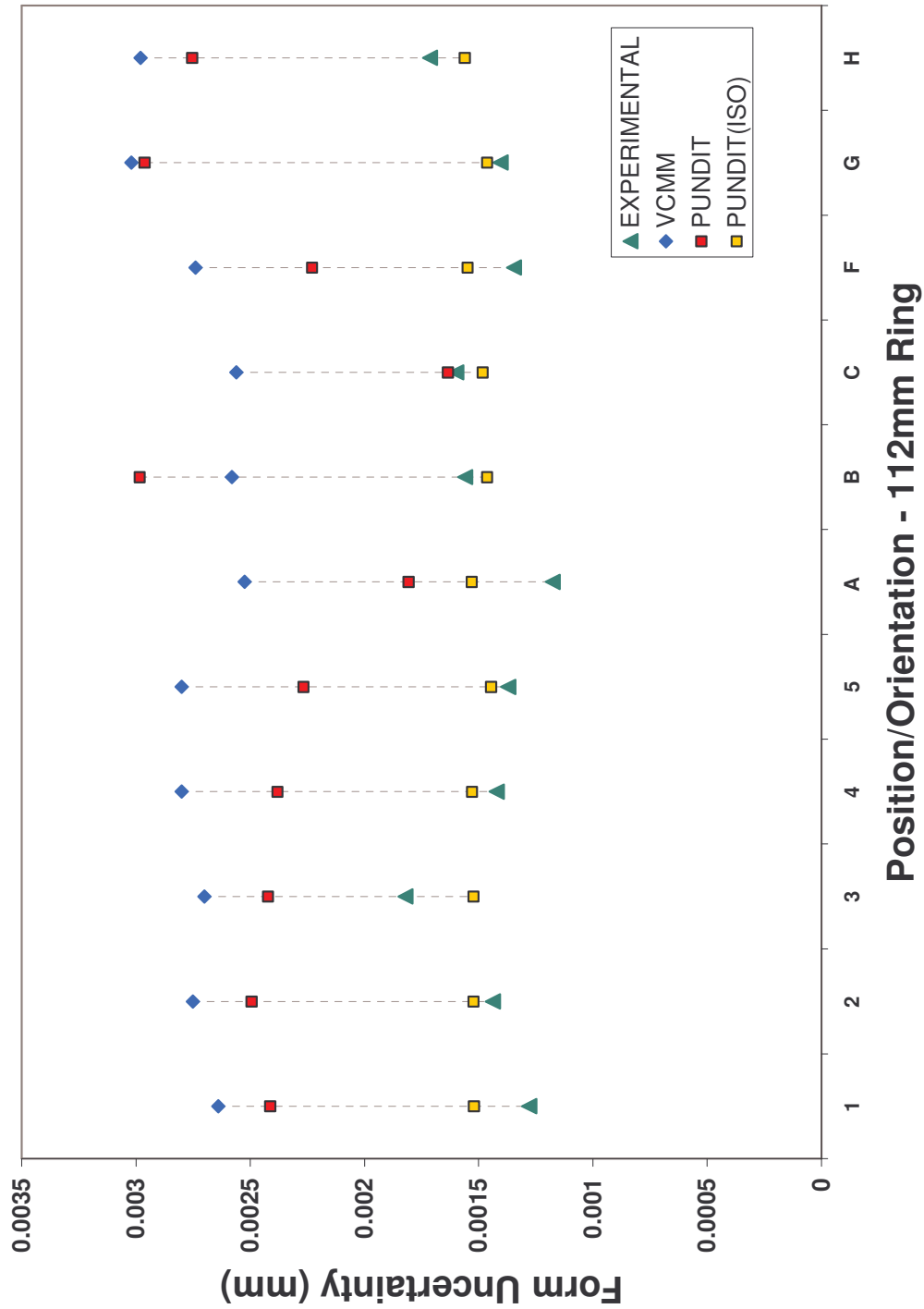


Figure 56: Form Results, 112mm Ring Gage, Averaged by Pos./Or

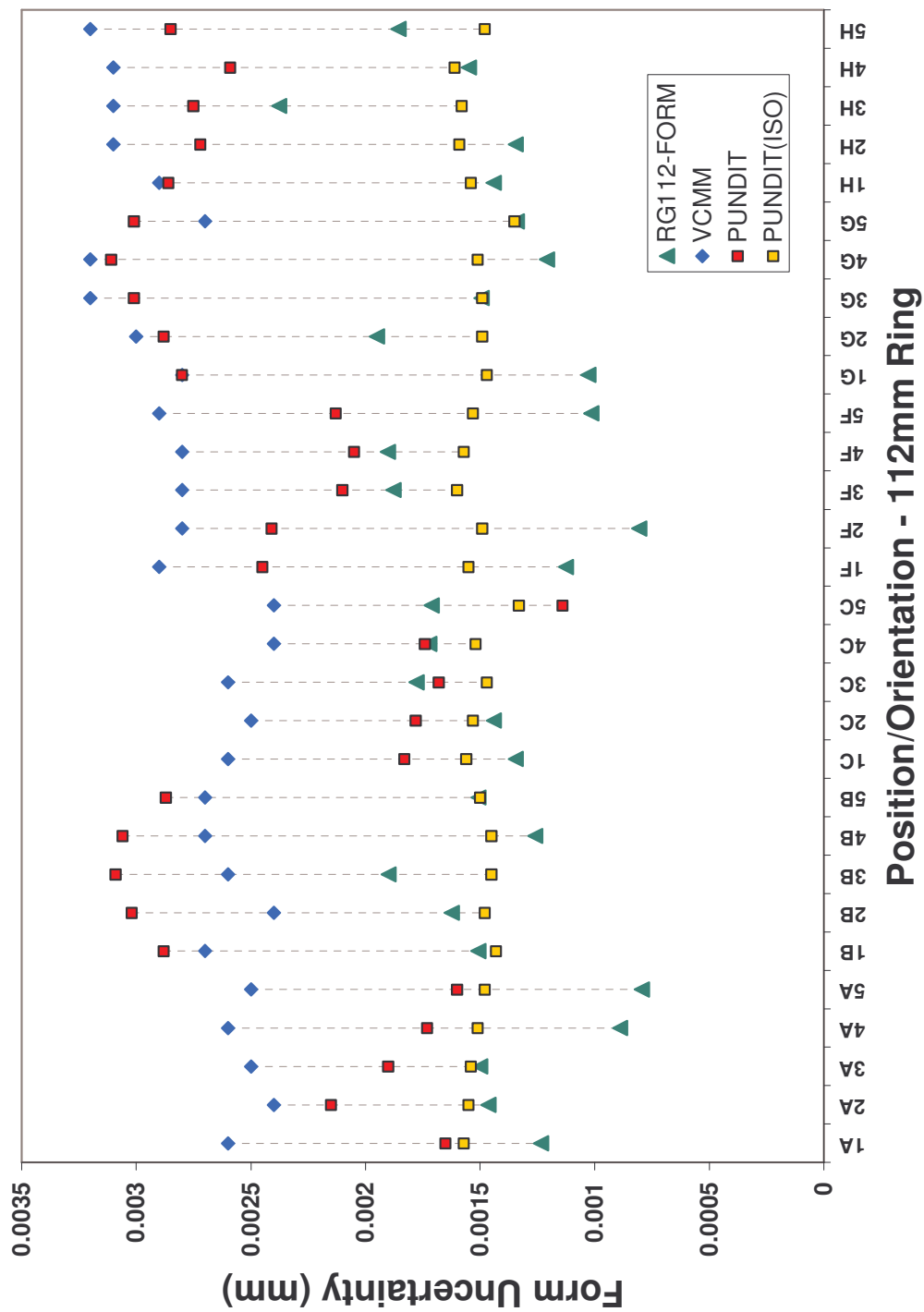


Figure 57: Form Results, 112mm Ring Gage

Table 10: Difference in Simulation and Experiment, Form, 112mm Ring Gage  
 112mm Ring Gage - Difference in Form Uncertainties (Simulation - Experimental) in  
 micrometers

POS.	ORI.	VCMM	PUNDIT(ISO)	PUNDIT(PAR.)
1	A	1.4	0.3	0.4
2	A	0.9	0.1	0.7
3	A	1.0	0.0	0.4
4	A	1.7	0.6	0.8
5	A	1.7	0.7	0.8
1	B	1.2	-0.1	1.4
2	B	0.8	-0.1	1.4
3	B	0.7	-0.4	1.2
4	B	1.4	0.2	1.8
5	B	1.2	0.0	1.4
1	C	1.3	0.2	0.5
2	C	1.1	0.1	0.3
3	C	0.8	-0.3	-0.1
4	C	0.7	-0.2	0.0
5	C	0.7	-0.4	-0.6
1	F	1.8	0.4	1.3
2	F	2.0	0.7	1.6
3	F	0.9	-0.3	0.2
4	F	0.9	-0.3	0.1
5	F	1.9	0.5	1.1
1	G	1.8	0.4	1.8
2	G	1.1	-0.5	0.9
3	G	1.7	0.0	1.5
4	G	2.0	0.3	1.9
5	G	1.4	0.0	1.7
1	H	1.5	0.1	1.4
2	H	1.8	0.2	1.4
3	H	0.7	-0.8	0.4
4	H	1.6	0.1	1.0
5	H	1.3	-0.4	1.0
<b>Average (Absolute Difference)</b>		<b>1.3</b>	<b>0.3</b>	<b>1.0</b>
<b>Maximum (Absolute Difference)</b>		<b>2.0</b>	<b>0.8</b>	<b>1.9</b>

Form uncertainties for the 112mm ring, for both parametric options, are greater than experimental values for nearly all of the test cases. Both of the parametric models show increased values in uncertainty for the increased size of the artifact. The PUNDIT results predict more variability than the VCMM results over the entire range of orientations which matches the variability in the experimental results. The average of the absolute difference values for the PUNDIT(ISO) results was only 0.3 micrometers from



the experimental values though the variability in the experimental cases was not replicated.

#### 4.2.3 Line Tests

Line measurements were conducted on a granite square which was calibrated by way of straightedge reversal (the line was measured on the block, then the block was rotated 180 degrees about the axis of the line, and remeasured at the same locations). The axis was measured in five horizontal and four vertical orientations and positions as shown in Figure 58. The vertical positions are denoted with a 'C'. The axis was approximately 150 mm in length and composed of 20 measurement points.

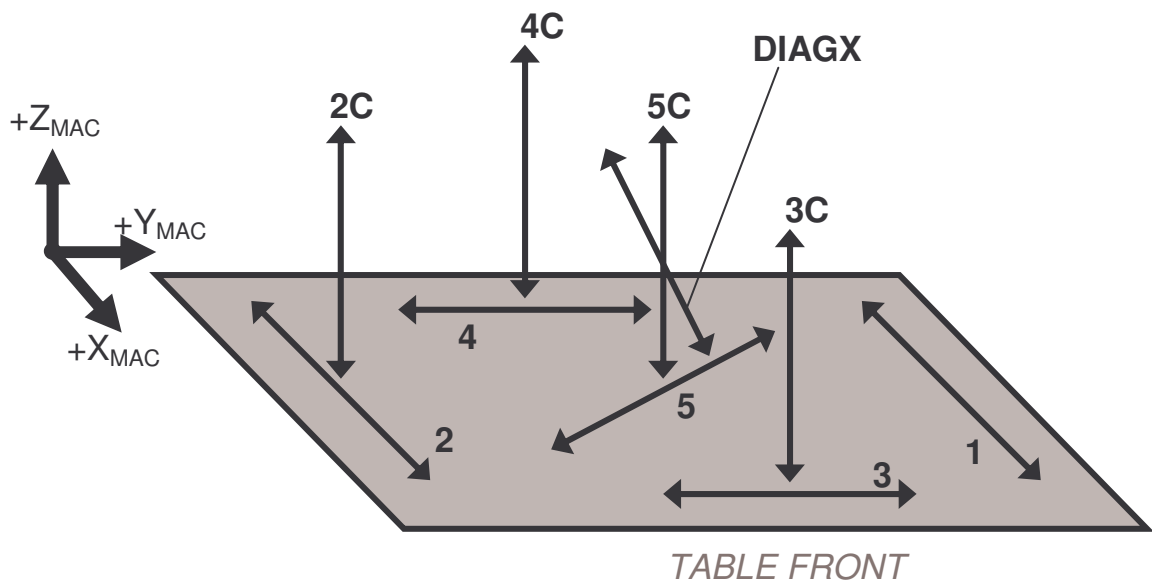


Figure 58: Positions/Orientations for Line Measurement

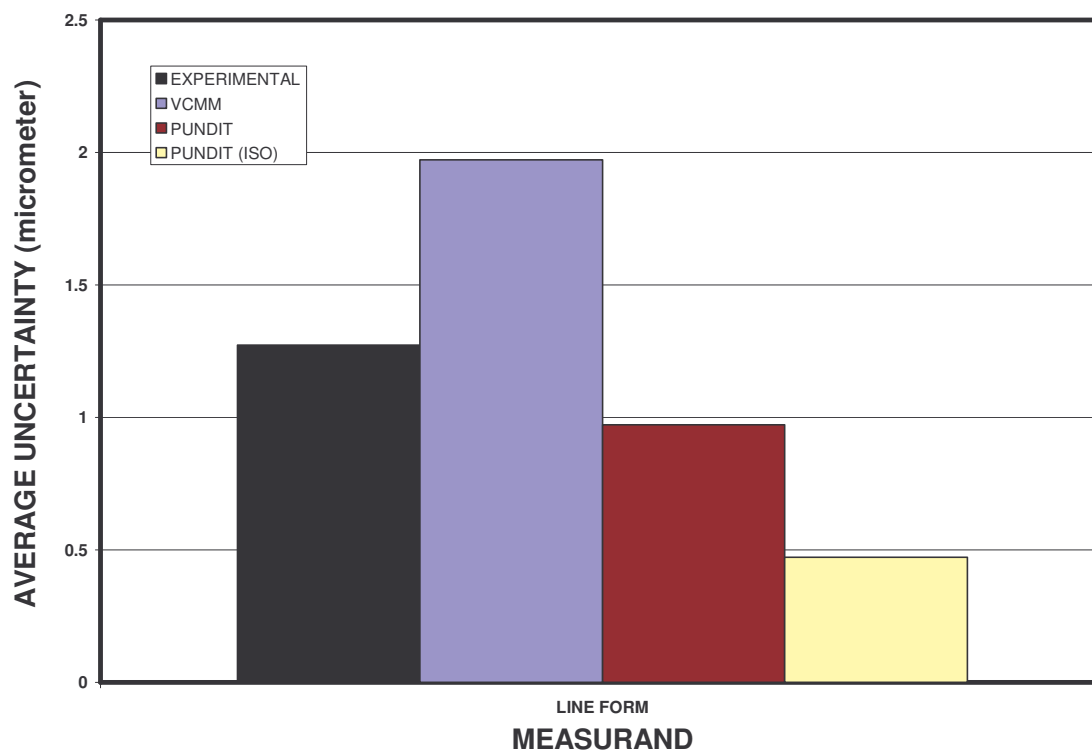


Figure 59: Average of All Line Measurements

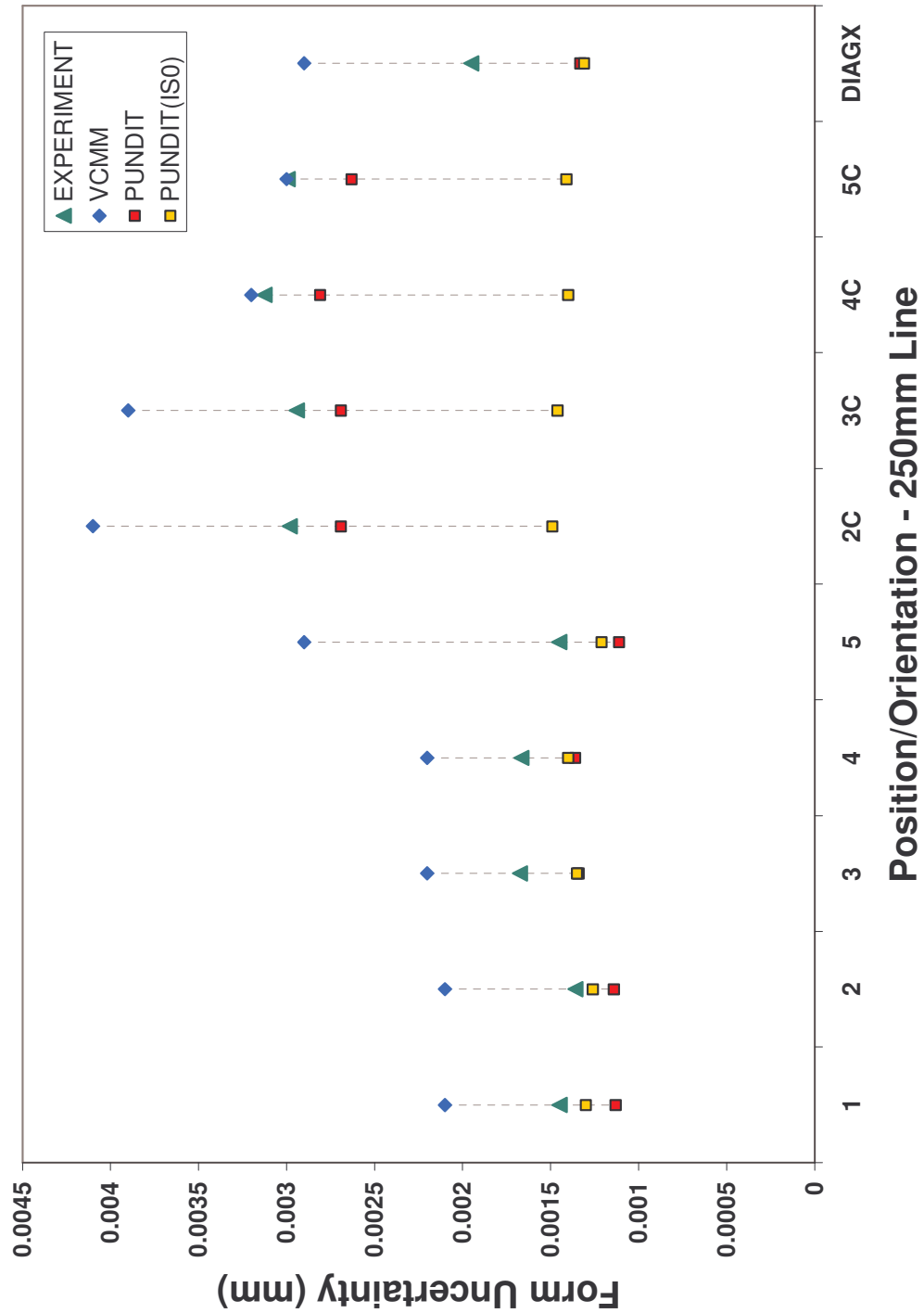


Figure 60: Form Results, 250mm Axis

Table 11: Difference in Simulation and Experiment, Form, 250mm Axis Lines - Difference in Form Uncertainties (Simulation - Experimental) in micrometers

ORI.	VCMM	PUNDIT(ISO)	PUNDIT(PAR.)
1	0.7	-0.1	-0.3
2	0.7	-0.1	-0.2
3	0.5	-0.3	-0.3
4	0.5	-0.3	-0.3
5	1.4	-0.2	-0.3
2C	1.1	-1.5	-0.3
3C	1.0	-1.5	-0.3
4C	0.1	-1.7	-0.3
5C	0.0	-1.6	-0.4
DIAGX	0.9	-0.6	-0.6
<b>Average (Absolute Difference)</b>	<b>0.7</b>	<b>0.8</b>	<b>0.3</b>
<b>Maximum (Absolute Difference)</b>	<b>1.4</b>	<b>1.7</b>	<b>0.6</b>

The parametric simulations show close approximation of actual results, though only VCMM results are greater than the experimental values. While the PUNDIT(ISO) results track closest to the experimental data for the horizontal positions, the lack of orientation dependent modeling does not account for the increased uncertainty when measuring vertically. Both of the parametric models account for this shift in uncertainty value, including the slightly lessened value for the DIAGX position.

#### 4.2.4 Point to Point Distance Tests

Gage blocks were used to evaluate point to point distances. Two smaller gage blocks (25mm measured horizontally and 20mm measured vertically) and a larger gage block (300mm) were measured in the orientations shown in Figure 61 and Figure 62, respectively.

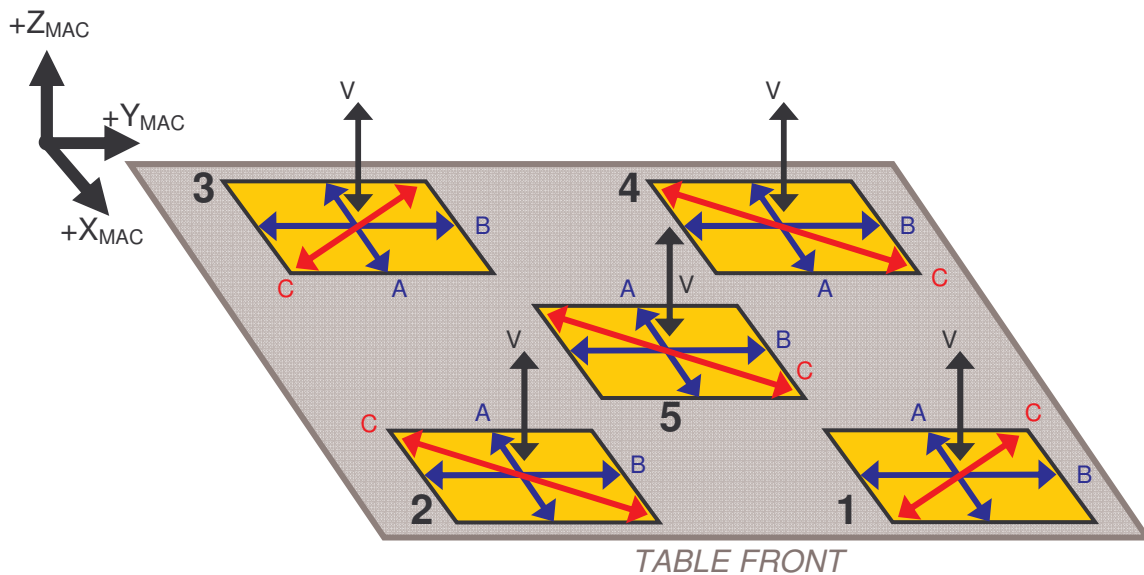


Figure 61: Positions and Orientations for 25mm and 20mm Gage Block

The positions for the 25/20 mm gages are shown as 1-5 with orientations shown as, horizontally, A,B,C and vertically as V. Orientations A were parallel to the X-axis, B to the Y-axis, and C at 45 degrees to the X and Y axes.

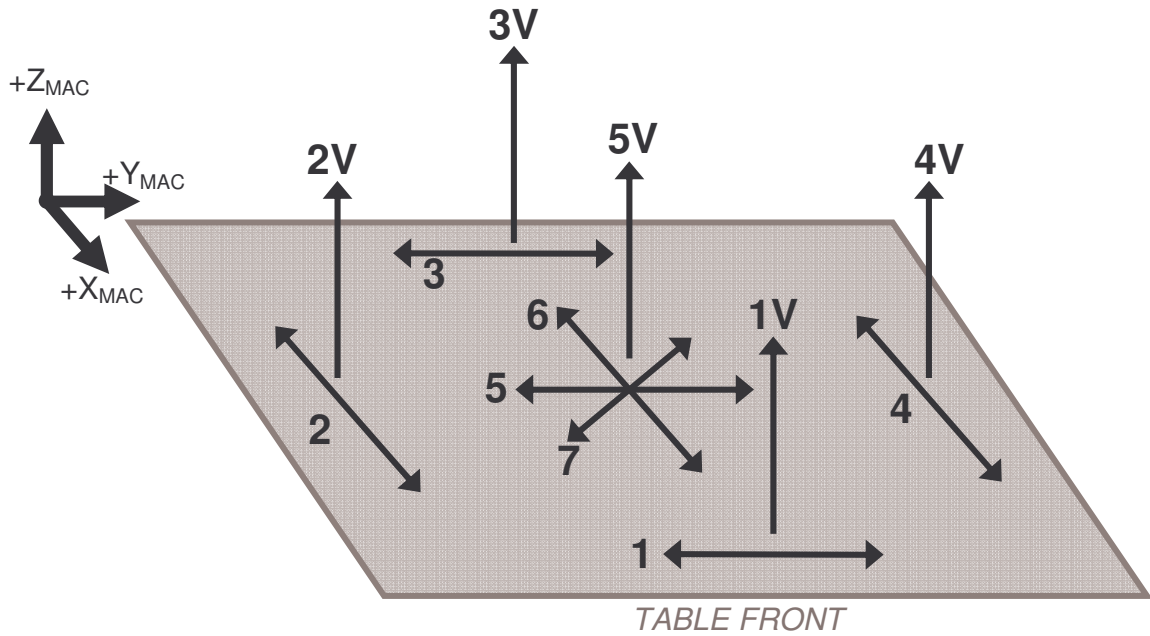


Figure 62: Positions and Orientations for 300mm Gage Block

The positions and orientations are denoted differently for the larger gage to facilitate fixturing. Horizontal positions are 1-7 and the corresponding vertical orientations are denoted with a 'V'. Positions 2,4,6 (even) were oriented parallel to the X-axis, 1,3,5 (odd) parallel to the Y-axis, and 7 at 45 degrees to the X and Y axes.

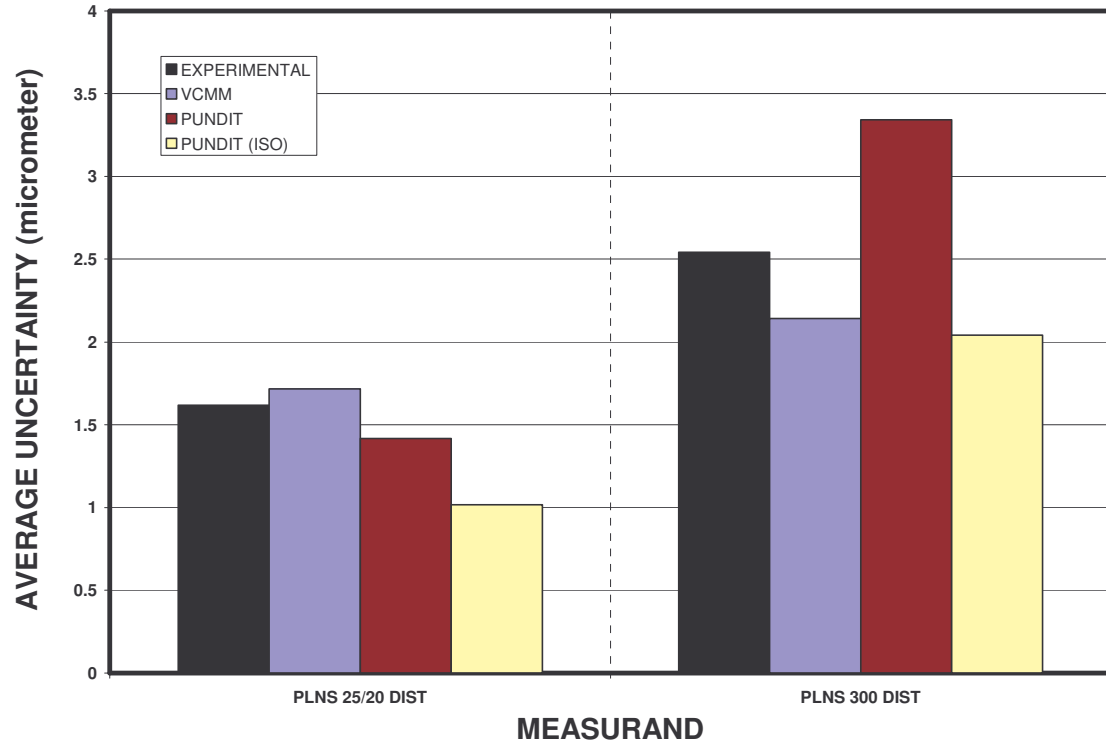


Figure 63: Averages of All Pt. to Pt. Measurements

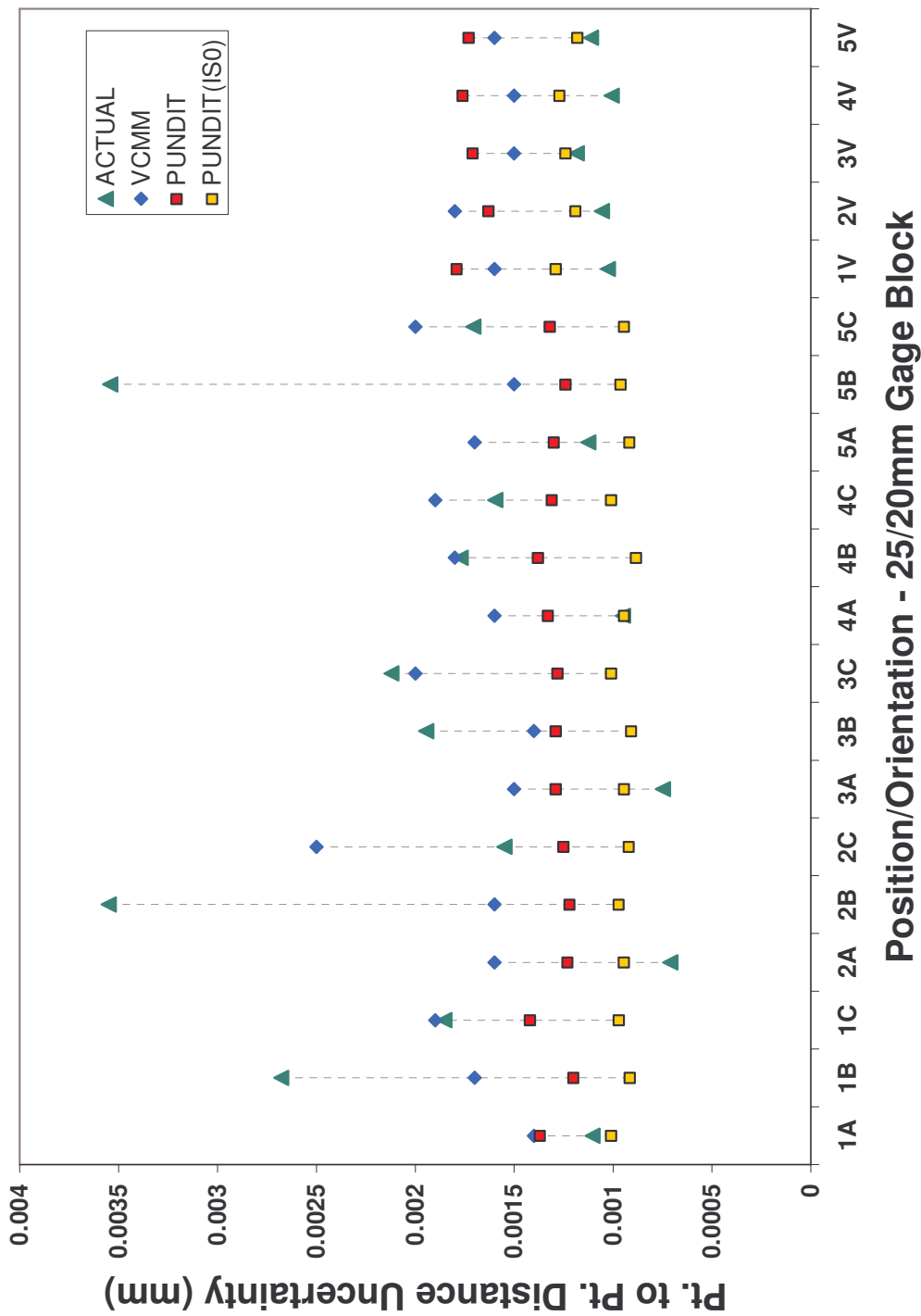


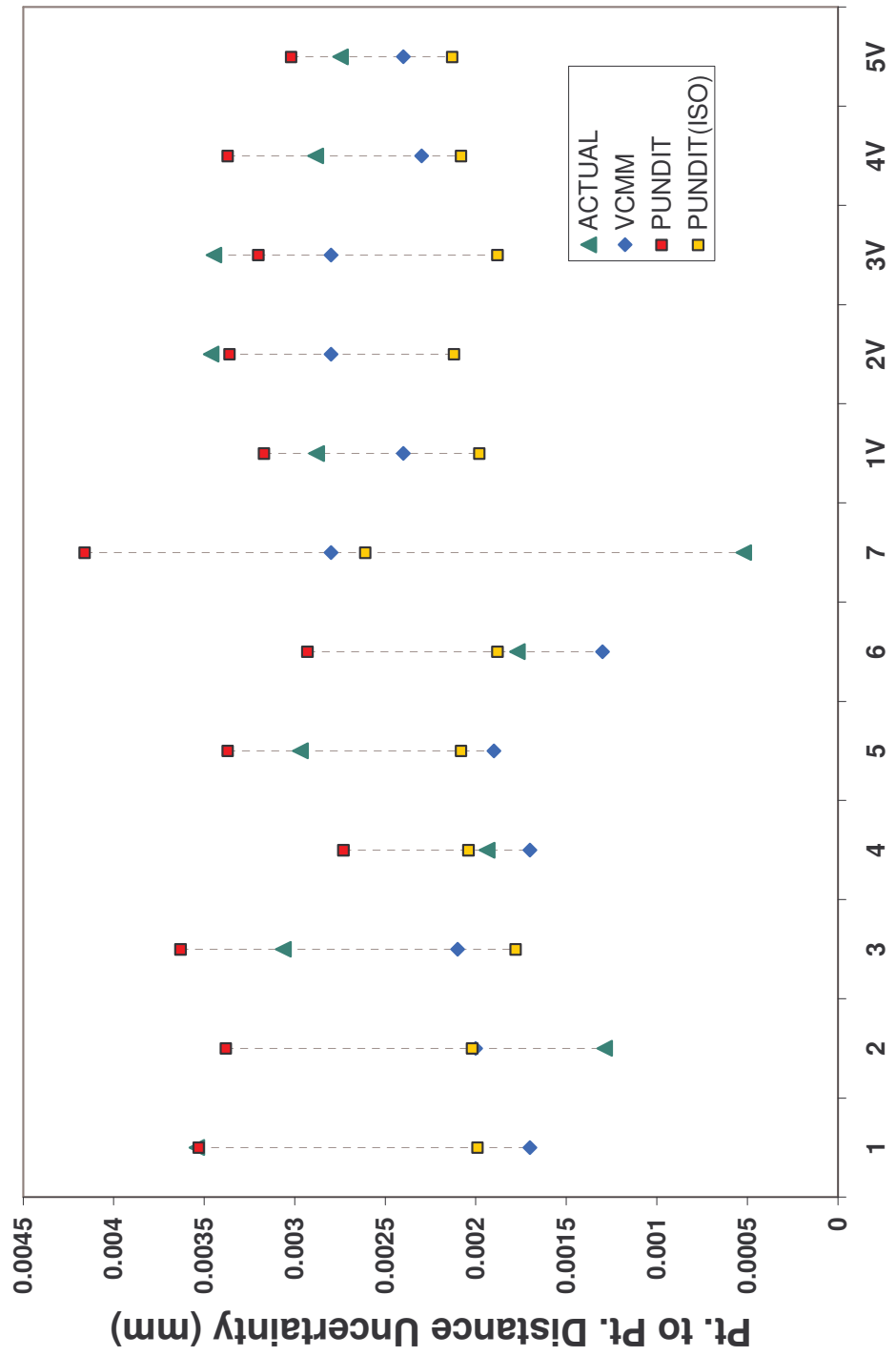
Figure 64: Point to Point Distance Results, 25mm and 20mm Gage Block



Table 12: Difference in Simulation and Experiment, 25mm and 20mm Gage Block Planes 25/20 mm Gage Blocks - Difference in Form Uncertainties (Simulation - Experimental) in micrometers

POS./ORI.	VCMM	PUNDIT(ISO)	PUNDIT(PAR.)
1A	0.3	-0.1	0.3
1B	-1.0	-1.8	-1.5
1C	0.0	-0.9	-0.4
2A	0.9	0.2	0.5
2B	-2.0	-2.6	-2.3
2C	1.0	-0.6	-0.3
3A	0.8	0.2	0.5
3B	-0.5	-1.0	-0.7
3C	-0.1	-1.1	-0.8
4A	0.7	0.0	0.4
4B	0.0	-0.9	-0.4
4C	0.3	-0.6	-0.3
5A	0.6	-0.2	0.2
5B	-2.0	-2.6	-2.3
5C	0.3	-0.8	-0.4
1V	0.6	0.3	0.8
2V	0.7	0.1	0.6
3V	0.3	0.1	0.5
4V	0.5	0.3	0.8
5V	0.5	0.1	0.6
<b>Average (Absolute Difference)</b>	<b>0.7</b>	<b>0.7</b>	<b>0.7</b>
<b>Maximum (Absolute Difference)</b>	<b>2.0</b>	<b>2.6</b>	<b>2.3</b>

While the average of the absolute difference values for the simulation methods were only 0.7 micrometers indicating close approximation of overall uncertainty for the measurand, the variability in the experimental results was not closely modeled, having a range of 2.5 microns. VCMM showed the largest variability among the simulations, at 1.0 micron. The PUNDIT(ISO) values were at the lowest threshold of the experimental data, however they closely tracked the vertical orientation results.



**Position/Orientation - 300mm Gage Block**

Figure 65: Point to Point Distance Results, 300mm Gage Block

Table 13: Difference in Simulation and Experiment, 300mm Gage Block  
 Planes 300 mm Gage Block - Difference in Form Uncertainties (Simulation - Experimental) in  
 micrometers

POS./ORI.	VCMM	PUNDIT(ISO)	PUNDIT(PAR.)
1	-1.8	-1.6	0.0
2	0.7	0.7	2.1
3	-1.0	-1.3	0.6
4	-0.2	0.1	0.8
5	-1.1	-0.9	0.4
6	-0.5	0.1	1.2
7	2.3	2.1	3.6
1V	-0.5	-0.9	0.3
2V	-0.7	-1.3	-0.1
3V	-0.6	-1.6	-0.2
4V	-0.6	-0.8	0.5
5V	-0.3	-0.6	0.3
<b>Average (Absolute Difference)</b>	<b>0.9</b>	<b>1.0</b>	<b>0.8</b>
<b>Maximum (Absolute Difference)</b>	<b>2.3</b>	<b>2.1</b>	<b>3.6</b>

For the larger 300mm gage, the average absolute difference between the simulations and the experimental results ranged from 0.8 micrometers to 1.0 micrometers. In this case, the PUNDIT parametric results closely track the experimental uncertainties when considering relative variation for differing positions and orientations (excepting orientation 7) while the VCMM results tracked well in the vertical orientations. The overall experimental variation was again larger for the experimental data at ~3.0 microns. VCMM had the largest variation at ~2.0 microns.

#### 4.2.5 Sphere Tests

All of the sphere measurements were conducted with a  $-Z$  probe in five positions. Positions 1 and 2 were at the front of the table, positions 3 and 4 at the back of the table, and position 5 at the center of the table. Two artifacts were measured, the smaller sphere was a steel calibration sphere with a diameter of 19.049mm and the larger sphere was a glass 'fishbowl' of ~250mm. A total of 15 measurement points were used to measure the smaller sphere and 29 were used for measuring the larger sphere.

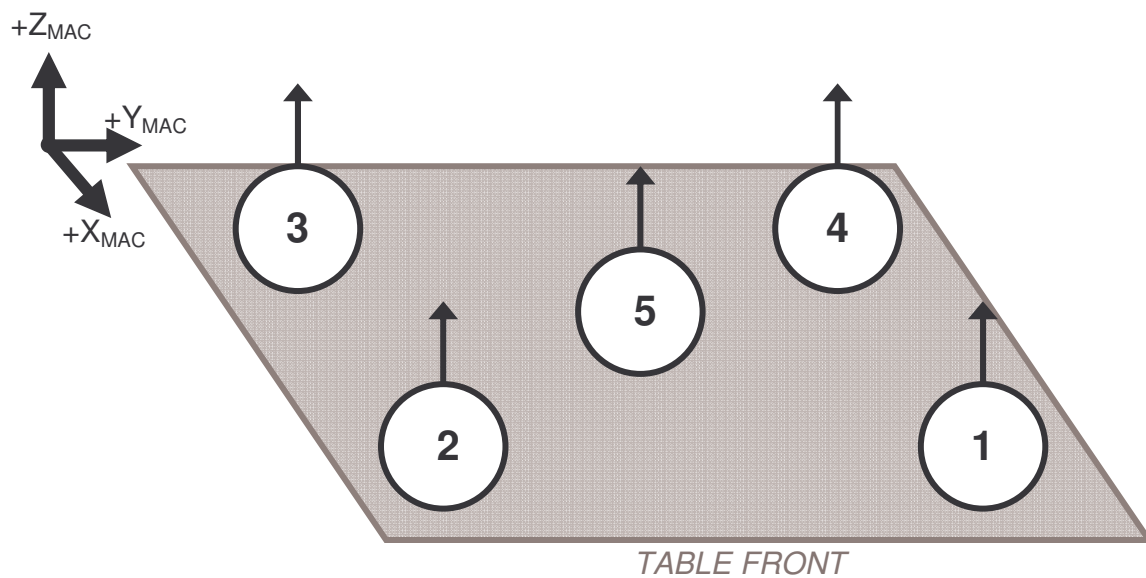


Figure 66: Positions/Orientations for Sphere Measurement

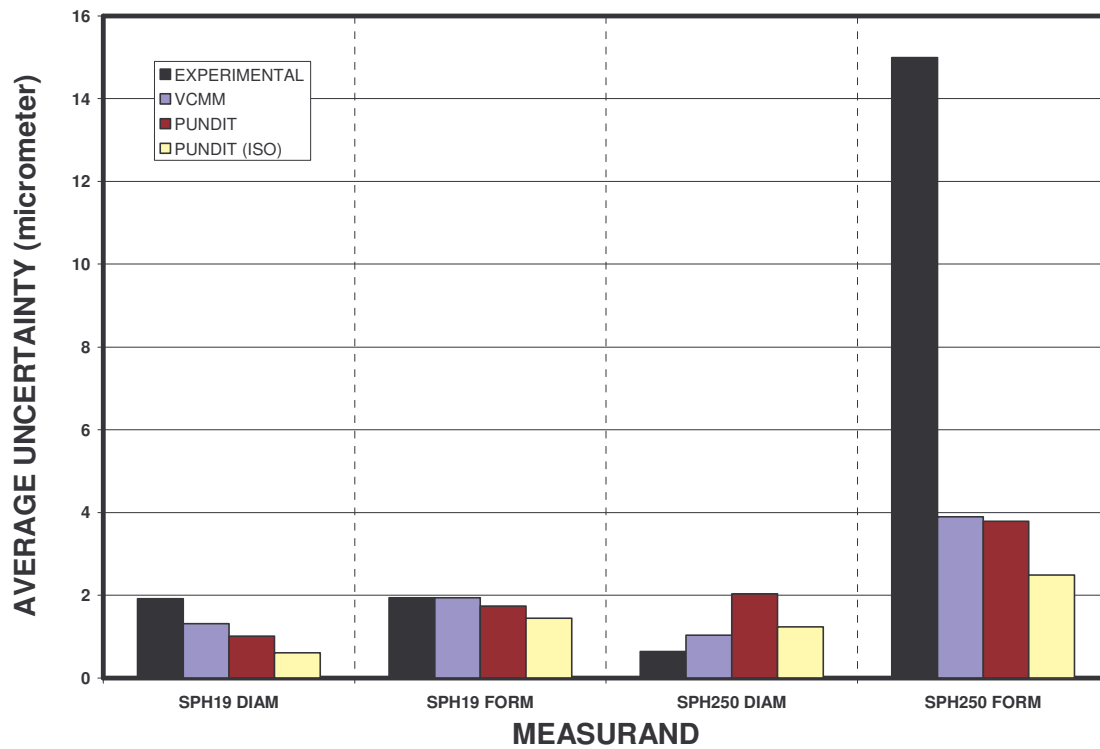
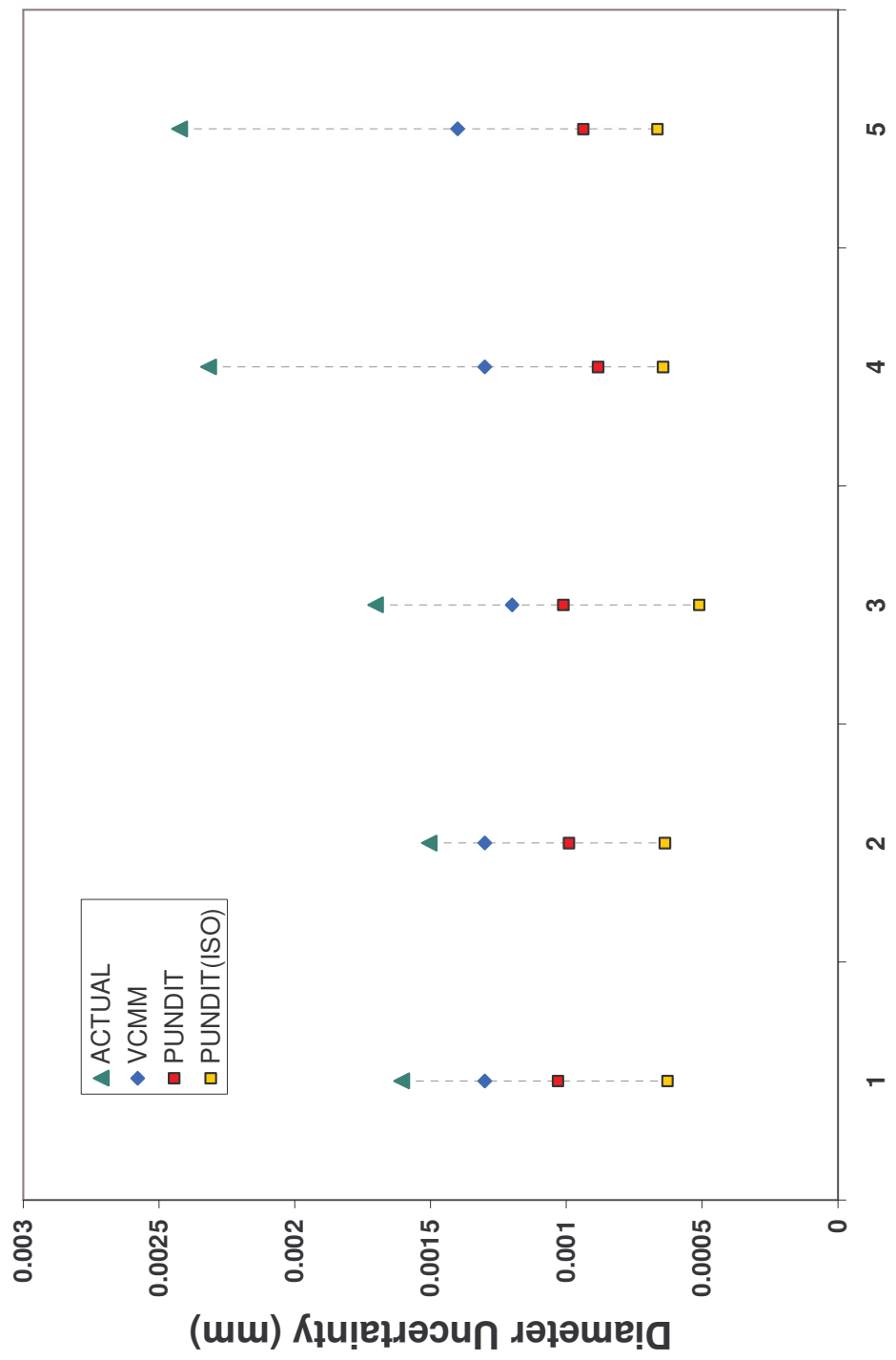


Figure 67: Averages of All Sphere Measurements



**Position/Orientation - 19.049mm Sphere**

Figure 68: Diameter Results, 19.049mm Sphere

Table 14: Difference in Simulation and Experiment, Diameter 19.049mm Sphere  
 19.049mm Sphere- Difference in Diameter Uncertainties (Simulation - Experimental) in  
 micrometers

POS./ORI.	VCMM	PUNDIT(ISO)	PUNDIT(PAR.)
1	-0.3	-1.0	-0.6
2	-0.2	-0.9	-0.5
3	-0.5	-1.2	-0.7
4	-1.0	-1.7	-1.4
5	-1.0	-1.8	-1.5
<b>Average (Absolute Difference)</b>	<b>0.6</b>	<b>1.3</b>	<b>0.9</b>
<b>Maximum (Absolute Difference)</b>	<b>1.0</b>	<b>1.8</b>	<b>1.5</b>

All of the simulation results for diameter uncertainty of the 19.049mm sphere were less than the experimental results. The PUNDIT and PUNDIT(ISO) results varied from the experimental results by an average absolute difference of 0.9 micrometers and 1.3 micrometers and the VCMM results by 0.6 micrometers. Additionally, the variation of ~1.0 microns for the experimental results was greater than the variation exhibited by the parametric simulations which had variations of ~0.5 microns.

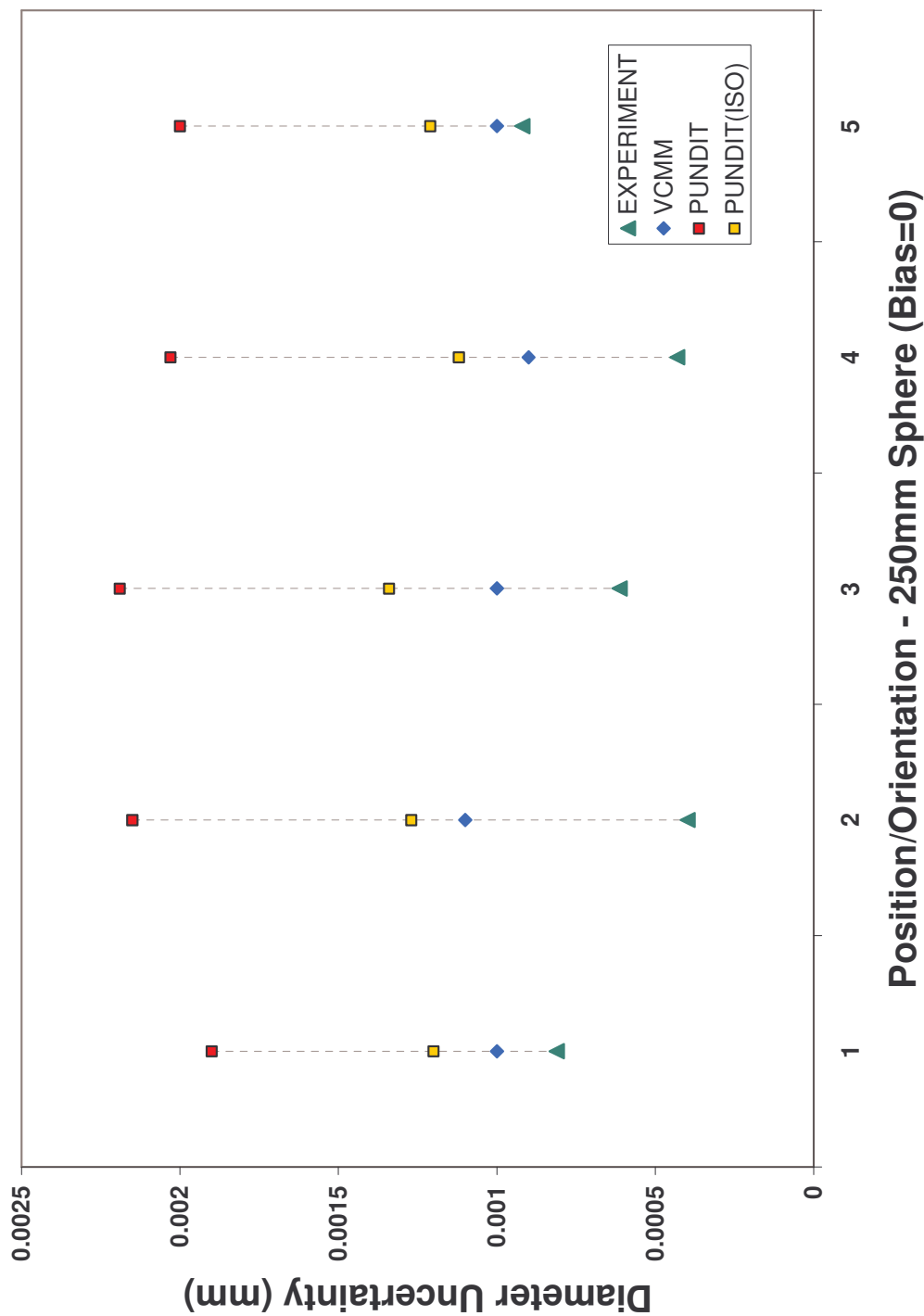


Figure 69: Diameter Results, 250mm Sphere



Table 15: Difference in Simulation and Experiment, Diameter 250mm Sphere  
 250mm Sphere- Difference in Diameter Uncertainties (Simulation - Experimental) in  
 micrometers

POS./ORI.	VCMM	PUNDIT(ISO)	PUNDIT(PAR.)
1	0.2	0.4	1.1
2	0.7	0.9	1.8
3	0.4	0.7	1.6
4	0.5	0.7	1.6
5	0.1	0.3	1.1
<b>Average (Absolute Difference)</b>	<b>0.4</b>	<b>0.6</b>	<b>1.4</b>
<b>Maximum (Absolute Difference)</b>	<b>0.7</b>	<b>0.9</b>	<b>1.8</b>

The experimental results for the 250mm sphere are incomplete as the calibrated value for the diameter is unknown. The results shown exhibit a diameter bias of zero. Given the dimension of the sphere a bias on the order of 1.0 to 2.0microns might be expected; however given the large form values of ~14.0microns it is difficult to rely on an estimate at this time. A comparison of the simulated results shows the PUNDIT case to be approximately 1.0 micrometer greater than the VCMM average of absolute differences. The variations of the parametric simulations results is approximately equal though slightly less than that of the experimental uncertainties.

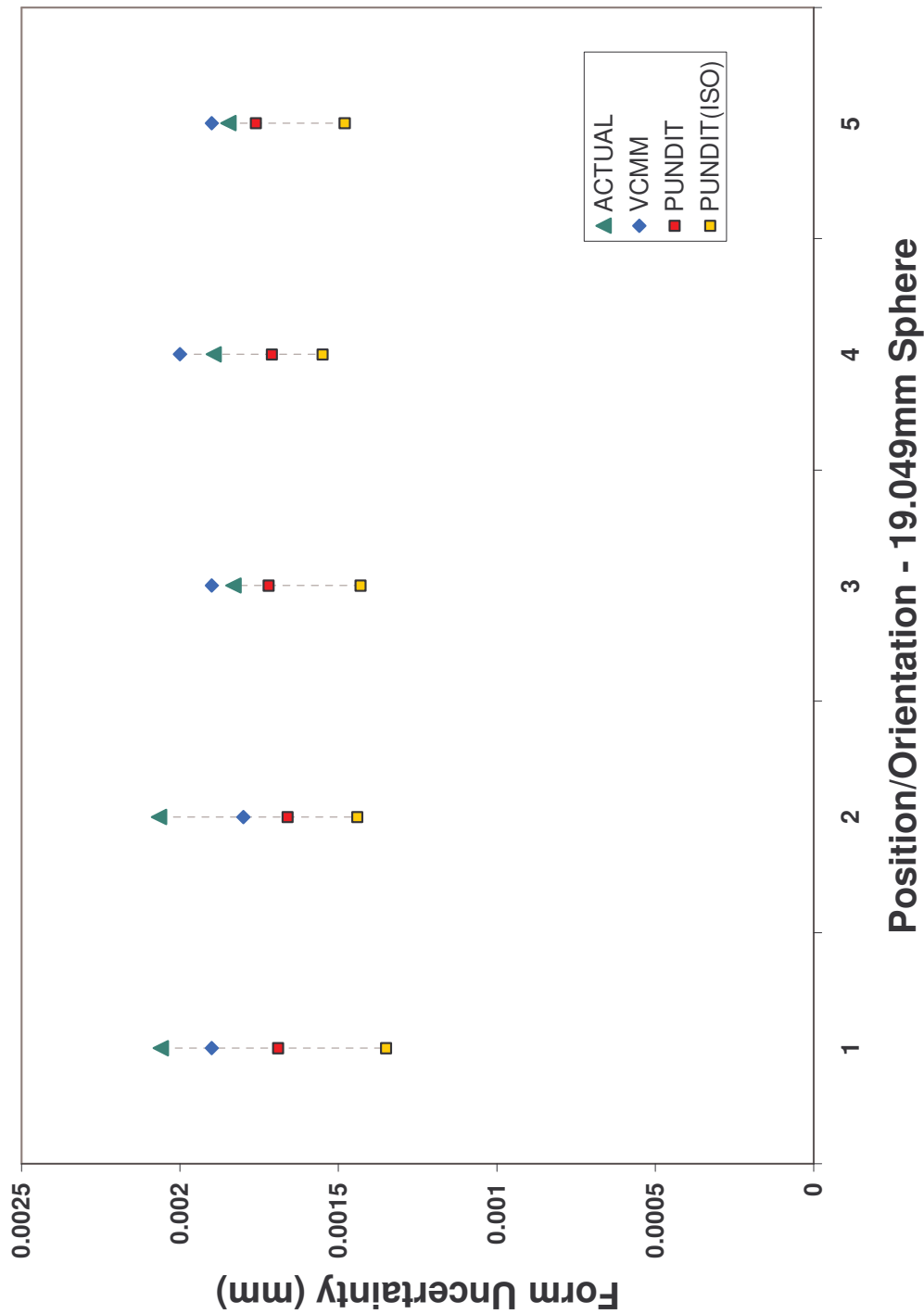


Figure 70: Form Results, 19.049mm

Table 16: Difference in Simulation and Experiment, Form 19.049mm Sphere  
 19.049mm Sphere- Difference in Form Uncertainties (Simulation - Experimental) in  
 micrometers

POS./ORI.	VCMM	PUNDIT(ISO)	PUNDIT(PAR.)
1	-0.2	-0.7	-0.4
2	-0.3	-0.6	-0.4
3	0.1	-0.4	-0.1
4	0.1	-0.3	-0.2
5	0.1	-0.4	-0.1
<b>Average (Absolute Difference)</b>	<b>0.2</b>	<b>0.5</b>	<b>0.2</b>
<b>Maximum (Absolute Difference)</b>	<b>0.3</b>	<b>0.7</b>	<b>0.4</b>

The form uncertainty results for the smaller sphere show close agreement with the parametric simulations with VCMM averaging an equal value to the experimental data uncertainties. The PUNDIT(ISO) values are the furthest from the experimental values, by an average absolute difference of 0.5 micrometers. The range of variation of both parametric simulations is also approximately equal to the variation in the experimental results.

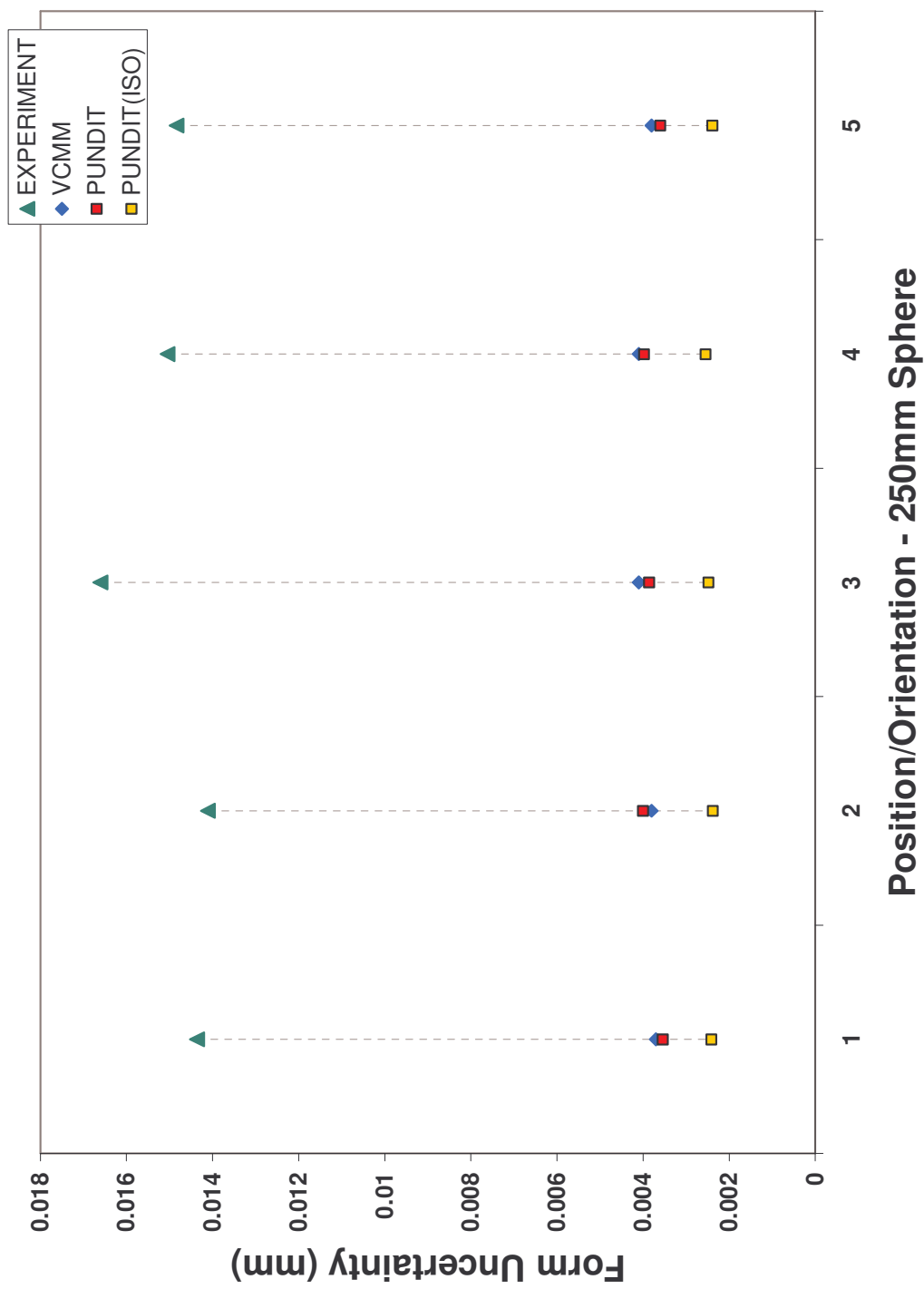


Figure 71: Form Results. 250mm Sphere

Table 17: Difference in Simulation and Experiment, Form 250mm Sphere  
 250mm Sphere- Difference in Form Uncertainties (Simulation - Experimental) in  
 micrometers

POS./ORI.	VCMM	PUNDIT(ISO)	PUNDIT(PAR.)
1	-10.7	-12.0	-10.8
2	-10.3	-11.7	-10.1
3	-12.5	-14.1	-12.7
4	-10.9	-12.5	-11.1
5	-11.0	-12.4	-11.2
<b>Average (Absolute Difference)</b>	<b>11.1</b>	<b>12.5</b>	<b>11.2</b>
<b>Maximum (Absolute Difference)</b>	<b>12.5</b>	<b>14.1</b>	<b>12.7</b>

Form uncertainty results for the 250mm sphere experimental data are not reliable in comparison to simulated values since the nature of the form error is unknown at this time. The magnitude of the form error is ~14.0microns. Results for the parametric simulations are comparable to within ~0.1 micrometers when considering the average of the absolute difference values, while the PUNDIT(ISO) values are ~1.5 micrometers greater than the parametric cases.

#### 4.2.6 Cylinder Tests

The cylinder test measurements were conducted on a 100mm cylindrical square artifact. The orientation of the artifact was not changed, with the cylinder axis parallel to the Z-axis of the machine. However as shown in Figure 72, four probing orientations were used (A,B,C,D). Probe orientations A and C were parallel to the X-axis and B and D were parallel to the Y-axis. Measurement positions of the artifact were located at 1-5, with 1 and 2 at the front of the table, 3 and 4 at the back of the table, and 5 at the center of the table. The cylinder measured length was ~250.0 mm and was measured with 33 points divided evenly at three levels along the cylinder axis.

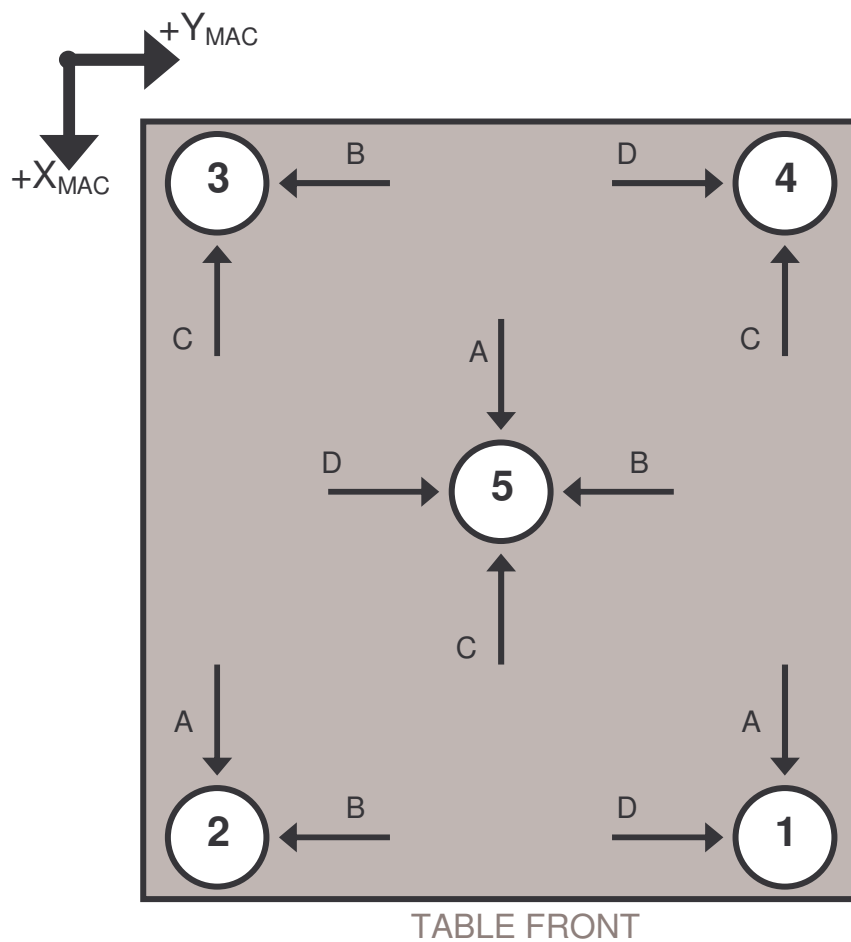


Figure 72: Positions/Orientations for 100mm Cylinder

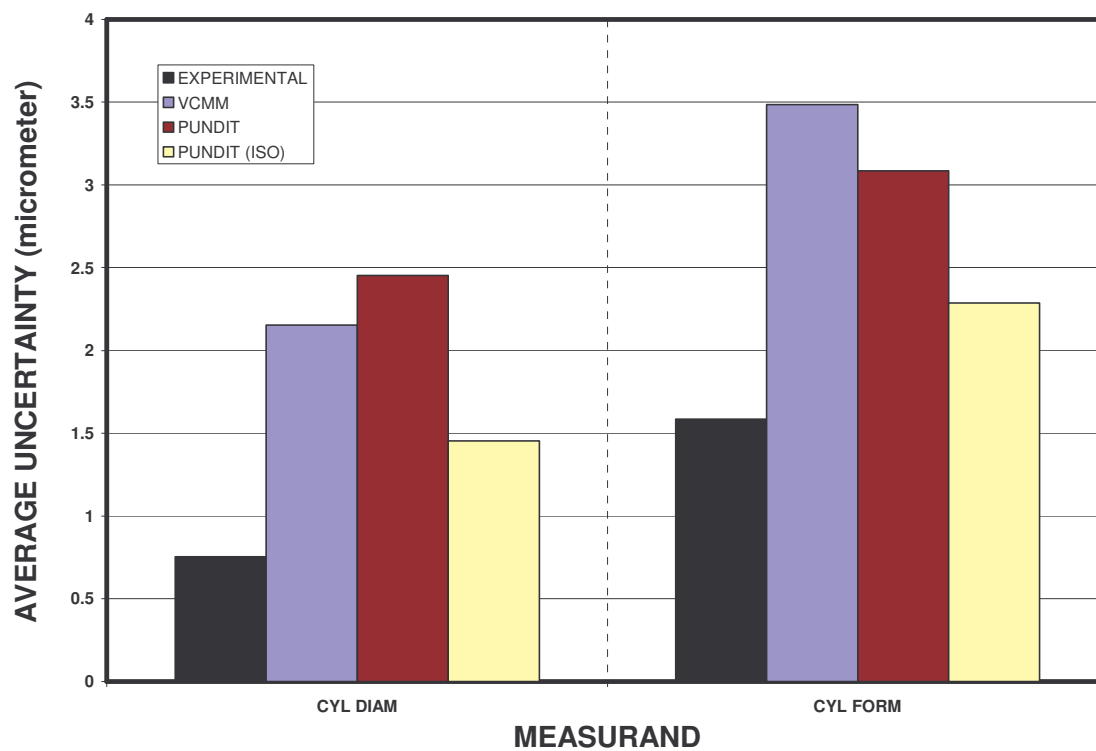


Figure 73: Averages of All Cylinder Measurements

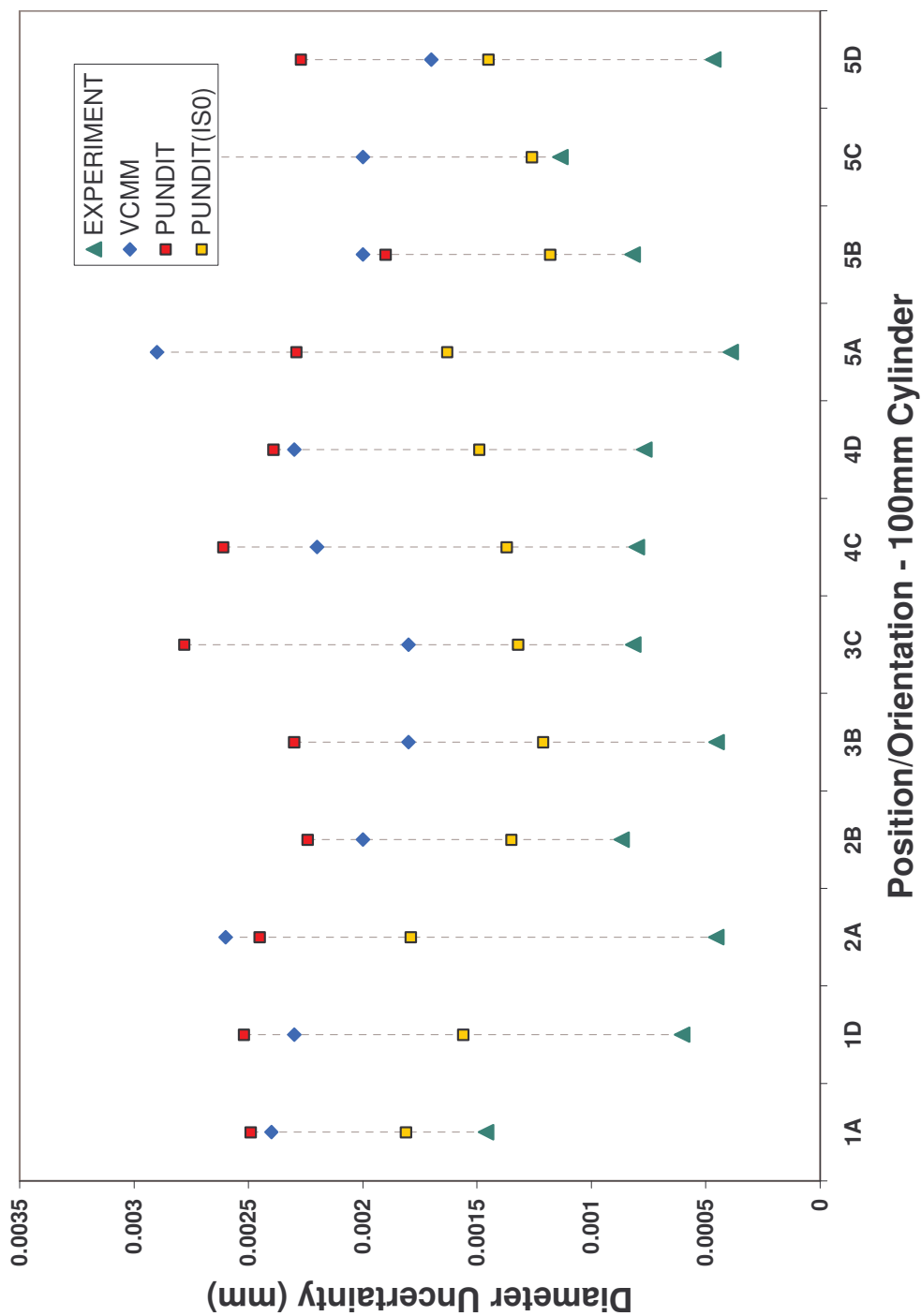


Figure 74: Diameter Results, 100mm Cylinder



Table 18: Difference in Simulation and Experiment, Diameter, 100mm Cylinder  
Cylinders - Difference in Diameter Uncertainty (Simulation-Experiment) in  
micrometers

POS/ORI	VCMM	PUNDIT(ISO)	PUNDIT(PAR.)
1A	0.9	0.3	1.0
1D	1.7	1.0	1.9
2A	2.1	1.3	2.0
2B	1.1	0.5	1.4
3B	1.3	0.8	1.8
3C	1.0	0.5	2.0
4C	1.4	0.6	1.8
4D	1.5	0.7	1.6
5A	2.5	1.2	1.9
5B	1.2	0.4	1.1
5C	0.9	0.1	1.5
5D	1.2	1.0	1.8
<b>Average (Absolute Difference)</b>	<b>1.4</b>	<b>0.7</b>	<b>1.7</b>
<b>Maximum (Absolute Difference)</b>	<b>2.5</b>	<b>1.3</b>	<b>2.0</b>

All of the simulations exceed the experimental uncertainty values for diameter. However, the cylinder artifact is not calibrated for diameter. Estimates of bias may be attainable by comparison to prior ring gage measurements of approximately 112mm. The value in that case is ~1.0microns. Adding this to the uncertainty result would place the experimental values at approximately those of the simulation data. Comparison to the parametric data show that the variation of uncertainty values to be in agreement with the variation of the experimental data though the variations do not track those of the experimental data. Comparison of the parametric simulations shows the average absolute difference varies about 0.3 micrometers, while the PUNDIT(ISO) values are less than these by ~1.0 micrometers.

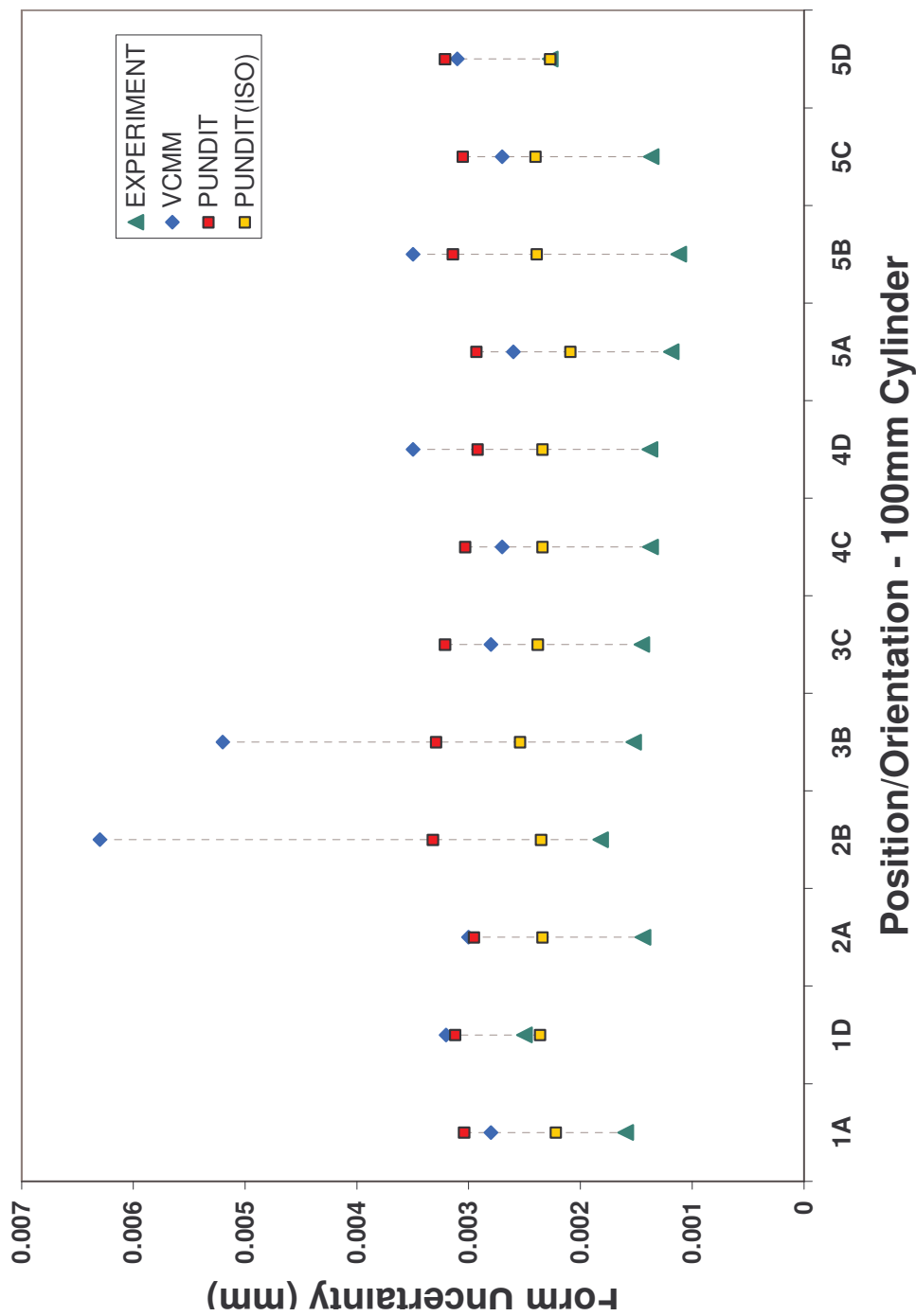


Figure 75: Form Results, 100mm Cylinder

Table 19: Difference in Simulation and Experiment, Form, 100mm Cylinder  
Cylinders - Difference in Form Uncertainty (Simulation-Experiment) in micrometers

POS/ORI	VCMM	PUNDIT(ISO)	PUNDIT(PAR.)
1A	1.2	0.6	1.4
1D	0.7	-0.1	0.6
2A	1.6	0.9	1.5
2B	4.5	0.5	1.5
3B	3.7	1.0	1.8
3C	1.4	0.9	1.8
4C	1.3	1.0	1.7
4D	2.1	1.0	1.5
5A	1.4	0.9	1.7
5B	2.4	1.3	2.0
5C	1.3	1.0	1.7
5D	0.8	0.0	0.9
<b>Average (Absolute Difference)</b>	<b>1.9</b>	<b>0.8</b>	<b>1.5</b>
<b>Maximum (Absolute Difference)</b>	<b>4.5</b>	<b>1.3</b>	<b>2.0</b>

The experimental form uncertainties show closest agreement to the PUNDIT(ISO) results. The average absolute differences for the parametric simulations range from 1.5 micrometers to 1.9 micrometers and track very closely together, though the VCMM data show a large spike in uncertainty for position/orientations 2B and 3B. Possible causes for this are large values in parametric error at the extents of the rotational errors involving the Z axis. Ball plate measurement in the Z direction did not cover the full extent of the Z-axis (~290mm/400mm). KALKOM, when calculating the parametric errors, extrapolates the errors to beyond the range of actual measurement to fill data to the extents of the machine axis. As a result, larger errors can result from an improperly constrained curve fit. Since the cylinder measurements reach in excess of 300mm +Z, this is likely an effect. Tests with 'perfect' plate data show the uncertainty value decreases for these cases (~1.0micron), however, reducing only the Z rotational errors artificially shows no decrease in the uncertainty values. The cause may be a combination of effects, including positional errors, rotational errors, and probe errors in the VCMM

model, since the other B orientation (5B) does not show the large increase in uncertainty and the PUNDIT results do not show the increase either, using the same parametric error data.

#### 4.2.7 Summary by Measurand

Data composed of average values from all of the measurand experiments is summarized below in Table 20 through **Error! Reference source not found.**

**Table 20: Absolute Difference – Measurand Summary**

**AVERAGES OF ABSOLUTE DIFFERENCES**  
 Difference = (simulation-experiment)  
 Avg. Absolute Deviation = mean[absolute(Difference)]

		VCMM	PUNDIT (ISO)	PUNDIT	EXPERIMENTAL
CIR25	DIAM	0.4	0.7	0.5	1.2
CIR25	FORM	0.5	0.3	0.5	1.1
CIR112	DIAM	0.4	0.3	0.6	1.0
CIR112	FORM	1.3	0.3	1.0	1.5
CYL	DIAM	1.4	0.7	1.7	0.8
CYL	FORM	1.9	0.8	1.5	1.6
LINE	FORM	0.7	0.8	0.3	1.3
PLNS 25/20	DIST	0.7	0.7	0.7	1.6
PLNS 300	DIST	0.9	1.0	0.8	2.5
SPH19	DIAM	0.6	1.3	0.9	1.9
SPH19	FORM	0.1	0.5	0.2	1.9
SPH250	DIAM	0.4	0.6	1.4	0.6
SPH250	FORM	11.1	12.5	11.2	15.0
<b>Avg. All</b>		<b>1.6</b>	<b>1.6</b>	<b>1.6</b>	
<b>Average (excluding sphere form)</b>		<b>0.8</b>	<b>0.7</b>	<b>0.9</b>	

The average of the absolute differences shows, regardless of sign, the average deviation of simulated from experimental estimates for uncertainty. Table 20 is a summary of these values for each measurand, and indicates an overall performance of the simulation. Most of the estimates are 1.0 micrometer or less and none of the results exceeds 2.0 micrometers, excepting the large sphere form case. (Values greater than 1.0 micrometer are shown in red text). The average of all measurands, for each simulation method, is also given. The indication is that all of the software simulations were very

close in comparison to each other, PUNDIT (ISO) with 0.7 micrometers average deviation, VCMM with 0.8 micrometers, and PUNDIT (parametric) with 0.9 micrometers.

**Table 21: Maximum Deviations – Measurand Summary**  
**MAXIMUM ABSOLUTE DIFFERENCE**

		VCMM	PUNDIT (ISO)	PUNDIT
CIR25	DIAM	1.0	1.4	1.3
CIR25	FORM	1.2	1.1	1.2
CIR112	DIAM	1.1	0.9	1.7
CIR112	FORM	2.0	0.8	1.9
CYL	DIAM	2.5	1.3	2.0
CYL	FORM	4.5	1.3	2.0
LINE	FORM	1.4	1.7	0.6
PLNS 25/20	DIST	2.0	2.6	2.3
PLNS 300	DIST	2.3	2.1	3.6
SPH19	DIAM	1.0	1.8	1.5
SPH19	FORM	0.3	0.7	0.4
SPH250	DIAM	0.7	0.9	1.8
SPH250	FORM	12.5	14.1	12.7

A summary of the maximum deviations of simulation from experiment is shown in Table 21. The values are the maximum difference in uncertainty for any one test case of the measurand indicated. With few exceptions, the values lie between 1.0 micrometer and 2.0 micrometers and only two (excluding the large sphere form) exceed 3.0 micrometers. (Values exceeding 2.0 micrometers are shown in red text). This indicates, in general, the maximum amount that each software deviated for a particular test case. Comparing the values of each simulation to each other also indicates no significant differences, with the notable exception of VCMM for the cylinder form case.

#### 4.2.8 Notes on Findings

The point to point tests in particular showed exceptionally large variation in experimental results on the order of ~3.0 microns, independent of size. This result is unexpected, especially for the smaller 25mm gage block. This might bring into question

the validity of the ISO 10360-2 values for this particular machine. After running some test measurements on a short gage block in various combinations of position and orientation, probe configuration, and varied calibration artifact, it was determined that the source of the error lies in the calibration measurement but not likely with the calibration artifact, probe styli type, or environmental conditions. The plots below show typical results from one of the tests in which the CMM was set to automatically measure a short gage block (8 times) and recalibrate in a continuous loop (in this case for 60 cycles). The routine actually measures the block first using the newest calibration and then reverts to the first calibration before recalibrating for the next cycle, so simultaneous comparison can be made. In the figure below, the darker line shows the average (of 8 measurements) error for each cycle measured with the new calibration 'PRB(i)', and the lighter line show the errors for the first calibration 'PRB(1)'.

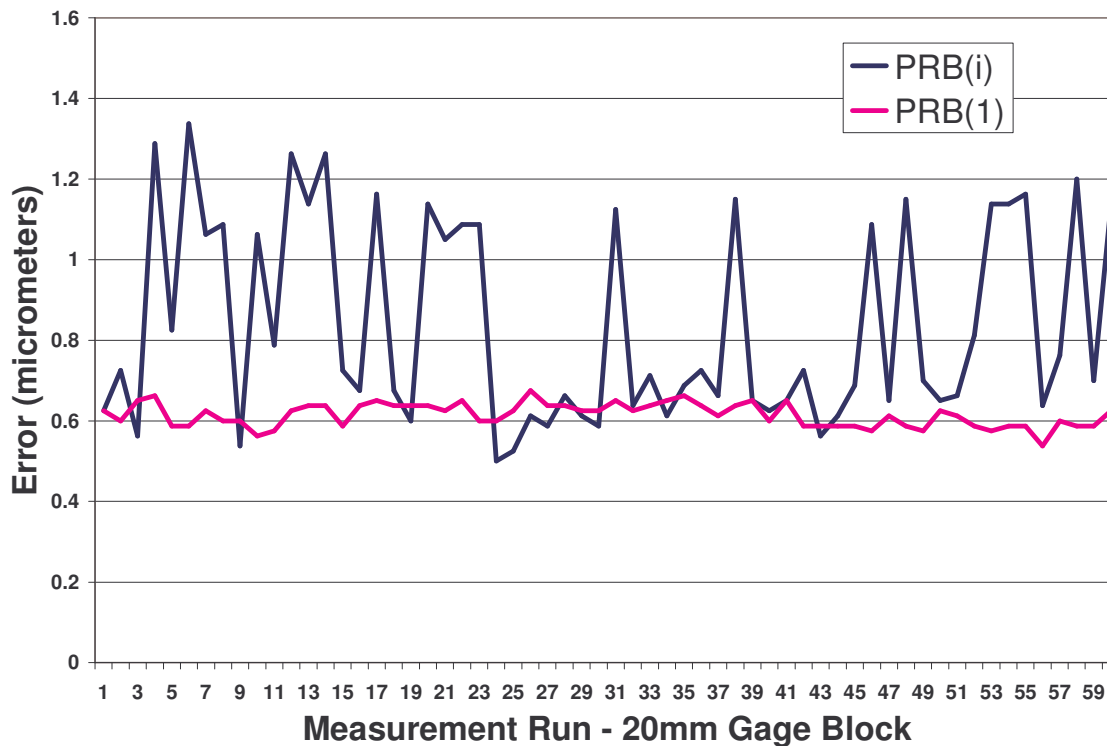


Figure 76: Comparison of Consecutive Measurement of a 20mm Gage Block Through 60 Cycles of One Calibration and New Calibrations of the Same Probe

From these results the measurements for the first probe calibration show a very repeatable measurement over an extended period of time under continuous measurement and machine axis exercise yielding no apparent drift. The measurements taken with the new calibrations of the same physical probe and taken side by side with the original probe calibration show much larger variations in results. Figure 77 shows these same results plotted with the corresponding directional component from the deflection matrix of the calibrations, in this case in the x-direction which corresponds to the direction of measurement of the gage block.

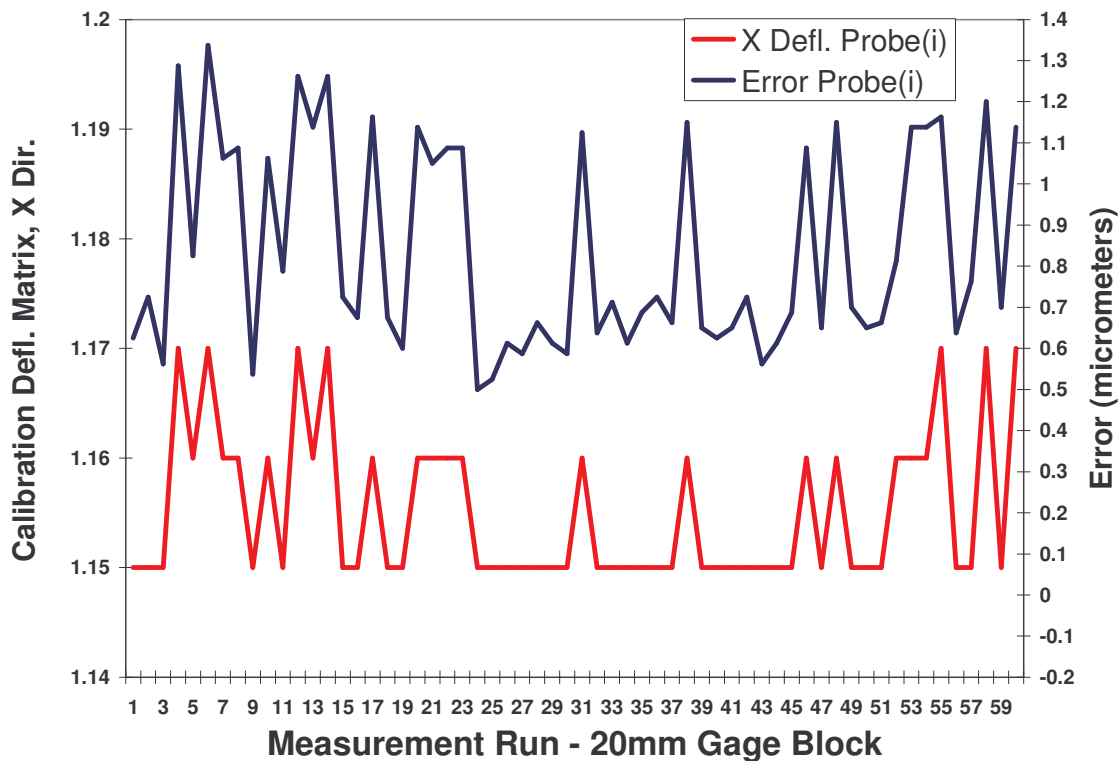


Figure 77: Two Axis Plot, Showing 60 Consecutive Calibrations and The Corresponding Probe Deflection From the Calibration Result

The indications are that the calibration procedure is potentially a source for large bias errors, especially in point to point measurement. In this experiment the errors are almost one to one with the calibration deflections. In order to simulate the uncertainties for any given measurement which takes into account the bias from calibration on this particular machine one would need to interpret the deflection matrix and input the corresponding terms as scale errors or some other input that is interpreted as a bias.



## Chapter 5: CONCLUSIONS AND REMARKS

A process for evaluating commercial software packages that estimate task-specific measurement uncertainties for a particular CMM, for sets of various measurands, was implemented. In this process, task-specific measurement uncertainties were determined in two ways: by direct measurement of artifacts producing a statistical basis for uncertainty calculation, and by software simulations of the physical measurements which produced a virtual basis from which uncertainties were calculated. The measurands evaluated were circle diameter and form, line form, cylinder diameter and form, point-to-point distances, and sphere diameter and form.

In this evaluation, the artifacts measured for experimental uncertainties were calibrated geometries with, in general, negligible surface roughness or form. The exception being the 'large' sphere artifact, which had a form 'error', by design, of unknown magnitude. Additionally, experiments were carried out in a well controlled laboratory, where environmental conditions were relatively stable. This allowed physically measured uncertainties to be determined by controlling the variables of the experiment, but also detracts from the evaluation in terms of robustness of the simulation packages.

The expertise level required to operate either software package requires, at the least, a basic understanding of error sources and influence quantities usually associated with CMM measurement, in a general sense and as it applies to a specific machine, or

machine class. Using VCMM requires much more in depth analysis of parametric errors and the ability to test these errors using a specific process defined for the software. On the other hand, PUNDIT is inherently simpler regarding machine error terms, though there is an option to include parametric errors. By design it was intended to be used with Maximum Permissible Errors (MPE) and volumetric errors which are usually designated by the manufacturer, though reverification of these values for specific instances are recommended. In either case, the user is still required to input quantities associated with the conditions surrounding the measurement and provide some information about the machine for the software's model of the machine's functions. Verification of these inputs, if either software package is to be implemented, is therefore essential for remaining in compliance with the GUM or any standard that regulates the definition of these terms, should a measurement with a simulated uncertainty be scrutinized. The level of user for these methods is likely above that of the typical technician/operator. It should be noted however, that despite the level of sophistication of these software packages, the method is still a simplification of direct analytical calculation of all input quantities that are required for a sensitivity type analysis which is the current method required for compliance with the GUM.

Comparing the simulated results to the experimental values showed that, for the geometries tested, realistic uncertainty values are attainable. Additionally, similar overall averages for the absolute difference in simulation and experiment were attained for each simulation method, though a case by case basis indicates the methods were less reliable than the overall averages suggest. Additionally, in some cases the uncertainties were underestimated, which, assuming the experimental values were valid, is an undesirable

result. The PUNDIT (simulation by constraints) method was the most likely to underestimate uncertainties, and in certain instances weakness in the method was shown when systematic effects accounted for by the full parametric models was not by the PUNDIT method. In the same respect, both parametric simulations were equally likely to overestimate uncertainties in certain instances by systematic effects that were not represented in the experimental data. From a reliability standpoint, this indicates that the parametric methods might be preferred, but from an accuracy standpoint, the methods are more equal. It would be inherently simpler to adjust estimates for the simulation by constraints method to “cover” the uncertainties, if a process such as this were used to validate the method. Though, discrepancies in estimates for uncertainty by the parametric methods would be more difficult to correct, comprehending the correction type necessary would be more likely. For example, a large systematic influence, incorrectly estimated by the error measurement procedure might be indicated in the comparison of simulation to physical experiment, and would therefore allow the error to be more closely examined, i.e. by re-evaluating and correcting the erroneous error estimate. Hypothetically, if either software was implemented for determining the uncertainty of a part inspection, there is currently no mechanism to indicate the validity of the software result other than testing of this type. The part is an unknown and the reliability of the software and input quantities are the only assurances against an invalid uncertainty estimation.

In this experiment, artifacts were measured in particular position and orientation scenarios. Repeated measurements were taken for each. A first look at the data for most of the measurands for these individual scenarios indicates that both simulation and

experiment are noisy, in that the differences in scenario to scenario are not matched by the simulations. Taking the uncertainty estimations across various scenarios shows a closer relationship in uncertainty value between measured and simulated methods. This effect is likely, in part, due to the number of measurements in each case. The more scenarios included in the uncertainty calculation, the more likely variation in the measurement process is emulated, for all methods. This might also, however, indicate that in order to rely on a simulation to determine uncertainty for a particular machine and measurand, that a larger set, more inclusive of multiple conditions (i.e. a large number of positions and orientations, measurement strategies, and possibly long term effects) be used. Currently, neither software would allow for this type of evaluation. They were designed to encompass the specific scenarios associated with a task specific uncertainty. However, the limits of accurate determination of input values and verification of the simulation results based on those inputs is determined by skill level, cost, and time. By designing the software to encompass various scenarios at once, these factors may be reduced and the reliability of the software increased.

The large unknown form error that was encountered with testing of the 250mm sphere artifact, indicates also the effect this extrinsic factor may have on the simulation methods. To be clear, both methods allow a certain compensation in the form of input harmonics, but require some knowledge of the form error magnitude and frequency. Encountering a situation where a form error is undetected might not be an uncommon occurrence in certain situations for part inspection. It is evident that the uncertainty values simulated for this scenario may not be valid.

The simulation methods tested, for the experimental scenarios conducted in this dissertation, show the concept is valid. Especially if estimates are considered across several measurement scenarios. Though, underestimation is still possible and certain extrinsic factors need to be accounted for, future work may resolve this by determining certain practices or standards for the determination of errors sources specific to simulation use and for defining what scenarios the simulations can be considered valid. It is also interesting to note the performance in many cases of the simulation by constraints method was close to that of the parametric model simulations, especially considering uncertainties across different scenarios. Since only a manufacturer specified MPE value was used to input the machine error description, it is significant. Though these simulation methods are potentially useful and make determining task specific uncertainties accessible to a wide scope of users, the techniques used in this dissertation illustrate the difficulty in accepting the reliability of the results for general application.

## REFERENCES

1. Trapet, E., Waldele, F., 1995, The Virtual CMM Concept, *Advanced Mathematical Tools in Metrology II*, *World Scientific* **40**, pp. 238–247.
2. Phillips, S.D., Borchardt, B., Sawyer, D., Estler, W.T., Ward, D., et al., 1997, The Calculation of CMM Measurement Uncertainty via The Method of Simulation by Constraints, *The Proceedings of the American Society for Precision Engineering*, pp. 443-446.
3. Abbe, M., Nara, M. Takamasu, K., 2007, Uncertainty Evaluation of CMM by Modeling with Spatial Constraint, 9<sup>th</sup> Annual International Symposium on Measurement and Quality Control (ISMQC), pp. 121-125.
4. Balsamo, A., Di Ciommo, M., Mugno, R., Rebaglia, B.I., Ricci, E., Grella, R., 1999, Evaluation of CMM Uncertainty Through Monte Carlo Simulations, *Annals of the CIRP*, 48/1 pp.425-428.
5. Bosch, J. A., 1995, *Coordinate Measuring Machines and Systems*, Marcel Dekker, Inc.
6. JCGM 200, 2008, *International vocabulary of metrology — Basic and general concepts and associated terms (VIM)*.
7. Kirkup, L., Frenkel, B., 2006, *An Introduction to Uncertainty in Measurement*, Cambridge University Press.
8. JCGM 100, 2008, *Evaluation of measurement data — Guide to the expression of uncertainty in measurement (GUM)*.
9. ISO 14253-2, 2011, *Geometrical Product Specifications (GPS) – Inspection by Measurement of Workpieces – Part 2: Guidance for the Estimation of Uncertainty in GPS Measurement, in Calibration of Measuring Equipment and in Product Verification*.
10. NIST, 1994, *Guidelines for Evaluating and Expressing the Uncertainty of NIST Measurements*, NIST Technical Note 1297.
11. Wilhelm, R.G., Hocken, R., Schwenke, H., 2001, Task Specific Uncertainty in Coordinate Measurement, *CIRP Annals – Manufacturing Technology*, 50/2 pp. 553-563.
12. Summerhays, K.D., Baldwin, J.M., Campbell, D.A., Henke, R., 2005, A Versatile Tool for the Evaluation of CMM Task-Specific Measurement Uncertainty, *ACMC Annual Workshop*.
13. ISO/TS 15530-3, 2004, *Geometrical Product Specifications (GPS) –*

Coordinate Measuring Machines (CMM): Technique for Determining the Uncertainty of Measurement – Part 3: Use of Calibrated Workpieces or Standards.

14. Phillips, S.D., Borchardt, B., Abackerli, A.J., Shakarji, C., et al., 2003, The Validation of CMM Task Specific Measurement Uncertainty Software, ASPE Summer Topical Meeting, 29 pp.51-56.
15. Murray, P.G., Rasnick, W.H., 2004, Testing of Task-Specific Measurement Uncertainty Software for Coordinate Measuring Machines, Technology Development, Y-12 National Security Complex, BWXT Y-12, L.L.C.
16. Averitt, G.C., 2005, Comparison of Three Methods of Estimating Task Specific Measurement Uncertainty For a Coordinate Measuring Machine, Master's Thesis, The University of North Carolina at Charlotte, Charlotte, North Carolina.
17. Trenk, M., Franke, M., Schwenke, H., 2004, The "Virtual CMM" a Software Tool for Uncertainty Evaluation – Practical Application in an Accredited Calibration Lab, ASPE Proceedings, Uncertainty Analysis in Measurement and Design.
18. ISO/TS 15530-4, 2008, Geometrical Product Specifications (GPS) – Coordinate Measuring Machines (CMM): Technique for Determining the Uncertainty of Measurement – Part 4: Evaluating task-Specific Measurement Uncertainty Using Simulation.
19. Hocken, R., Simpson, J., Borchardt, B., Lazar, J., Reeve, C., Stein, P., 1977, Three Dimensional Metrology, Annals of the CIRP, 26/2 pp. 403-408.
20. ISO 10360-2, 2009, Geometrical Product Specifications (GPS) – Acceptance Test and Reverification Test For Coordinate Measuring Machines (CMMs) – Part 2: CMMs used for Measuring Linear Dimensions.
21. PTB, 2002, VCMM User Manual: Models, Parameters, Operation, Physikalisch-Technische Bundesanstalt, Coordinate Measuring Machines Section.
22. PTB, 2001, KALKOM 4 (User Manual): CMM Parametric Error Assessment.
23. Metrosage, 2005, PUNDIT/CMM: Uncertainty Evaluation for Coordinate Measuring Machines, Metrosage LLC.